NEAR INFRARED PHOTOMETRY OF SOME INTERESTING ASTRONOMICAL OBJECTS

BY

ASHOK MADHAV NAGARHALLI
PHYSICAL RESEARCH LABORATORY
AHMEDABAD-380009
INDIA

A THESIS

SUBMITTED TO THE GUJARAT UNIVERSITY
FOR THE DEGREE OF

DOCTOR OF PHILOSOPHY

JULY 1982

To

My Parents

CERTIFICATE

I hereby declare that the work presented in this thesis is original and has not formed the basis for the award of any degree or diploma by any University or Institution.

Author

N.M.ASHOK
Physical Research Laboratory
Ahmedabad-380009, India

Certified by

P.V.KULKARNI
Professor-in-charge
Physical Research Laboratory
Ahmedabad-380009, India

ABSTRACT

The discovery of X-ray burst sources has provided a powerful astrophysical probe to study the nature of the compact objects. The observations of the X-ray burst sources at other wavelengths provide valuable data about the physical processes at work in the surroundings of the compact objects. Among the X-ray burst sources the Rapid Burster, RB, (MXB 1730-335) displays a unique behaviour. The RB located in Liller I, a compact globular cluster experiences large visual interstellar extinction ($A_V \sim 11$) since it is located near the galactic center. Consequently it is very difficult to obtain the optical observations of either the RB or Liller I. Liller I having the the RB in it can be observed at IR wavelengths since the interstellar extinction is appreciably small in the IR spectral region ($A_K \sim 1.1$). We have recorded 6 IR bursts at 1.6 μm on 4/5 April 1979, for the first time, from the central region of Liller I which we believe are from the RB. The observed 2-3 second rise time and the peak luminosity $\sim 2 \times 10^{38}$ erg s^{-1} in 0.3 μm bandwidth centered at 1.6 μm indicate that the IR burst radiation is non-thermal in its origin. The possibility of proton-cylotron emission mechanism giving rise to the IR radiation is suggested.

The Be stars as a class have been studied. 55 Be stars were observed in the J, H and K bands. A few brighter members were also observed in the L band. Most of them show IR excess. The thesis contains new IR observations for 20 Be stars. The important result that has emerged from our analysis is the importance of the role played by stellar bolometric flux, L_*, in deciding the energetics of circumstellar envelope. From B0 to B8 L_* changes by two orders of magnitude and all through this range the total continuum luminosity, L_{IR}, of the circumstellar envelope is proportional to L_*. By geometric considerations it is shown that the energy input to the circumstellar envelope by Lyman continuum flux, L_L^o, from the central star cannot account for the observed continuum flux L_{IR}. The luminosity of the Balmer Hα emission line is shown to be proportional to the IR continuum luminosity of the circumstellar envelope, L_{IR}. As a result the IR excess becomes an indicator of Be phenomenon. Also a long term variability of infrared flux with a time scale of a few years is observed from the present and the previous available IR data. It has been shown that the IR variations are accompanied by variations in the equivalent width of the Hα line.

In addition to the IR observations of the RB and the Be stars, J H K photometry of XX Cam, a member of the group of peculiar variable stars known as RCB stars, is presented. It is shown that the absence of IR excess in XX Cam is related to its comparatively quiscent behaviour in the optical region.

List of Publications

1. Kulkarni P.V., Ashok N.M., Apparao M.K.V. and Chitre S.M.
Discovery of IR bursts from Liller I/MXB 1730-333,
Nature 280, 819-820 (1979).

2. Ashok N.M. and Kulkarni P.V.
A different kind of burst from infrared/X-ray burster
Liller I/MXB 1730-333,
Bull. Astron.Soc. India, 7, 47-48 (1979).

3. Chandrasekhar T., Ashok N.M. and Desai J.N.
Coronal interferogram in 5303 Å obtained during total
solar eclipse of 16th Feb.1980 and coronal temperatures,
Bull. Astron.Soc.India, 8, 87-89 (1980).

4. Kameswara Rao N., Ashok N.M. and Kulkarni P.V.
XX Cam - An inactive R CrB star,
Jnl. Astron and Astrophys. 1, 71-78 (1980).

5. Kameswara Rao N., Ashok N.M. and Kulkarni P.V.
Is HR 2947 a variable?
Bull. Astron. Soc.India, 9, 144-150 (1981).

6. Ashok N.M., Bhatt H.C., Kulkarni P.V. and Joshi S.C.
Near infrared photometric observations of Be stars,
Proceedings of the VII Annual Meeting of the
Astronomical Society of India at Roorkee,
Nov.29-Dec.1, (1981).

ACKNOWLEDGEMENTS

I would like to take this opportunity to express my deep sense of gratitude to Prof.P.V.Kulkarni, under whose guidance the work presented in this thesis was carried out. All through he has been very considerate and extremely helpful. His constant encouragement and valuable suggestions have greatly helped to complete the work in time. His active participation in all the observational programs solved most of the logistic problems that usually make any field trip tedious and troublesome.

I am extremely grateful to Prof.M.K.V.Bappu, Director Indian Institute of Astrophysics (IIA), for his encouragement. He has very generously made available the valuable telescope time and provided all the necessary help at the observatory site.

It is indeed a pleasant duty to express my deep gratitude to Prof.S.D.Sinvhal, the then Director of Uttar Pradesh State Observatory (UPSO) and also Prof.M.C.Pande the present Director of UPSO. Both of them have shown keen interest in my work. Without their offer of precious telescope time it would not have been possible to acquire the necessary observational data.

I am extremely grateful to the Director Prof.D.Lal for his encouragement. His attitude towards younger generation and strong belief in the necessity of venturing in new fields have left a deep impression on me.

I am very grateful to Prof.S.P.Pandya for all his help and encouragement.

I have greatly benefited from the numerous discussions with Prof.S.C.Joshi of UPSO. In particular the observational work on Be stars has been done with his collaboration. I am grateful to him for the same.

The observational program on RCB stars was done in collaboration with Dr.N.Kameshwara Rao of IIA. I have greatly enjoyed the observational work with Dr.NK Rao and would like to express my sincere thanks for the same.

Prof.J.N.Desai has been extremely helpful all through my work. I consider myself very lucky to be associated with him in different activities of the group - in particular Operation Celestron. The post-lunch tea strolls and evening discussions have greatly enlivened and made the duration of the present work rewarding. I owe him a deep sense of gratitude.

It is indeed almost an impossible task to convey my feeling of gratefulness to Chandrasekhar, Harish and Patro. Without venturing any further I would like to acknowledge their friendship with a simple THANK YOU ALL.

It is indeed a very pleasant duty to record my indebtedness to Manian. Apart from designing, fabricating and successfully operating the electronic instrumentation he has rendered great many other services. His enthusiasm and appreciation of the observational work have made the field trips very enjoyable. His innovations and suggestions have greatly helped in smooth functioning of the observational work. I once again thank Manian for all that he has done for me.

My special thanks are due to Mr.S.D.Rawat for maintaining the InSb dewars in good condition. His careful and delicate handling of the dewars has greatly helped in undertaking uninterrupted observational programs over the last four years. Mr.S.B.Banerjee was always ready to render a helping hand in many things - in particular cryogenic, vacuum and thin film coating facilities. I am extremely thankful to him for the same.

I would like to express my sincere thanks to Dr.A.G.Ananth ISAC, Bangalore. He was associated with

me in the initial stages of the work. His presence made the field experiments a delightful experience.

Over the years Messrs: N.S.Jog, R.T.Patel, A.R.Gupta, Ranjan and J.S.Chauhan have participated in different observational programs. I am extremely grateful to all of them for the same.

I am grateful to Kailash who undertook the tedious task of proof-reading of the stencils and did a thorough job.

I have greatly benefited from the helpful nature of other members of the group namely B.G. Ananda Rao, Mrs.S.K.Jani, H.I.Pandya, P.K.Kikani, R.Madhavan, F.M.Pathan, Mrs.Mary Thomas, R.K.Mahadkar, N.C.Shah and R.M.Parmar. Sincere "thank you" to all of them.

I am grateful to Mr.V.C.Mathew for all the help rendered by him. Without his enthusiastic support it would not have been possible to finish the thesis in time. He has always gladly incorporated last minute changes in the manuscript. His elegant typing almost without corrections has considerably reduced my work.

I am grateful to Mr.G.A.Panchal who helped in designing the mechanical assembly for the photometer. My

acknowledgements are also due to Messrs. G.A.Macwan, R.B.Chauhan and A.D.Patel for their services.

It is a pleasure to express my thanks to the Workshop personnel Messrs. V.R.Dave, Poonambhai, Jadhavbhai, Atmaram, Badia, K.P.Panchal and many others. They have always very cheerfully undertaken the jobs.

I would also like to express my thanks to Dr.Vijay Kumar and Messrs.D.R.Ranpura, J.G.Vora, Harishbhai Panchal and S.C.Bhavsar for the timely help rendered concerning photographic, drafting and xeroxing work.

I am also extremely grateful for the helpful attitude of the library staff and Dr.Dinesh Patel and other administrative staff.

It is a pleasant duty to record my thanks to Professors P.D.Angreji, G.Subramanian, A.R.Prasanna, S.K.Alurkar and M.R.Deshpande for their keen interest in my work.

With a sense of extreme happiness I recall the splendid cycling trips that were undertaken over the past few years. I would like to thank the team members who made this possible viz., Nagesh, Nautiyal, Neeraj,

Bhaskaran, Jha and Anjanikumar. At the same time I would also like to thank all my colleagues who have helped in no less measure, namely Kamalesh, Sekhar, Shyamlal, Ambastha, Pankaj, Avinash, Rhama, Mohan, Venkat, Jiten, Pal, Ajay, Hussain, Manab, Kutti Krishna Kumar, Jayaraman, Dhiraj, Kar, Potdar, Debhashish, Vishnu and all others.

I am very thankful to Mr.Muralidhar for the neat and meticulous cyclostyling of the thesis.

I would like to take this opportunity to express my deep sense of gratitude to Drs.H.S.Mahra and C.D.Kandpal of UPSO for their encouragement and help. The fellow observers of UPSO, Dr.J.B.Srivastava, Dr.S.K.Gupta, Dr.Umesh Joshi, Mr.U.S.Chaubey and Mr.Paramjeet have always extended their co-operation during the observing programs. Their help is gratefully acknowledged. I would also like to record my indebtedness to Sri. R.C. Tripathi and other library staff and Sri.N.Dass and other workshop staff.

I am very thankful to Raveendran and Mekkadan of IIA for numerous astronomical discussions as well as non-academic gossipping (only during cloudy nights) that provided much needed break from monotonous observational

work. I also take this opportunity to express my thanks to all observatory staff at Kavalur - in particular Messrs: Shanmugan, Ganesan, Kuppuswamy, Jayarajan, Rosario, Gabriel and other workshop staff and Rajendran and cateen staff. I would be failing in my duty if I do not record my indebtedness to IIA library staff at Bangalore who have always helped me during my stop-overs at Bangalore.

My sincere thanks are also due to Mr.TN Rajaraman who has helped me in many ways. Very often I recollect with nostalgia the happy days spent with him.

C O N T E N T S

CHAPTER I

INTRODUCTION

1.1 INFRARED ASTRONOMY - AN INTRODUCTION

Sir W.Herschel in the year 1800, alongwith discovering the infrared part of the electromagnetic spectrum also obtained the first infrared astronomical observations. In fact he observed the sun at infrared wavelengths. The next historical advancement was done by Charles Piazzi Smyth through his studies of infrared radiation from the moon in the year 1856. It is interesting to note that inspite of the discovery of infrared spectral region as early as 1800, only during the last 20 years or so astronomical observations in the infrared have gained the recognition as one of the major branches of observational astronomy. The main reason for the late development of this field was non-availability of detectors with sufficient sensitivity. Also the standard model stellar atmospheres do not allow the photospheres to have sufficiently low temperatures (< 2000 K) because in that case photosphere will not be stable against gravitational collapse. Hence stellar sources with most of the emitted energy at wavelengths longer than 10 μm were not suspected. The early results indicating the presence of substantial flux at 10 μm

(Mendoza 1966; Low and Smith 1966) came as a pleasant surprise and greatly accelerated the growth of infrared astronomy.

Because of necessity the initial efforts were concentrated mainly towards ground based observations. Consequently one could work only in the existing atmospheric windows transparent to infrared radiations. These windows and hence the ground based observations are restricted to wavelengths shorter than 25 μm on the lower side and longer than 350 μm on the higher side of wavelength. In certain high altitude dry sites observations at 35 μm are possible. At wavelengths longer than 1 μm mainly water vapour (H_2O) and carbon-di-oxide render the atmosphere opaque except in certain windows. The weaker bands of methane (CH_4), nitrous oxide (N_2O), carbon-monoxide (CO) and ozone (O_3) which are minor constituents of the atmosphere also cause partial obscuration to infrared radiation. However, in recent years the availability of different space platforms has made the entire infrared spectral region amenable for astronomical studies. Conventionally, the spectral region with wavelengths longer than 40 μm is referred to as far infrared and it merges into submillimeter region. After acquiring the initial

rudimentary observations, in last few years sophisticated instruments are being flown above the atmosphere (Soifer and Pipher, 1978). However, the development of sensitive detectors working in the far infrared region still remains as one of the urgent needs of the astronomical community.

The advent of infrared astronomy has served two purposes. It has made possible to study the sources and phenomena that could only be studied in the infrared. For example, objects with temperatures less than 3000 K emit most of their energy in the infrared and under certain astrophysical conditions the non-thermal radiation is emitted prominently in the infrared. Because of steep decline in the interstellar extinction in the infrared, the highly obscured regions such as dense dark clouds, center of our galaxy etc. become transparent in the infrared, and hence can be studied most effectively in the infrared. Observations in the visible region of such objects are not possible due to high extinction (Strom et al. 1975; Rieke, 1978). The other aspect of the astronomical studies in the infrared is adding new information about the objects already studied in other spectral regions. For example, the IR light curves of novae carry definitive information on grain formation and

growth (Ennis et al. 1977; Szkody et al. 1979; Gehrz et al. 1980). IR observations will provide important constraints for the structure and extent of accretion discs in cataclysmic variables (Sherrington et al. 1980; Frank et al. 1981). Close binary systems undergo mass transfer during their evolution. IR observations of these objects will reveal important information about dust and gas components (Phillips et al. 1980). The thermal emission from cometary dust peaks in the IR and consequently IR observations are very valuable in understanding their nature (Ney, 1976). Dust present in the H II regions is most effectively studied at IR wavelengths.

Another example of usefulness of IR spectral region is the possibility of studying astrophysically important molecules whose vibration-rotation lines lie mainly in this wavelength region. The abundant molecules of H_2, CO and H_2O present in the stellar spectra can be observed only in the IR, while other molecules like VO and CN and atoms like neutral helium, carbon and sulphur have their strongest transitions in the 2 μm region. IR observations have provided important data about the abundances of light elements in stellar atmospheres (Spinard and Wing, 1969). Also, the isotopic abundance

studies have become possible (Thompson and Johnson 1978) with the advent of high resolution IR spectroscopy and these are very helpful in understanding the nuclear processes taking place in stellar interior and mixing phenomenon in the stellar surface layers. Studies of oxygen isotopes ^{17}O and ^{18}O have shown evidence for enrichment of ^{17}O in cool giants (Maillard, 1974 and Geballe et al. 1977).

1.2 INFRARED ASTRONOMY FROM SPACE

As noted earlier, beyond 25 μm the terrestrial atmosphere is completely opaque and at wavelengths less than 25 μm the atmosphere is transparent only within restricted ranges. Progress in this field has been coupled to the development of the detector and technical capability to place the payload above substantial portion of the atmosphere.

Far infrared observations have been obtained from (a) high flying aircrafts (h $\sim$ 10-12 km), (b) balloons (h $\sim$ 30 km), (c) rockets (h $\sim$ 200-500 km, for a few minutes only). Already the data acquired by these space platforms has brought surprising and unexpected new results.

Far infrared observations of H II regions and molecular clouds have shown that they are very bright at $\lambda = 100$ μm (Low and Aumann, 1970). These observations have emphasised the role of dust in determining their energy balance and evolutionary sequence.

Remarkable decrease in the interstellar extinction at IR wavelengths provides new means of studying the galactic structure. Large scale infrared emission in the galactic plane and from the galactic centre has been observed all through the IR spectral region - 2.4 μm to 100 μm. The reasons for the near infrared observations from balloon are weak intensity gradient and large angular extent. The unique gap between the OH bands of the atmosphere at 2.4 μm allow the observations to be made without airglow interference. First far infrared observations of our galactic centre region showed that 100 μm emission is common throughout the galactic plane (Hoffmann et al. 1971), emphasising the importance of dust emission. In general far infrared and radio continuum surface brightness are well correlated (Alvarez et al. 1974). An interesting observational result that has emerged out of the detailed mapping of the galactic center region at far infrared wavelengths is the double lobed

structure (Harvey et al. 1976; Rieke et al. 1978). Further the two lobes of peak brightness at 100 μm are located on either side of the galactic center region where 30 μm observations show a peak (Gatley and Becklin, 1981). The map of the 2.4 μm emission in the galactic plane shows a distribution characteristic of edge-on galaxy (Okuda, 1981) consisting of two components, disc and bulge, with the bulge brightness peaking at galactic center. Also the 5 kpc complex, where different constituents of the galactic disc like OB star, H II regions, CO emission and H 166α radiation peak, shows up in the 2.4 μm maps (Hayakawa et al. 1976; Okuda et al. 1977).

In case of extragalactic studies, the most astonishing result was the discovery of prodigal amount of energy in the far infrared from Seyfert Galaxies (Low and Aumann, 1970). Because of the limited available apertures, the sizes of the infrared emitting regions in the Seyferts have been deduced from the temporal variability studies. These studies which provide upper limits for the sizes have hinted at non-thermal processes. High spatial resolution far infrared studies of Seyfert galaxies will provide clues for the emission mechanisms.

The Wein part of the 3 K blackbody distribution falls in the realm of far infrared spectral region. As a result, far infrared observations have provided valuable data for studying cosmic background radiation, (Robson et al. 1974; Woody et al. 1975).

The first sky survey from space was carried out by Air Force Geophysical Laboratory using rocket borne instruments at the following 4 wavelengths viz. 4 μm, 11 μm, 20 μm and 27 μm (Price and Walker, 1976). The far infrared sky survey experiment (FIRSSE) presently - 1982 - in progress will extend the wavelength coverage to 120 μm (Price et al. 1981). The possibility of achieving considerably higher sensitivities in space has been demonstrated by AFGL rocket sky survey (Price and Walker, 1976). However, the rockets provide data over a very limited time interval and for long duration observations IR satellite is the only way out. The first IR space mission is the Infrared Astronomical Satellite (IRAS) scheduled for launch in late 1982. IRAS will use 0.6 m telescope cooled to $\sim$ 15 K and its main scientific objective is an all sky survey in 4 bands covering the wavelength region 8 to 120 μm. The next committed space mission is the space telescope

(ST) observatory, with an uncooled 2.4 m primary mirror, which will have IR photometer as one of the focal plane instruments. The main advantages of ST are improved spatial resolution and exceptional pointing accuracy (Moorwood, 1978).

1.3 GROUND BASED INFRARED ASTRONOMICAL STUDIES

The extensive stellar infrared photometric studies by Johnson and his group in the early stages of the development of this field provided the basic data of importance to stellar studies. In his review paper Johnson (1966) has summarised the results about stellar colour indices, bolometric corrections and effective temperatures. The next important development was the sky survey at 2 μm by the CIT group (Neugebauer and Leighton, 1969). It gave an idea of how the infrared sky looks.

As mentioned earlier the ground based studies are carried out through the atmospheric windows which are centered at the following wavelengths viz. 1.25 μm (J), 1.65 μm (H), 2.2 μm (K), 3.4 μm (L), 5.0 μm (M), 10.0 μm (N) and 22 μm (Q). Conventionally 1 to 5 μm

region is referred to as the near infrared and 6 to 35 μm as the middle-infrared region.

One of the important results of stellar infrared studies is that a significant number of sources show departures from the blackbody spectra in their energy distribution. Given the spectral class of a star, which decides the effective temperature, one can obtain the expected blackbody energy distribution. If the observed radiation exceeds the expected radiation in any spectral region then the object is said to have excess radiation in that particular spectral region. With present understanding the observed infrared excess is usually attributed to (a) dust re-emission or (b) plasma emission processes - thermal and non-thermal. The ground based galactic infrared observations cover a wide variety of objects - stars, H II regions, dark clouds, molecular clouds, planetary nebulae, novae and galactic center. Extragalactic coverage is also equally impressive-normal galaxies, quasars, BL Lac objects and Seyferts.

The early (1960's) infrared astronomical work done using the ground based telescopes and space platforms is summarised by Neugebauer et al. (1971). Later review articles by Fazio (1976), Beckman and Moorwood (1979)

and Reike and Lebofsky (1979) discuss the subsequent developments. Proceedings of IAU Symposium No.96 on Infrared Astronomy (edited by Wynn-Williams and Cruikshank, 1981) - covers extensively recent observations, their interpretation and the theoretical aspects in infrared astronomy and astrophysics.

1.4 SCOPE OF THE PRESENT WORK

The work presented in this thesis consists of ground based near infrared photometric observations of selected objects at J H K L bands.

The instrumental set up used for the said observations is described in Chapter II.

The following three different kinds of celestial sources are studied.

1. The X-ray Rapid Burster MXB 1730-335
2. The Be stars
3. The RCB stars.

The discovery of X-ray burst sources has provided a powerful astrophysical probe for studying the compact objects and their environments. Amongst the X-ray burst

sources the Rapid Burster, RB, (MXB 1730-335) is indeed a remarkable object and has greatly influenced the course of theoretical attempts to understand the nature of the burst sources.

Observations of the X-ray burst sources in other spectral regions will provide important clues to the emission mechanism and the nature of these sources. As a result of worldwide coordinated observational campaigns simultaneous optical and X-ray bursts have been observed from three burst sources: MXB 1735-44 (Grindlay, et al.78) MXB 1837+05 (Hackwell et al. 1979) and MXB 1636-53 (Pedersen et al. 1979). However, the case is different for the R B.

The RB is located in the highly reddened globular cluster Liller I which is near the galactic center and falls in the Scorpius constellation. The large interstellar extinction, $A_V \sim 11$, (Kleinmann et al. 1976) makes optical observations of RB almost impossible. Under these circumstances near infrared studies can be employed as powerful diagnostics to study the RB. The theoretical calculations of Drs.Apparao and Chitre (1979) indicated that IR bursts should accompany X-ray bursts from the RB.

Also the prior knowledge of the approximate active period of RB makes it possible to plan observational program in advance. The results of our successful detection of IR bursts from RB are presented in Chapter III.

The Be stars are characterised by the presence of hydrogen Balmer series lines ($H\alpha$, $H\beta$ ...) in emission. In the generally accepted model of a Be star the origin of circumstellar envelope is attributed to the material lost from the central star from its equatorial region. The relevance of IR studies of Be stars comes about because of the following reasons. The presence of a circumstellar envelope around a central star is the cause for all peculiar behaviour of Be stars. So to understand the nature of Be phenomenon it is essential to study the structure and physical conditions of the envelopes of Be stars. Infrared photometry is one of the powerful tools for studying Be star shells since the shell emits a substantial part of its total energy in this wavelength region. With this end in view JHKL observations for a group of Be stars were taken. In the present work the Be stars are studied as a class and no emphasis is given to detailed behaviour of individual members of the class. An attempt is made to

work out the details of energetics of the circumstellar shells. Correlation studies of the total continuum shell flux, the physical parameters of the central star and the hydrogen emission line strengths have been done. Also long term-few years time scale - photometric variability of Be stars is studied. This work is presented in Chapter IV.

R CrB is the prototype of a peculiar class of variable stars known as RCB stars characterised by the following properties. Their brightness normally constant, suddenly drops by several magnitudes at irregular intervals and then slowly recovers to the initial level. Spectroscopically they are distinguished by overabundance of carbon and deficiency of hydrogen. Another characteristic feature is the presence of excess infrared radiation at all times.

The excess infrared emission from RCB stars is due to different mechanism than those operating in the case of RB and the Be stars. The hypothesis of thermal reradiation of the stellar flux at longer wavelengths satisfactorily accounts for the observed infrared excess in RCB stars. The occasional mass ejection episodes which manifest as fading of the star in the optical

region, replenish the circumstellar material. Of all the RCB stars XX Cam has shown virtually no change except only once of visual fading during last 80 years. JHK observations of XX Cam have been taken to look for the infrared excess. These results are presented and discussed in Chapter V.

The data presented in this thesis were obtained with 1 m Sampurnand reflector of the Uttar Pradesh State Observatory, Nainital, and 1 m reflector of the Indian Institute of Astrophysics, Bangalore at Kavalur. A few observations of some bright Be stars were also taken on the 0.5 m reflector at Kavalur.

CHAPTER II

INSTRUMENTATION

2.1 INFRARED PHOTOMETRY - AN INTRODUCTION

Infrared photometry as at any other wavelength consists of measuring the amount of radiation coming from a region of the sky which contains the object of interest. However, the peculiarities of the infrared radiation demand special techniques for the successful detection of the precious signal from astronomical objects. For ground based observations the main problem is the terrestrial atmosphere. Over years, the observational procedures that permit acquisition of IR astronomical data, inspite of the severe limitations of the earth's atmosphere, have been improved and perfected. These have been very nicely reviewed by Low and Rieke (1974) and Lena (1978). The following paragraphs briefly describe the details of the procedure currently followed by ground based infrared observers.

In the atmospheric windows, alongwith the star light all the time thermal emission from the sky which is wavelength dependent will be reaching the detector. Because of this the contrast between the source and the background is considerably reduced making signal

detection difficult. In addition, this thermal emission from the atmosphere itself varies. This variation, conventionally referred to as sky noise, is site dependent and in a given place it varies with changing meteorological conditions. Very few attempts have been done to study the behaviour of the sky noise (Blanco et al. 1976; Allen and Barton, 1981). The limited available data indicates that the power spectrum of the sky noise is flat in 1-3 μ m wavelength range at $>$ 1 Hz and for frequencies less than this it shows 1/f dependence (Allen and Barton, 1981). In order to surmount these difficulties the beam switching technique is adopted for infrared observations. Two beams, one containing the object of interest and the other one looking at adjacent sky are alternately presented to the detector. Only the difference between these two signals, which is proportional to the source strength, is tapped from the detector for further processing. By carrying out this alternate sampling at the appropriate rate (usually $>$ 10 Hz) a modulated signal with its a.c. component proportional to the incident stellar flux is generated rejecting the lower frequency noise.

Any room temperature object in the field of view of the detector radiates profusely in the infrared

($\lambda > 3$ μm) and reduces the signal to noise ratio. So it is necessary to cool all the detector associated components of the photometer. In the near infrared liquid nitrogen cooling is adequate and beyond 5 μm liquid helium cooling becomes essential.

2.2 INFRARED PHOTOMETER

We have used our photometers in conjunction with the reflectors meant for optical astronomy. These optical reflectors have neither the provision for vibrating the secondary nor for nodding the telescope to accomplish the chopping. Therefore a vibrating tertiary mirror near the focal plane had to be used for presenting alternately the star plus sky and nearby sky fields to the detector. To avoid microphonics the chopper and detector housing were always independently mounted on the Cassegrain plate. This reduced the transfer of microphonics due to moving parts of the chopper to the detector since the mechanical coupling between these two is only through the telescope. The telescope damps the vibrations very efficiently since it has a large weight.

PbS Photometer:

In the first version of the photometer, which was really for our own training, uncooled lead sulphide (PbS) detector was used. Because of high noise equivalent power (NEP) of PbS detector, stars fainter than zero K magnitude could not be observed (with S/N $\sim$ 4) and consequently no results obtained with this photometer are presented in this thesis. For the sake of completeness the details of the PbS photometer are listed in Table 2.1.

Table 2.1

Details of the PbS detector and pre-amplifier

a. Characteristics of PbS detector

NEP (K; 750 Hz, 500 K)	= 10^{-11} W $Hz^{-\frac{1}{2}}$
Cell size	= 1.0 mm x 1.0 mm
Time constant	$\sim$ 1 ms
Energy gap	E_g = 0.42 eV
Long wavelength cut-off	λ_c = 2.9 μm

b. Specifications of Pre-amplifier

Input impedance	= 10 MΩ
Output impedance	= 2 KΩ
Gain	= 60 (0.16 - 1 KHz)
Noise	= 5 nV $Hz^{-\frac{1}{2}}$ at 16 Hz.

In the second version of the above photometer the detector was cooled to 195 K. The gain in sensitivity was marginal.

InSb Photometer:

Indium antimonide (InSb) detector not only covers the wavelength from 1 to 5.5 μm but also has lower NEP value. Hence in the later version of our photometer we have incorporated liquid nitrogen cooled InSb dewar (supplied by IR Laboratories, Tucson, USA). The schematic diagram of the optical and mechanical arrangement is given in Fig.2.1. The system diagram of the photometer, signal processor and data acquisition system is given in Fig.2.2.

The InSb dewar has double walled vacuum isolation and provides liquid nitrogen (LN_2) temperature for the InSb detector, filters, apertures, Fabry mirror and first stage of the preamplifier. To reduce the radiation due to thermal background falling on the detector, extensive baffling is provided. For manual selection of the filter and focal plane aperture, controls have been brought outside the dewar through vacuum seals. The dewar is fitted with a calcium fluoride (CaF_2) window which can

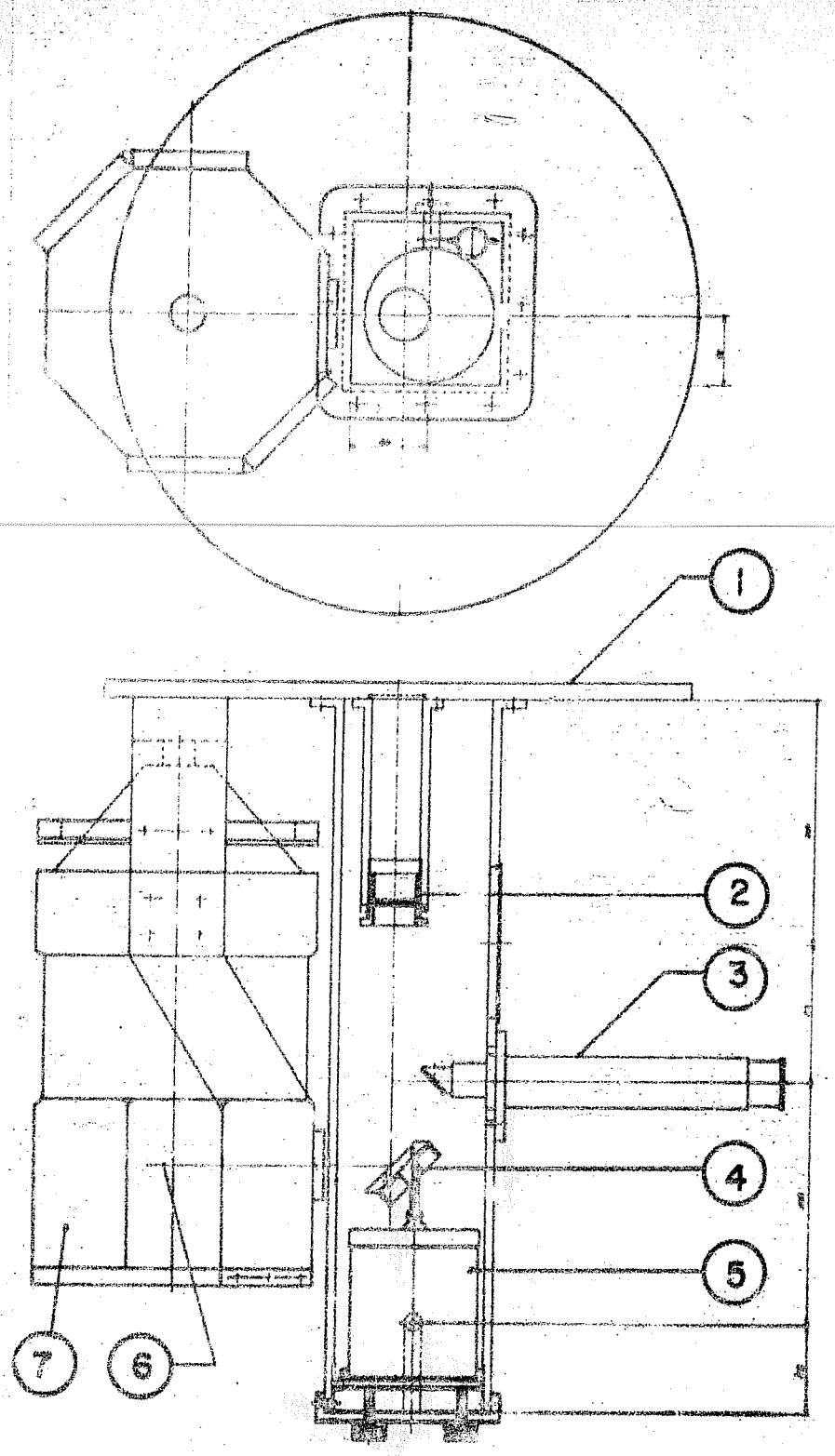

1. Cassegrain plate 2. Relaying lens
3. Retractable mirror and eye-piece assembly
4. Chopper mirror 5. Vibrator
6. Focal plane 7. Dewar

Fig.2.1 : Schematic diagram of the optical and mechanical arrangement of the InSb photometer.

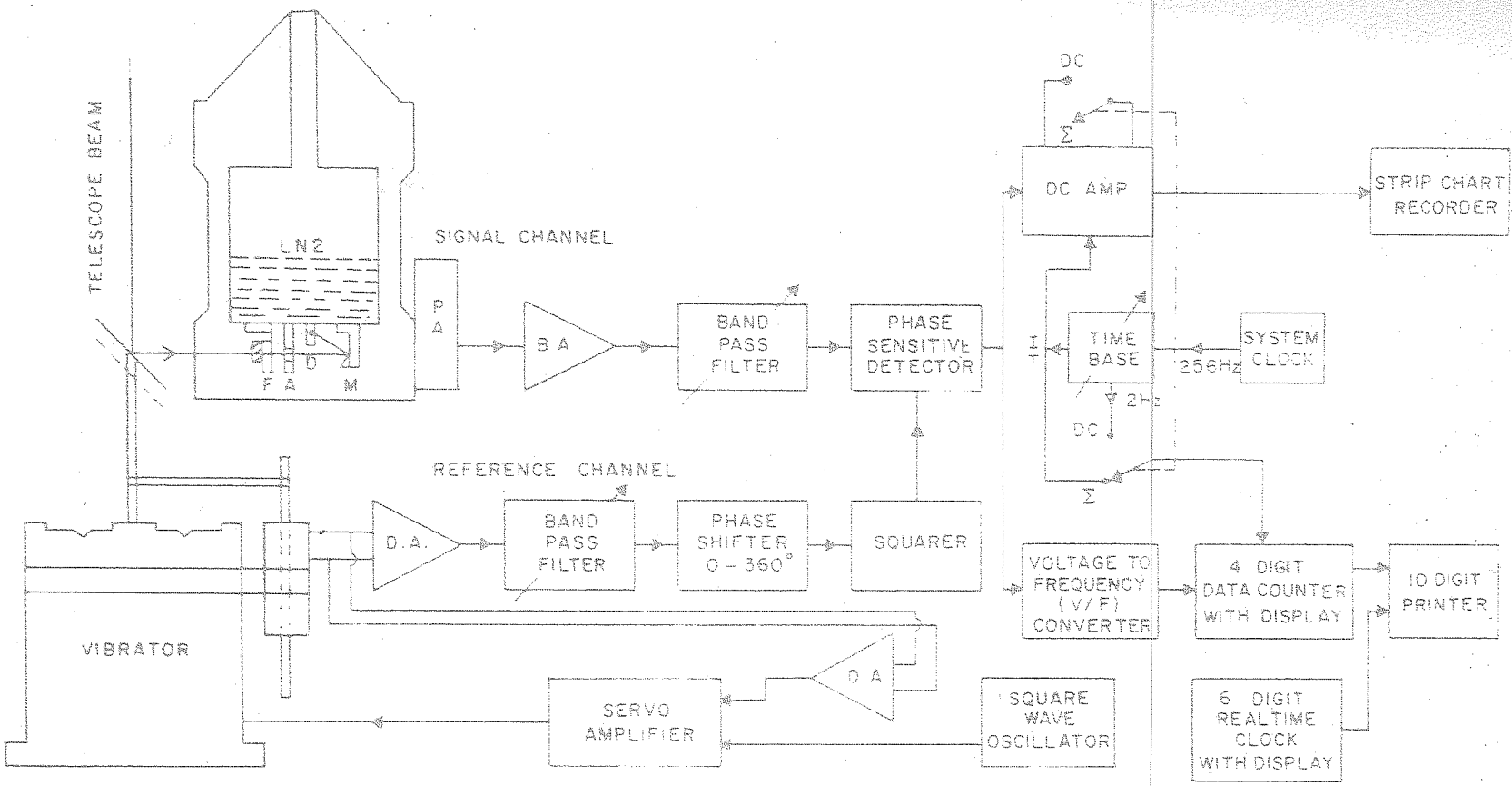

F: Filter, A: Aperture, D: Detector, M: Fabry Mirror

Fig.2.2 : Block diagram of the InSb photometer, signal processor and data acquisition system.

withstand the vacuum behind it and is able to transmit 90-95% of IR radiation upto 7 μm. A small box containing molecular sieve material is mounted on the cold work surface inside the dewar to retain vacuum and consequently give longer LN_2 hold time. For imaging the primary mirror of the telescope onto the detector an off-axis concave Fabry mirror was used.

The InSb detector and preamplifier details are given in Table 2.2.

Table 2.2

InSb detector and preamplifier details

a) Characteristics of InSb detector

Phtovoltaic Mode

NEP : 2.4×10^{-15} W $Hz^{-\frac{1}{2}}$ at 2 μm)
1.0×10^{-15} W $Hz^{-\frac{1}{2}}$ at 5 μm) for 5-50 Hz

Energy gap E_g (77 K) = 0.23 eV

Long wavelength cut off λ_c = 5.4 μm

Impedance at 77 K : $3 \times 10^9 \Omega$

Cell size : 0.5 mm diameter

Time constant : 1 μs

b) Preamplifier Specifications

Frequency Response : DC to 25 KHz (3 dB)

Noise at 77 K 20 nV $Hz^{-\frac{1}{2}}$ (5-40 Hz)

Output impedance 250 Ω.

The preamplifier model IA2 is designed to operate the InSb detector in current mode i.e. monitoring of current by holding the voltage across p-n junction of the detector constant. This results in linear responsivity of the detector over a very large range and hence suitable for astronomical purposes. The dual matched FET and the feed-back resistors are mounted on the cold work surface along-with the detector to reduce the contribution due to Johnson noise. There is a provision to adjust the bias voltage to near zero value resulting in maximum signal to noise ratio. The pre-amplifier is dc coupled to the detector. Because of this, at pre-amplifier output a large offset corresponding to the background radiation will be present. The pre-amplifier is ac coupled to the next stage to avoid saturation when large dc background is present. The signal processor developed was such that the detector noise limited the performance of the IR photometer. We have used the method of phase sensitive detection (PSD) which very efficiently detects the low signal in the presence of high noise. For PSD, the reference signal was derived by mechanically coupling a position transducer to the vibrating mirror.

The vibration of the tertiary mirror was controlled by a servo system. The servo system helps the chopper

mirror to execute square wave motion and retain steady mean position. A duty ratio of $\sim$75%(stable trapezium waveshape)was realised at 16 Hz with an amplitude of 2.5 mm on the chopper tertiary mirror.

On the data acquisition side several facilities increased the IR photometer efficiency. Of these the most important was the linear data integrating facility for increasing S/N ratio on weak stellar sources. The analog data could be integrated upto 99 seconds in steps of 1 second and the voltage output was linear upto 15 V. The time base that controlled the integration time was accurate to 4 milliseconds.

To facilitate data reduction the analog signal was digitised using a voltage to frequency (V/F) converter with a conversion factor of 10 KHz/10V and a linearity error of less than 0.1%. The observed characteristic curve of V/F converter is shown in Fig.2.3. V/F count rate output was accumulated in 4 decade counters for a specified time interval. The resulting outputs of these counters alongwith 6 digit real time information (1 millisecond accuracy and 1 sec. resolution) were printed with a 10 digit printer. The broad band interference filters were calibrated using Beckman dual beam spectrophotometer

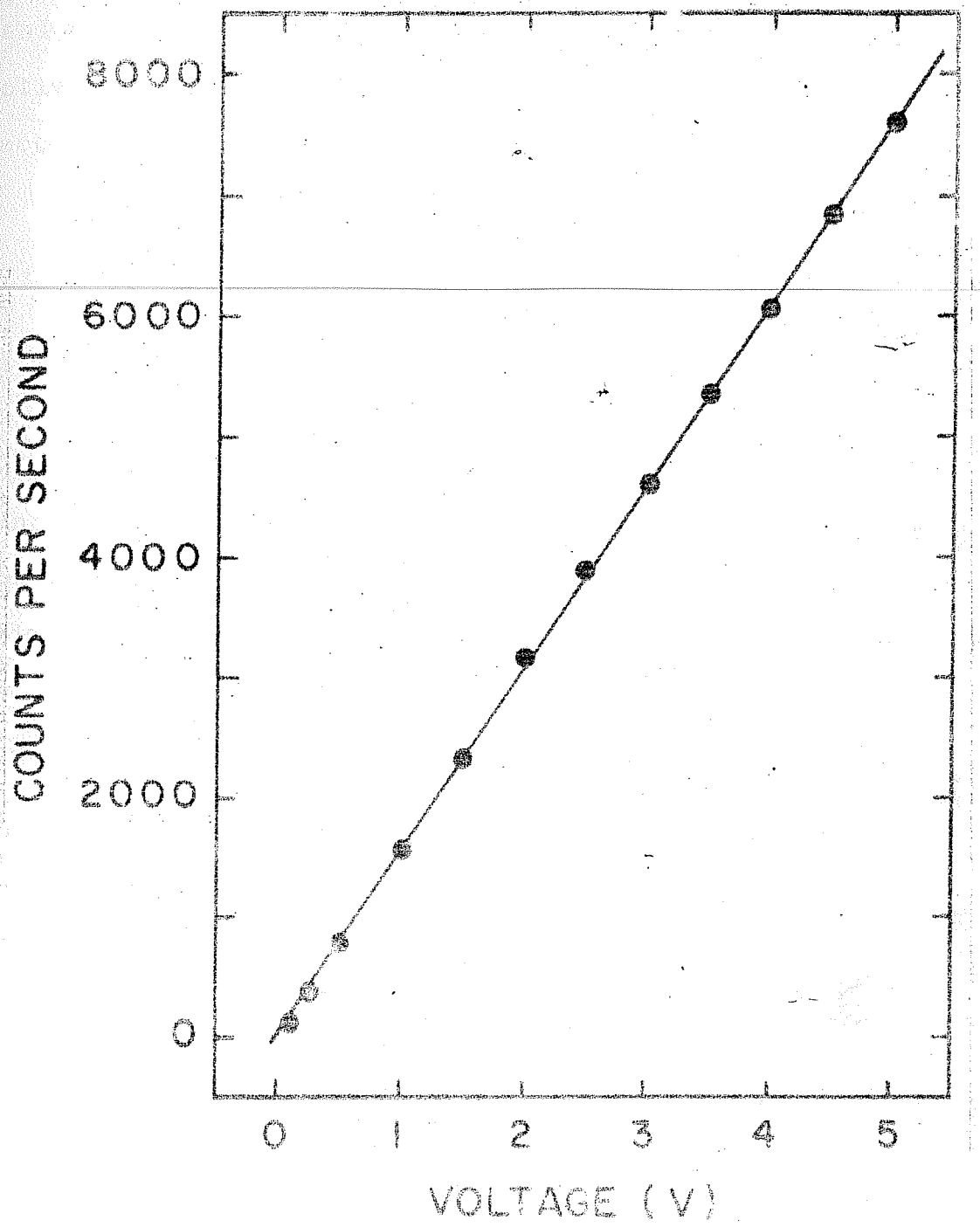

Fig.2.3 : Characteristic curve of the voltage to frequency (V/F) converter.

and transmittance curves are shown in Fig.2.4. The effective wavelength λ_e for each filter was determined according to the following relations.

$$\lambda_e = \frac{\int_{\lambda_1}^{\lambda_2} \lambda\, T_\lambda\, d\lambda}{\int_{\lambda_1}^{\lambda_2} T_\lambda\, d\lambda} \qquad \ldots\ldots \quad (2.1)$$

λ_1 and λ_2 are cut off wavelengths at 0.1% transmission and T_λ is the filter transmittance at a given wavelength λ. The characteristics of the interference filters are listed in Table 2.3.

Table 2.3

Interference filter characteristics

Photometric Band	Effective wavelength λ_e (μm)	Percentage Transmission at λ_e	Effective Bandwidth $\Delta\lambda_e$ (μm)	Flux for zero* magnitude $F(\lambda)$ (W cm^{-2} μm^{-1})
J	1.26	69	0.27	3.4×10^{-13}
H	1.65	77	0.28	1.28×10^{-13}
K	2.23	73	0.39	3.9×10^{-14}
L	3.64	80	1.16	8.1×10^{-15}

* Adopted from Johnson (1966).

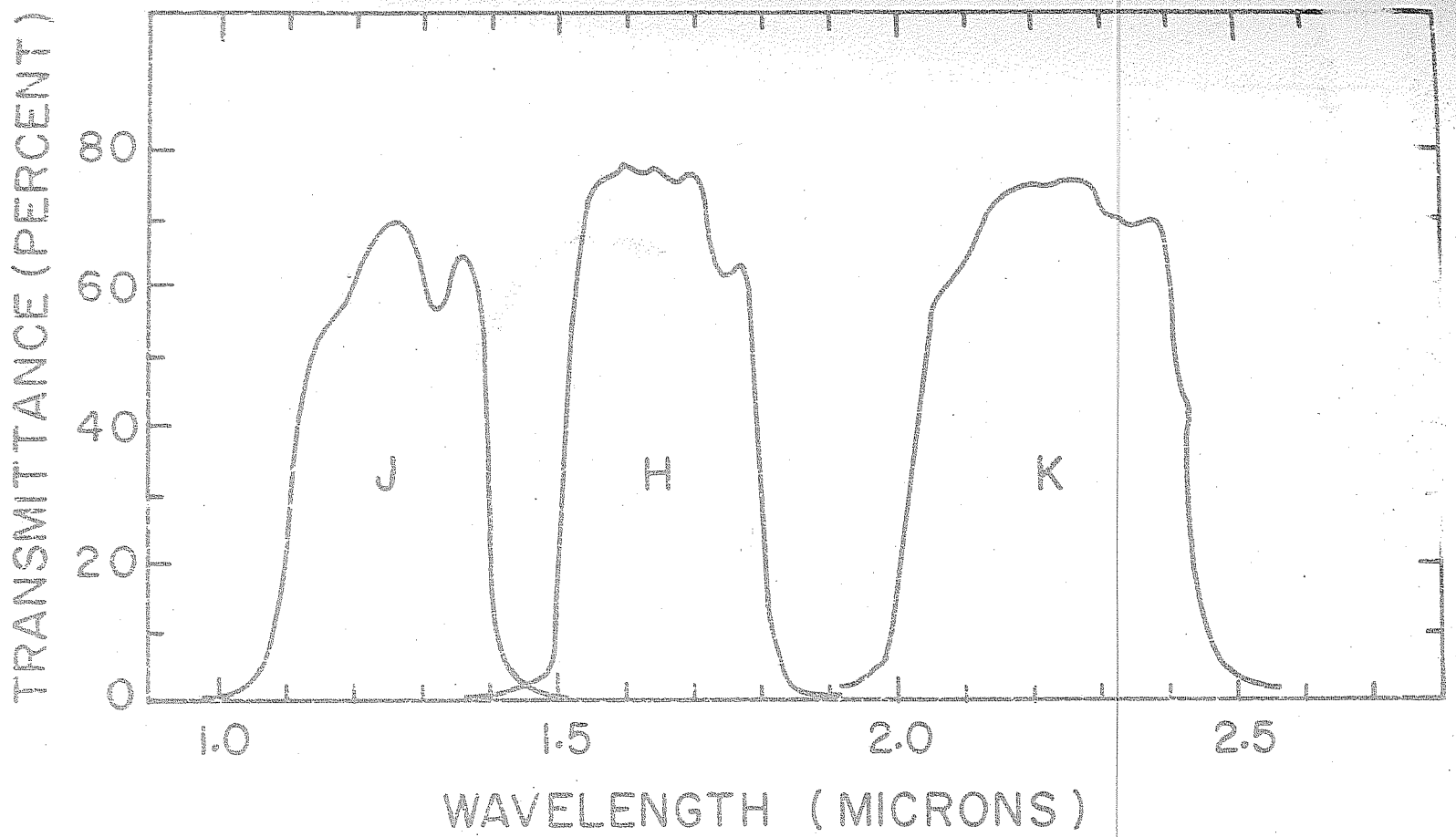

Fig. 2.4a : Transmittance curves of J (1.26 μm), H (1.65 μm) and K (2.23 μm) filters.

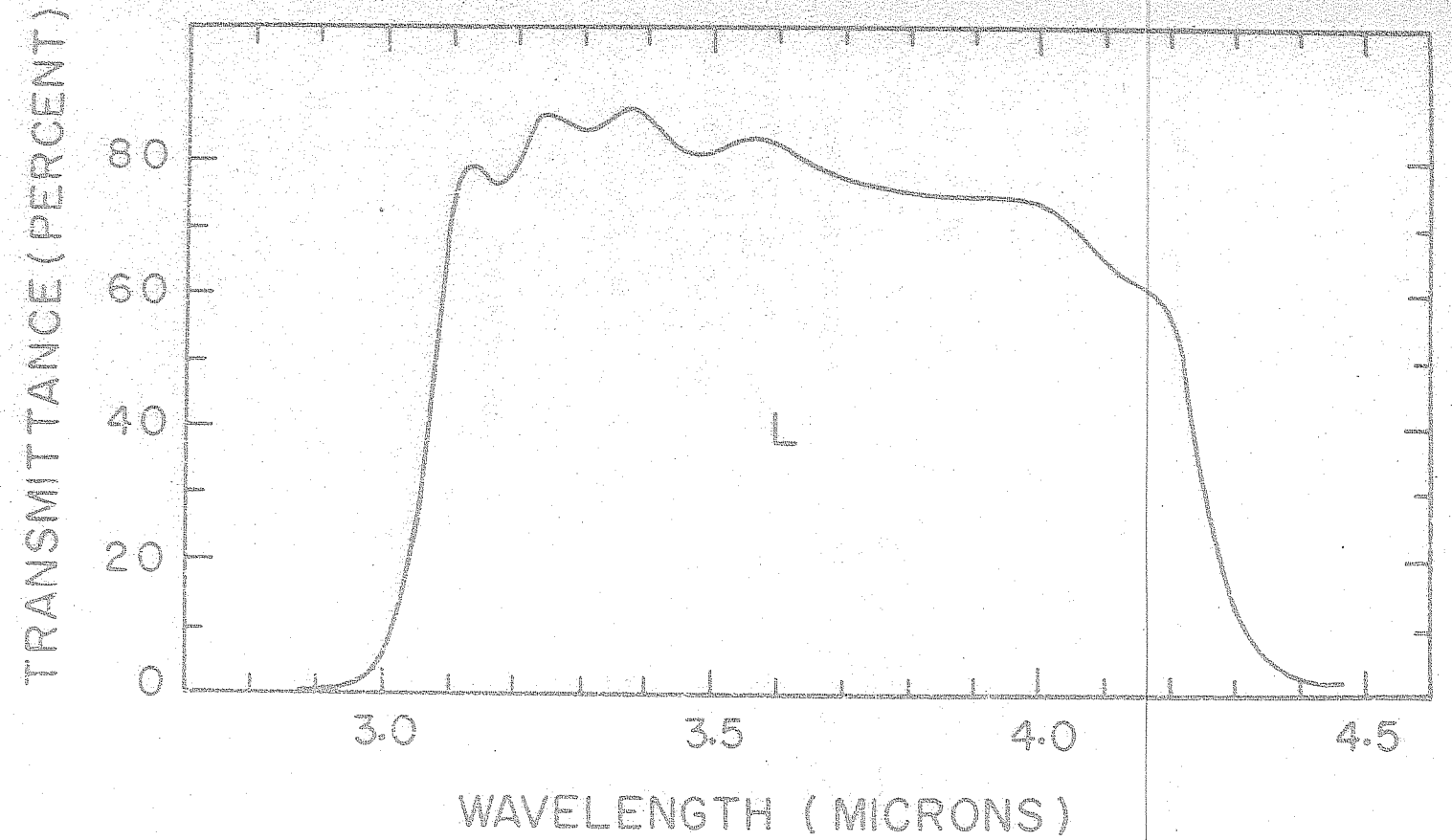

Fig. 2.4b : Transmittance curve of L (3.64 μm) filter.

The technical details of the infrared photometry program are given in Table 2.4.

Table 2.4

Characteristics of the Infrared Photometry Program

Telescope diameter	: 1 metre reflector
Telescope set up	: Cassegrain optical system
Telescope f/no	: f/13
Modified f/no	: f/20 (by optically relaying)
Focal plane apertures	: 0.5 mm, 1.0 mm, 2.0 mm
Plate scale factor	: 10 seconds of arc per mm
Detector field of view matched to	: f/13
Chopping frequency	: 12 to 16 Hz
Sensor cryogen	: Liquid Nitrogen
Focal plane temperature Detector Filter Fabry Mirror FET pair and feedback resistor	: 77 K

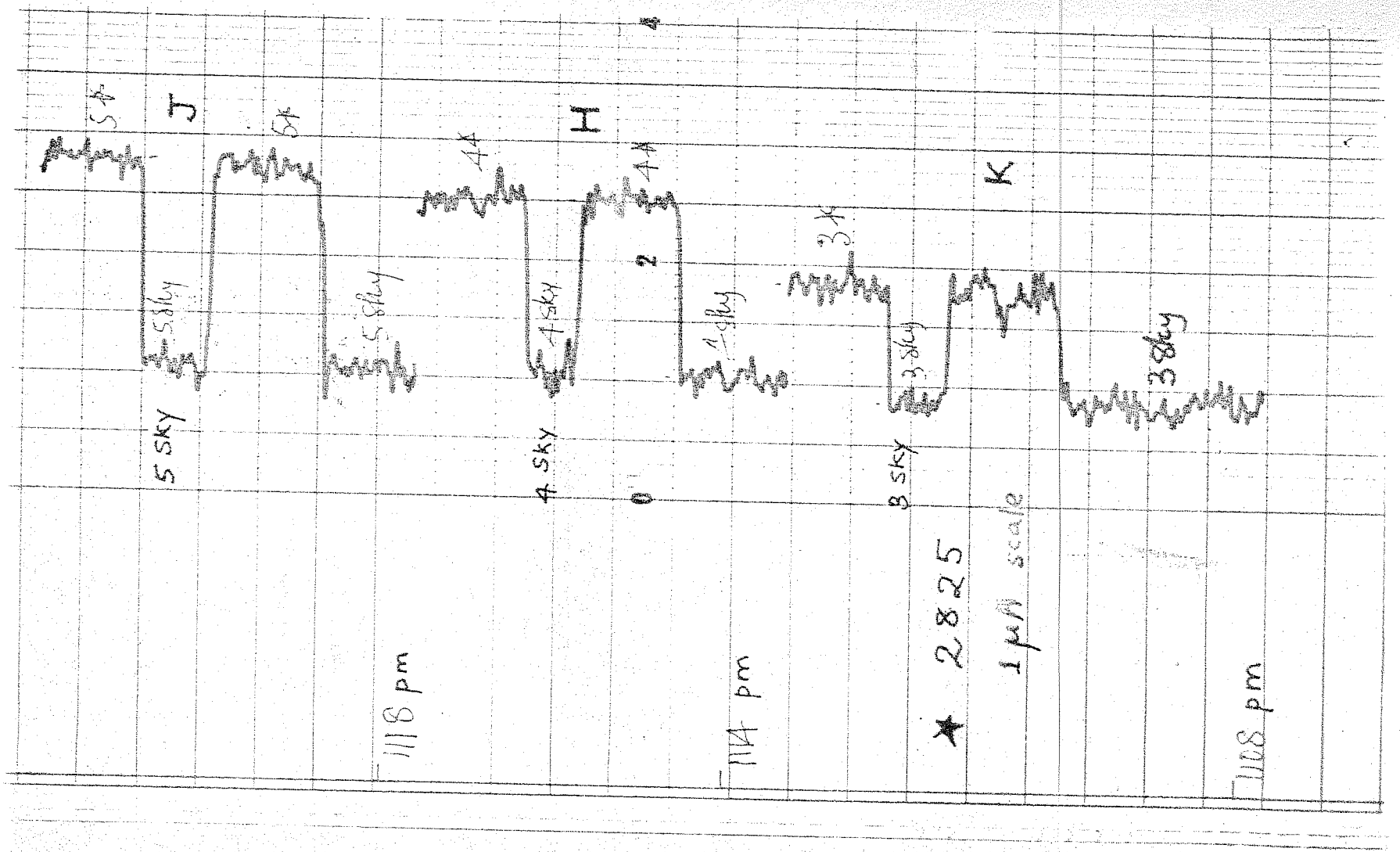

Fig.2.5 : A typical section of the chart record.

A typical section of the chart record is shown in Fig.2.5. The details of the observing sites are listed in Table 2.5.

Table 2.5

Observing site details

	Kavalur	Nainital
Latitude	+12° 34.58'	+29° 21.65'
Longitude	78° 49' 45" E ($5^h 15^m 19^s$)	79° 27' 24" E ($5^h 17^m 49.71^s$)
Altitude	725 m (2380 ft)	1927 m (6322 ft)

2.3 DETECTOR CALIBRATION

The response R of the detector is defined as the voltage output per unit incident flux. This is one of the basic parameters that characterise a detector and is given by

$$R = V_s/W \quad VW^{-1} \qquad \ldots\ldots (2.2)$$

where V_s and W are the rms values of the fundamental components of the signal voltage at the detector output and power incident on the detector respectively.

The response of the InSb detector was determined in the laboratory using a blackbody source. The incident power P was determined using the following equation.

$$P = A \Omega N_{\lambda_e}(T) \Delta\lambda \; T_f \qquad \ldots\ldots \quad (2.3)$$

where
- A : etendue (cm^2 sr) = $A_1 A_2/d^2$
- A_1 : detector area (cm^2)
- A_2 : blackbody aperture area (cm^2)
- d : distance between the blackbody aperture and the detector (cm)
- $N_{\lambda_e}(T)$: radiance of blackbody at temperature T at effective wavelength λ_e (W cm^{-2} μm^{-1} sr^{-1})
- $\Delta\lambda$: Effective bandwidth of interference filter (μm)
- T_f : Transmittance of the filter at the effective wavelength.

(Product $N_{\lambda_e}(T)\ \Delta\lambda\ T_f$ is a reasonable approximation for $\int_{\lambda_1}^{\lambda_2} N_\lambda T_\lambda\, d\lambda$ where λ_1 and λ_2 are the wavelengths where filter transmission T_λ is less than 0.1%).

$N_{\lambda_e}(T)$ was calculated using the following equation.

$$N_{\lambda_e}(T) = \frac{1.2 \times 10^{-16}}{\lambda_e^5 \left(\exp\left(1.44/\lambda_e T\right) - 1\right)} \text{ W cm}^{-2}\ \mu\text{m}^{-1}\ \text{sr}^{-1} \quad \ldots\ (2.4)$$

(λ_e in cm and T in K)

Experimental values of parameters for calculations of R are listed below.

$A_1 = 1.963 \times 10^{-3}$ cm^2 (d_1 = 0.5 mm)

$A_2 = 3.167 \times 10^{-3}$ cm^2 (d_2 = 0.635 mm)

d = 324 cm

T = 973 K

A = 5.921×10^{-11} cm^2 sr

The incident radiation on the detector was modulated using a square wave chopper at 20 Hz. However,

the incident power on the detector has to be specified in terms of rms value of the fundamental component. For a square wave the rms value of the fundamental component is 0.45 times the peak to peak amplitude (Hudson, 1969), therefore $W = 0.45\ p$.

The laboratory measurement of detector noise yielded a value of $V_n = 30\ \mu V\ Hz^{-\frac{1}{2}}$ at 20 Hz. The noise equivalent power (NEP) was calculated using the relation

$$NEP = \frac{V_n}{R}\ W\ Hz^{-\frac{1}{2}} \qquad .... \qquad (2.5)$$

The results of the detector calibration for the experimental values listed above are given in Table 2.6.

Table 2.6

Detector response at effective wavelengths of JHKL bands

Filter	(λ_e) μm	W(rms) watts	V(rms) volts	R VW^{-1}	NEP(λ_e, 20 Hz) $W\ Hz^{-\frac{1}{2}}$
J	1.26	1.49×10^{-13}	7.5×10^{-5}	5.05×10^{8}	5.94×10^{-14}
H	1.65	7.17×10^{-13}	3.0×10^{-4}	1.12×10^{9}	2.68×10^{-14}
K	2.23	2.17×10^{-12}	5.3×10^{-3}	2.44×10^{9}	1.23×10^{-14}
L	3.64	8.10×10^{-12}	1.5×10^{-2}	1.85×10^{9}	1.62×10^{-14}

At the telescope, a value of 1.9×10^{-14} W $Hz^{-\frac{1}{2}}$ for NEP (2.23 μm, 16 Hz) was attained. This slightly higher value of NEP (compared to the laboratory value) may be due to the additional noise contribution from mirror baffles, telescope structure, etc.

2.4 ATMOSPHERIC EXTINCTION AND TRANSFORMATION TO STANDARD SYSTEM

The first step in reduction of the observations was the calculation of instrumental magnitudes j, h and k. They were obtained using the following equations.

$$j = -2.5 \log d_J \quad .... \quad (2.5a)$$

$$h = -2.5 \log d_H \quad .... \quad (2.5b)$$

$$k = -2.5 \log d_K \quad .... \quad (2.5c)$$

where d's are observed deflections normalised to a particular fixed scale.

On all observation nights it was not possible to get an extended set of observations to determine the atmospheric extinction coefficients. So it was decided to adopt the following extinction coefficients which were determined on 11/12 Feb.1981 at Kavalur.

$$k_J = 0^m.15 \ , \quad k_H = 0^m.07 \text{ and } k_K = 0^m.09 \qquad \ldots (2.6)$$

Manduca and Bell (1979) have calculated the theoretically expected atmospheric extinction coefficients, for the filter sets employed in Kitt Peak National Observatory instrument, as a function of water vapour expressed in precipitable mm. The absorption in infrared is mainly due to molecular bands of water vapour. The transmission characteristics of the interference filters employed in our InSb photometer are similar to the ones used in KPNO instrument. The observed values of water vapour at Nainital for 18 days in November/December 1976 range from 2.5 to 4.3 mm (Kulkarni et al. 1977). The theoretical extinction coefficients for 5 mm water vapour are $0^m.10$, $0^m.07$ and $0^m.07$, for Kitt Peak J, H and K filters respectively. The extinction coefficients used in the present calculations (equation 2.6) are in general agreement with the calculations of Manduca and Bell (1979). To minimise the extinction corrections comparison stars, lying within 5 to 10 degrees of program stars, were almost always observed. Further, on most of the occasions both program and comparison stars were observed at zenith angles less than 45°.

The extra-atmosphere magnitudes and colours denoted by the subscript zero were obtained using the equations given below.

$$k_o = k - k_K Z \quad \ldots\ldots \quad (2.7a)$$

$$(j-k)_o = (j-k) - (k_J - k_K) Z \quad \ldots\ldots \quad (2.7b)$$

$$(h-k)_o = (h-k) - (k_H - k_K) Z \quad \ldots\ldots \quad (2.7c)$$

where Z is the zenith angle.

The extra-atmosphere colours and magnitudes in the instrumental system were then transformed to the standard photometric system of Johnson (1966) with the help of following equations (Hardie, 1962).

$$(J-K) = \mu_{JK} (j-k)_o + \zeta_{JK} \quad \ldots\ldots \quad (2.8a)$$

$$(H-K) = \mu_{HK} (h-k)_o + \zeta_{HK} \quad \ldots\ldots \quad (2.8b)$$

$$K = k_o + \varepsilon (J-K) + \zeta_K \quad \ldots\ldots \quad (2.8c)$$

where J, H and K are magnitudes in Johnson system. The scale constants μ's & ε and zero-point constants ζ's were determined with the help of observations of standard stars from the list of Johnson et al. (1966) and they are listed in Table 2.6. The

errors in the observation were estimated by calculating the standard deviation of zero-point constant values determined from standard star observations. The typical errors on most of the nights are $\pm$ $0^m.07$ and $\pm$ $0^m.1$ when seeing was poorer than average. The L band observations were taken only for the selected bright program stars. Because of the limited L band observations transformation to the standard system was not done. The L band fluxes were directly converted to magnitudes with the help of standard star observations.

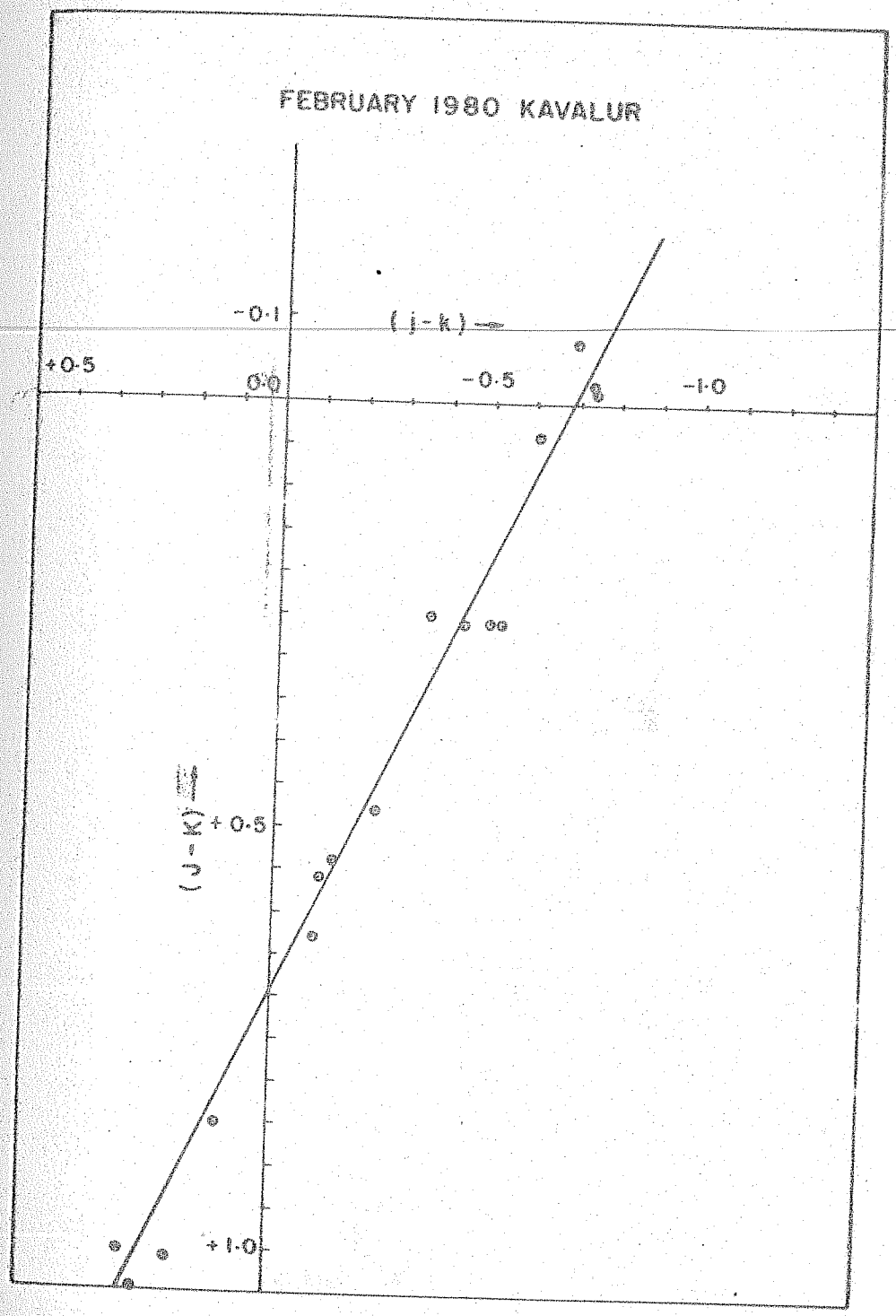

Fig. 2.6a: Transformation curve: $(j-k)_o$ to $(J-K)$.

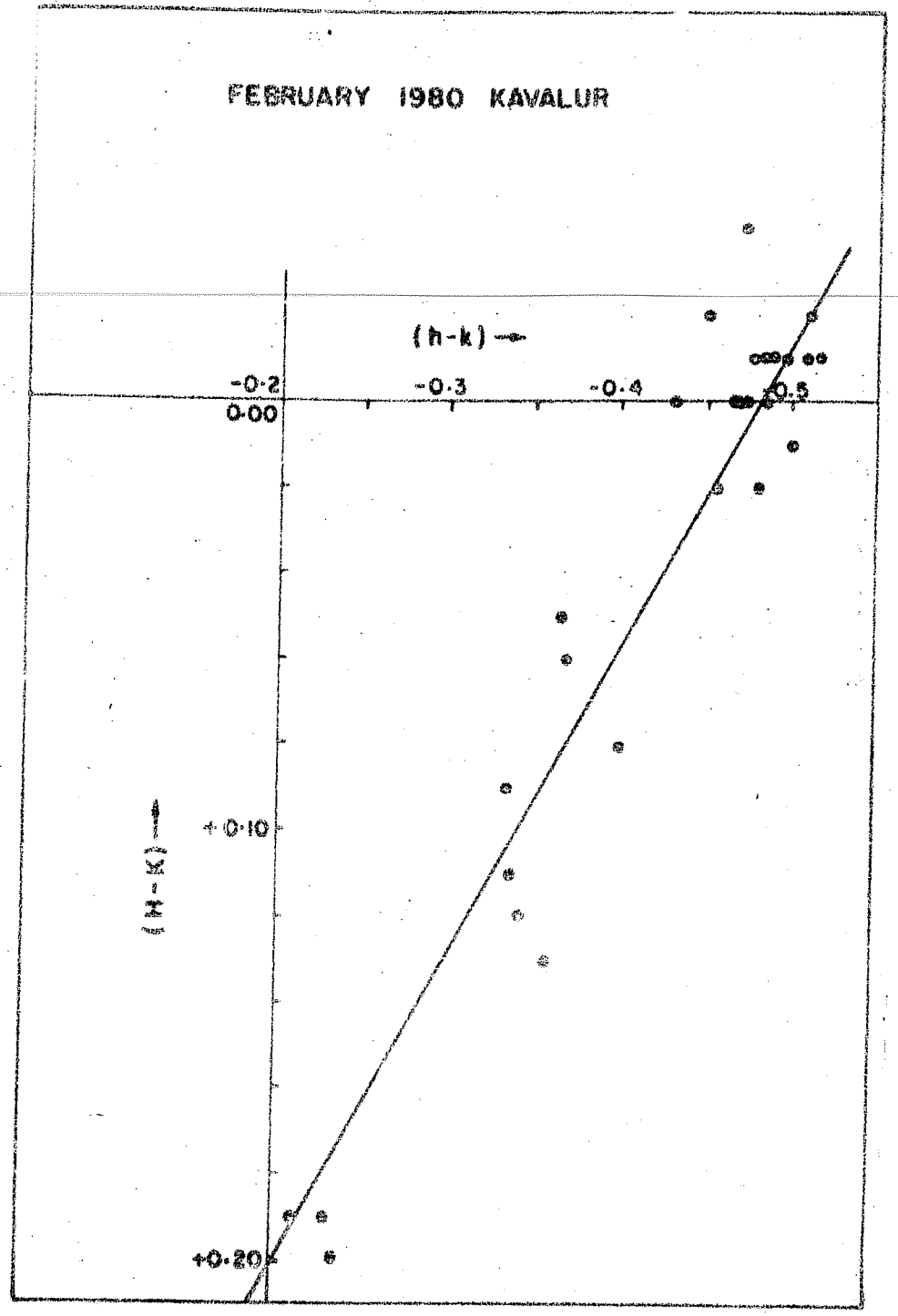

Fig.2.6b : Transformation curve: $(h-k)_o$ to (H-K).

Table 2.6

Transformation Coefficients

Date	Month	Year	Place	μ_{JK}	ζ_{JK}	μ_{HK}	ζ_{HK}	ε_K	ζ_K
16-17	Feb	1980	Kavalur	1.107	0.72	1.076	0.45	-0.155	8.22
18-19	Feb	1980	Kavalur	0.934	0.70	0.866	0.49	-0.130	8.66
23-24	Apr	1980	Nainital	1.036	0.75	0.857	0.43	+0.090	8.93
15-16	Oct	1980	Nainital	0.984	0.70	0.757	0.33	+0.125	8.72
11-12	Jan	1981	Kavalur	0.992	0.69	0.551	0.26	+0.060	8.93
15-16	Feb$^{\$}$	1981	Kavalur	1.056	0.85	0.563	0.29	+0.004	7.51
16-17	Mar	1981	Nainital	1.071	0.76	1.053	0.41	+0.084	9.08

$ observations done with 20" telescope.

CHAPTER III

THE X-RAY RAPID BURSTER MXB 1730-335/LILLER I

3.1 INTRODUCTION

The discovery of celestial X-ray sources has dramatically changed our perception of the nature. The study of these X-ray sources has been extremely rewarding in gathering host of data which possibly explain the physics of some of the exotic objects such as white dwarfs, neutron stars and black holes. The observational evidence indicates that gravitational energy released during the accretion of matter onto a compact object adequately explains the X-ray emission from a large number of these sources (Blumenthal and Tucker, 1974). The galactic binary systems at an appropriate stage in their evolutionary sequence have the necessary physical environment for X-ray emission to originate. With the advent of satellite observatories large number of X-ray sources were detected (Forman et al. 1978; Cooke et al. 1978) and extended observations of individual sources have become available. The modulation collimators have yielded more precise position information of the X-ray sources than that found in the earlier surveys and as a result optical identifications of large number of galactic X-ray sources became possible (Bradt et al. 1979).

The X-ray sources with early type, O or B, optical counterparts emerged as a homogeneous group. Most of the X-ray pulsars (15 out of 19) have OB companion stars. In general this class is known as massive X-ray binaries. The X-ray luminosity of these massive X-ray binaries is quite large, $L_x \sim 10^{34}$ to 10^{38} erg s^{-1} and the ratio L_x/L_{opt} where L_{opt} is the bolometric luminosity, varies from 10^{-4} to $\sim$ 1.

In 1975 December, Grindlay and Heise (1976) discovered an entirely different kind of X-ray source located in the globular cluster NGC 6624, since then known as X-ray burst source. Most of the time this source emits a certain amount of steady X-ray flux and all of a sudden in less than few seconds it literally bursts, attains ten times higher flux level and in the next few tens of seconds it comes down to the original level. The discovery frame of the X-ray burst from NGC 6624 is shown in Fig.3.1. Immediately after this discovery Lewin's group at MIT (Lewin, 1977) and Swank's group at GSFC (Swank, 1976a, 1976b) made impressive contributions to this newly emerged branch by discovering other $\sim$ 20 X-ray burst sources.

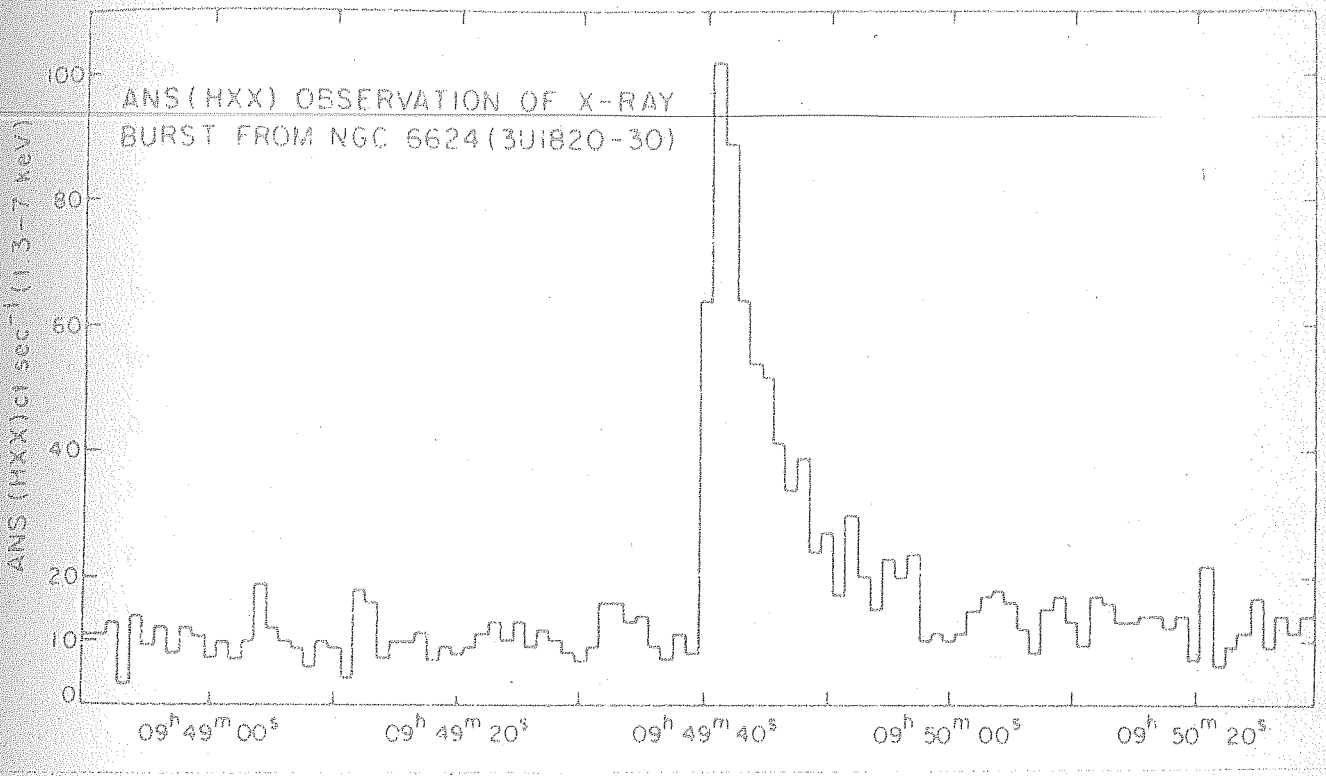

Fig.3.1 : The discovery of X-ray burst. Counting rate from the globular cluster NGC 6624 (3U 1820-30) in 1.3 - 7 keV energy range. This figure is from Grindlay et al. (1976).

At present (1982) the total number of known X-ray burst sources is around 30. Lewin and Joss (1981) have reviewed in detail the properties of the X-ray burst sources. The following paragraphs briefly discuss the general characteristics of the X-ray burst sources.

The X-ray burst sources belong to a group of bright X-ray sources known as galactic bulge sources which are different from the massive X-ray binaries discussed earlier (Lewin, 1980). The galactic bulge sources form a distinct group of bright ($L_x \gtrsim 10^{34}$ erg s^{-1}) X-ray sources. The main distinguishing feature between galactic bulge sources and massive X-ray binaries, that leads to a variety of differing observed properties, seems to be the companion star: low mass late type companion in galactic bulge X-ray sources and early type companion in massive X-ray binaries.

A typical X-ray burst has the following characteristics:

i. Rise time to peak luminosity in less than few seconds.

ii. Maximum luminosity, $L_x \sim 2 \times 10^{38}$ erg s^{-1}.

iii. Decay with time scale of about $\sim$ 10 s.

The range in the recurrence time of the bursts is from few hours to days and individual sources have burst active and quiescent periods.

The early attempts at optically identifying the X-ray burst sources were successful in associating the globular clusters as the seat of these burst sources. It was not possible to pin-point a particular object as the burst source because of the high central stellar densities of the globular clusters. The optical identification of MXB 1735-44 (McClinktock, 1978) was an important observational clue since it is an isolated point source ($V \sim 17^{m}.5$). Subsequently five more burst sources have been optically identified with faint blue objects having stellar appearances (Lewin and Joss, 1981).

The optical spectra of X-ray burst sources consist of smooth continuum with a few emission lines of HeII, OIII, N III and conspicuously lack in normal stellar absorption lines (Canizares et al. 1979). This behaviour closely resembles optical spectra of Sco X-1 and cataclysmic variables at minimum light (Bluementhal and Tucker, 1974). The spectral similarly suggested that the bursters could also be binaries having an accretion disc around the neutron star. Canizares et al. note

that the suspected binary companions are main sequence stars having spectral type later than F0. The direct evidence for binary nature of X-ray bursters was obtained by Walter, White and Swank (1982) who discovered absorption dips recurrent with a 50 min period from 4U 1915-05. White and Swank (1982) attribute this period to the underlying orbital period of the system.

Of the 30 known X-ray burst sources MXB 1730-335 discovered by Lewin et al. (1976a) stands out from the rest by its unique behaviour. It has been very aptly named as the Rapid Burster (RB). Series of X-ray bursts from RB during its active phase in March 1976 are shown in Figure 3.2. When active, the RB emits thousands of bursts in a single day. The availability of large number of bursts from RB has made its detailed studies possible.

Recognition by Hoffmann et al. (1978) that the X-ray bursts from the RB could be classified into two types was a major advancement towards understanding the origin and production mechanism of the X-ray bursts. They classified the X-ray bursts from the RB into type I and type II. The phenomenological classification details are given below.

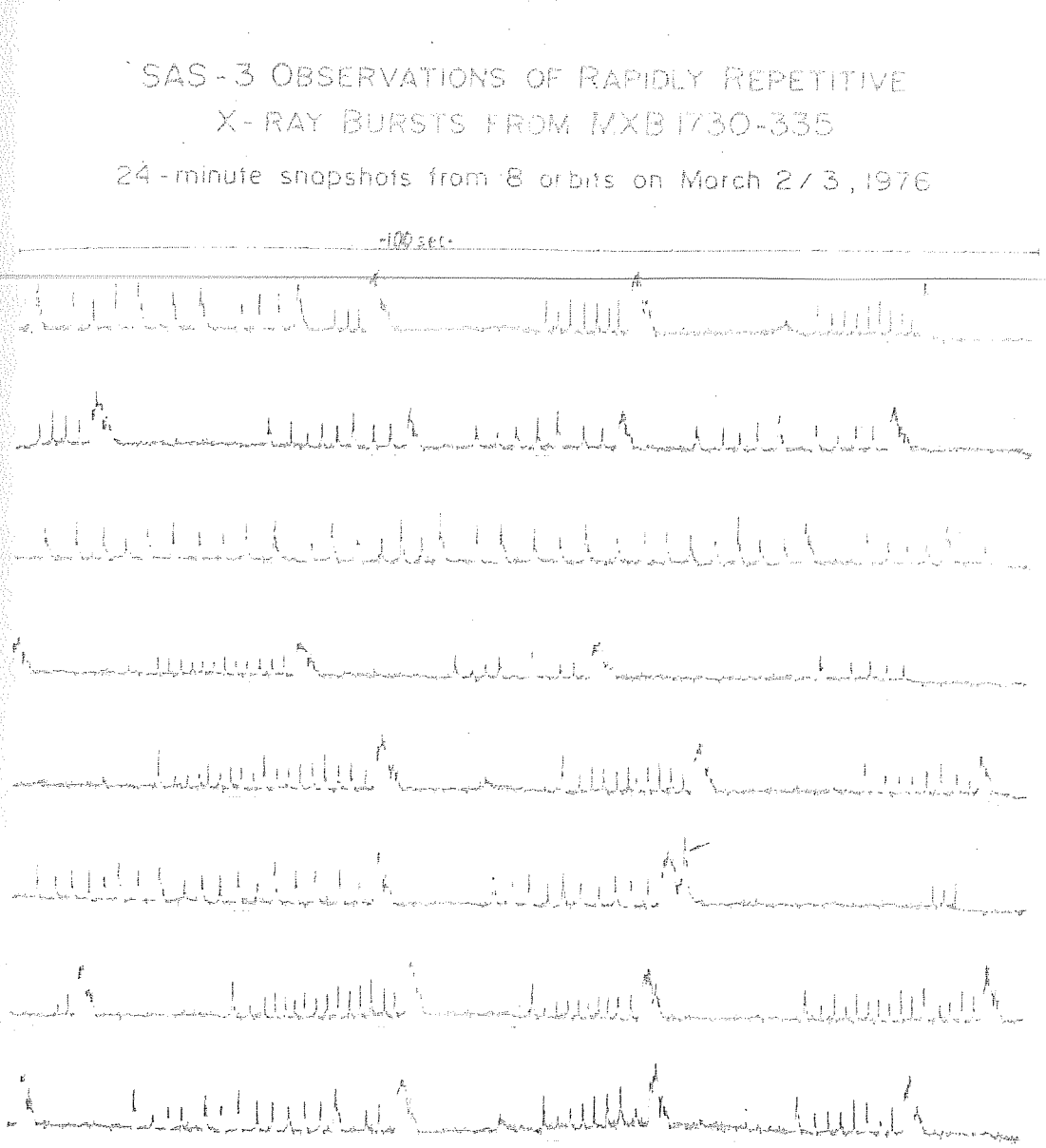

Fig.3.2 : The type II X-ray bursts from the Rapid Burster (MXB 1730-335). The relation between burst energy E, which is proportional to integrated counts in a burst and the waiting period $\triangle t$ for the next burst to occur is apparent. This figure is from Lewin and Joss (1981).

Type I X-ray bursts:

(i) Burst intervals of hours to days (may be even longer)

(ii) Distinct spectral softening during burst decay.

Type II X-ray bursts:

(i) Burst intervals of seconds to minutes.

(ii) No distinct spectral softening during burst decay.

Blackbody spectrum with temperature $T \sim 2 \times 10^7$ K fits reasonably well into the observed X-ray data of type II bursts from the RB and the temperature T of the blackbody remains same all through the burst duration (Hoffmann et al. 1978). On the other hand though blackbody spectrum fits the observed energy distribution of type I bursts from RB and other burst sources, the temperature of the blackbody decreases during the burst decay (Swank et al. 1977; Hoffmann et al. 1978).

3.2 CHARACTERISTICS OF RB

The total energy values of the individual bursts are spread over two orders of magnitude: 10^{36}-10^{38} erg.

The majority of the bursts from RB follow E - $\triangle$t relation where E is the integrated energy of individual burst and $\triangle$t is the waiting period for the next burst to occur i.e. larger is the total burst energy longer will be the time taken by the immediate following burst to make its appearance. However, at the lower end of the range of total burst energy the linear relation ceases to operate and $\triangle$t the waiting period attains a value which is independent of E. Because of reasonably good positional accuracy attained by SAS-3 it was known that the RB is directionally very close to the galactic center. Consequently heavy interstellar obscuration made the optical identification almost impossible. Following the announcement of the discovery of RB, Liller (1976) undertook a photographic program to identify this source. By photographing the region of the sky containing RB at 0.8 μm Liller found a faint, highly reddened, compact extended object. Liller noted that most likely this object is a globular cluster. Kleinmann et al. (1976) using 1-5 μm photometry to overcome stupendous interstellar extinction convincingly showed that the faint object found by Liller, since then known as Liller I, is indeed a globular cluster. By performing multiaperture photometry at 2.2 μm Kleinmann et al. showed that Liller I

is a highly concentrated globular cluster. They also estimated the total visual extinction suffered by Liller I to be $A_v \sim 11$ magnitudes.

After the burst active phase in April 1976 of RB when the discovery was made, it was found that RB became burst active again in April-May 1977 and September 1977. This suggested that RB is a recurrent X-ray source.

Marshall et al. (1979) made detailed study of 10,000 type II bursts from the RB acquired during March-April 1976 and divided them into mode I and mode II, according to their burst energy. When the RB is in mode I, the burst energy ranges from $\sim 5 \times 10^{37}$ erg to $\sim 5 \times 10^{39}$ erg with the burst distribution being bimodal. Majority of the mode I bursts have energies around $\sim 2 \times 10^{38}$ erg while very few have $\sim 4 \times 10^{39}$ erg. During mode II all the bursts have roughly the same energy $\sim 10^{39}$ erg and the spread in energy is only a factor of 10.

Combining 1976, 1977 and 1978 data Marshall et al. (1979) note that RB seems to become burst active about every 6 months with the active phase lasting 2 to 6 weeks. They also suggested that most likely each active period starts with mode I and ends with mode II.

3.3 IR OBSERVATIONAL PROCEDURE

The RB was observed with the InSb photometer during April 1979 and August-September 1979 with the 1 metre reflector at Kavalur. The April observational program was planned to coincide with the expected X-ray burst active period, based on the previous 3 years X-ray data. The August-September program was undertaken after receiving the intimation (Hakucho group) of the beginning of X-ray burst activity of RB. The details of the IR observations are given in Table 3.1.

As mentioned in 3.2 the globular cluster Liller I experiences heavy interstellar extinction and is not seen even on the yellow plate taken with 4 m telescope (Liller, 1977). This means that even though Liller I is reasonably bright at IR wavelengths (Kleinmann et al. 1976) acquisition of the same in the focal plane of the photometer has to be done blindly. The Carl Zeiss reflector at Kavalur has Star Changing Device (SCD) as an accessory. SCD has the capability of manoeuvring the telescope to pre-assigned position from any given reference point. SCD can move the telescope either in Right Ascension (RA) or Declination (Dec.) axis in steps of one second of arc. The relative pointing accuracy of SCD is few seconds of

Table 3.1

Infrared observations of the rapid burster

Date (1979)	Observation time (UT) Begins	Ends	Duration h	m	Remarks
3-4 April	2330	0015	0	45	Monitoring in H band; No bursts.
4-5 April	2130	0010	2	40	Monitoring in H band; 6 bursts.
15 April	2210	2350	1	40	Monitoring in H band. No bursts.
16 April	-	-	-		No observations could be done because of cloudy sky.
18 April	-	-	-		
19-20 April	2315	0015	1	00	Monitoring in K band; Double enhancement observed.
20 April	2205	2350	1	45	Monitoring in H band (50 mins) and in K band (55 mins); No bursts.
21 April	2105	0005	3	00	Monitoring in H band (50 mins) and in K band (2h 10 m); No bursts.
22 April	-	-	-		No obs could be done because of cloudy sky.
23 April	2130 2240	2220 2400	2	10	Monitoring in K band; No bursts.
22 to 26 August 29 August	-	-	-		No obs. because of cloudy sky.
30 August	1415	1545	1	30	Monitoring in J, H and K bands. No bursts.
1 Sept	1445	1555	1	10	Monitoring in J, H and K bands. No bursts.
2-4 Sept.	-	-	-		No obs. because of cloudy sky.

arc for angular telescope movement of few degrees. Using IRC-30317, which is $\sim$ 2.5° east in RA and $\sim$ 0.75° north in Dec. with respect to the RB, as the reference object, the RB was acquired in the photometer beam. Immediately a guide star was obtained in 8" finder telescope by off-setting it and then on, main telescope was guided manually using the finder telescope.

3.4 IR OBSERVATIONS AND DATA ANALYSIS

In the month of April RB rises after mid-night and culminates around 0400 hrs local time at an altitude of 45° at Kavalur. Observations of the RB with its altitude greater than 30° could be taken for about 2 hours in the early morning. Standard star photometry was conducted prior to RB observations.

The InSb photometer described in Chapter II is basically designed for point sources. The largest available aperture is 2 mm which corresponds to $\sim$ 20 seconds of arc on the sky. For all RB observations 2 mm focal plane aperture and 2 mm chopper throw was used. Since Liller I is an extended object (angular diameter $\theta \sim$ 80 seconds of arc) our smaller chopper throw will modify the observed magnitude values of Liller I's steady

emission. However, any variations in the RB contribution to the IR flux of Liller I will be faithfully recorded by our instrument since RB is most likely a point source.

The IR photometer being a single channel instrument, continuous monitoring of any given source can be done in only one waveband at a time. On April 4 and 5, 1979 observations were carried out in the H band. The photometer was looking at the central portion of the globular cluster Liller I with a 20" arc field of view.

3.4:1 Steady IR emission from Liller I:

The flux and magnitude values of Liller I were obtained from the observations of calibration stars. The list of calibration stars used for this purpose and their IR magnitudes are given in Table 3.2. On 1979 April 3/4 and 4/5 continuous observations were taken in H band. During the second set of observations in later part of April 1979 steady IR emission from Liller I was measured in J H and K bands. The observed magnitudes are listed in Table 3.2. Also given in Table 3.2 are the magnitude values of Liller I as reported by Kleinmann et al.(1976). Before comparing our values with those of Kleinmann et al. it is necessary to take into account the differing

Table 3.2

IR Magnitudes of Liller I

SOURCE	FILTER	J	H	K	
Present Work		8.86	7.47	6.53	(a)
		8.32	6.93	5.99	(b)
Kleinmann et al.		8.16	6.41	5.75	
Calibration Stars$					
	HR No.				
	3188	2.82	2.38	2.28	
	3903	2.56	2.12	2.02	
	4550	4.94	4.49	4.38	
	4689	-	3.73	3.75	
	4983	3.24	2.96	2.90	
IRC-30317		1.8	0.85	0.60	

(a) Observed magnitudes with 20 seconds of arc beam diameter (Θ) and chopper throw (d) of 20 seconds of arc.

(b) Magnitudes after correction due to smaller aperture and throw as compared to that of Kleinmann et al.'s values of Θ = 24" and d=90".

$ Magnitude values of calibration stars are taken from Johnson et al. (1966) except for HR 4689 whose magnitude values are taken from CIT Standard star list (Neugebauer, Private communication).

observing conditions in these two cases. Kleinmann et al. observed Liller I with 24 seconds of arc aperture and a chopper throw of 90 seconds of arc where as for our observations both aperture size and chopper throw were 20 seconds of arc. Taking the 2.2 μm flux dependance on the beam size as given by Kleinmann et al. we estimated the correction to be applied for our observations due to the smaller aperture and smaller throw, as $\triangle m_K = 0.54$. The corrected magnitudes are also listed in Table 3.2. It is seen from Table 3.2 that after necessary correction our J andK magnitudes agree within experimental errors with those of Kleinmann et al. However, the reasons for H magnitude difference ($\sim 0^m.5$)is not clear .

3.4:2 Detection of IR bursts:

On the night of 4/5 April 1979 we detected six bursts during 2 hours and 40 minutes of observation time. During the observations the zenith angle of RB varied between 54° and 47°. We have not applied extinction corrections to the observations because of the proximity (2.5° E and $0^\circ.75$ N of the RB) of calibration source IRC-30317 and not too large zenith angles. Time was manually marked at regular intervals on the paper

chart roll using event marker facility to an accuracy of about 1 second. The chart speed during continuous monitoring was 20 mm min^{-1}. Taking into consideration these factors, the time accuracy in reading the data is about 2 seconds.

The profiles of all the 6 bursts observed on 4/5 April 1979 are shown in Fig.3.3. These burst events are labelled from 1 to 6. It should be noted that the burst number 6 has a composite structure and the two components are designated 'a' and 'b'. The individual characteristics are separately listed for these two components in Table 3.3.

The peak flux is derived by comparing IR burst observations with measurements of standard stars on the same night. The integrated burst flux is estimated by measuring the area enclosed by burst profiles. Interstellar extinction correction at 1.65 μm is obtained on the basis of $1/\lambda$ dependance for the interstellar extinction. One gets $A_H = 1.47$ for the adopted value of $A_K = 1.1$ (Kleinmann et al. 1976). For calculating peak luminosity and total energy of the IR bursts distance of the RB and the source geometry are required. Assuming isotropic radiation and a distance of 10 kpc (Kleinmann et al. 1976), peak luminosity L^p_{IR} and total burst energy E_{IR} for each burst are calculated using Eqns 3.1 and 3.2.

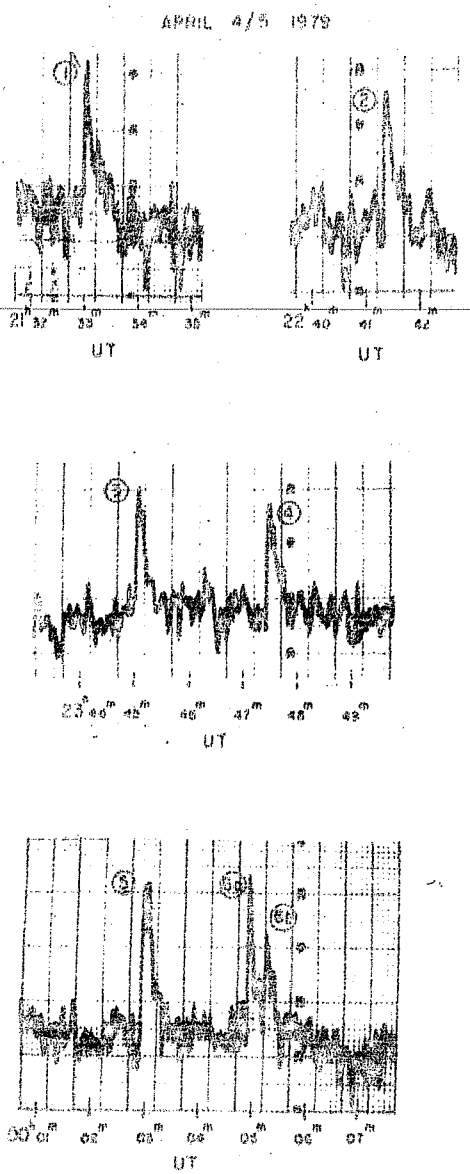

Fig.3.3: Profiles of 6 IR (1.6 μm) bursts from the Rapid Burster (MXB 1730-335). Note the composite structure of burst number 6; the two components are designated a and b.

Table 3.3

IR bursts from Liller I/MXB 1730-335

Burst No.	Time of occurrence (UT)	Rise time (s)	Duration (s)	FWHM (s)	Peak luminosity (10^{37} erg s^{-1} in 0.3 μm interval at 1.6 μm)	Burst energy (10^{38} erg in 0.3 μm interval at 1.6 μm)
1	$21^h33^m00^s$	2	37	12	2.2	3.0
2	22 41 24	2	36	12	1.9	2.0
3	23 45 06	3	36	12	2.0	2.6
4	23 47 30	3	24	9	1.7	1.5
5	00 03 00	2	36	10	2.2	2.5
6a	00 04 54	2	20	6	2.3	1.7
6b	00 05 12	2	19	6	1.6	0.9

$$L_{IR}^{p} = 4\pi d^2 \; F_{IR}^{p} \qquad \ldots\ldots \quad (3.1)$$

$$E_{IR} = 4\pi d^2 \int F_{IR}(t)\, dt \qquad \ldots\ldots \quad (3.2)$$

where d is the distance and $F_{IR}(t)$ the flux at time t.

The details of the time of occurrence, rise time, duration, full width at half maximum (FWHM), peak luminosity and burst energy are listed in Table 3.3. Inspection of Table 3.3 reveals that all the characteristics of IR bursts have a close similarity with each other and are in general phenomenologically similar to the X-ray bursts. The salient features of these bursts are listed below.

1. A total of 6 bursts during $\sim$ 160 minutes of observation at 1.6 μm.
2. The rise to the maximum is fast $\sim$ 2-3 s, followed by a slow, almost exponential decay in next $\sim$ 30 seconds.
3. The average peak luminosity is $\sim 2 \times 10^{37}$ erg s^{-1} and the average total burst energy is $\sim 2.4 \times 10^{38}$ erg in a bandwidth of 0.3 μm centered at 1.6 μm.

3.4:3 Detection of Double enhancement:

After two nights observations on 3/4 and 4/5 April, extended monitoring of RB was carried out from 15 to 23 April and 22 August to 4 September 1979. The observational set up was identical to that of April first week. The duration and times of the observation are listed in Table 3.1. During April observations comprising of 9.5 observational hours, no bursts were detected either in H or K band. However, on one occasion, 19th April 1979, a double enhancement of flux in K band was observed. The temporal characteristics of these enhancements do not resemble those of the IR bursts detected on 4/5 April 1979. The profiles of the enhancements are shown in Fig.3.4 and have been labelled as A and B; the details are given in Table 3.4. The second enhancement occurs immediately after the first one. The profiles are symmetric about the peak value. A correction of $A_K = 1.1$ due to interstellar extinction (Kleinmann et al. 1976) has been applied while calculating the burst energy. It is interesting to note that the energy contained in the enhancements is of the same order as the average burst energy of the H band bursts of 4/5 April 1979.

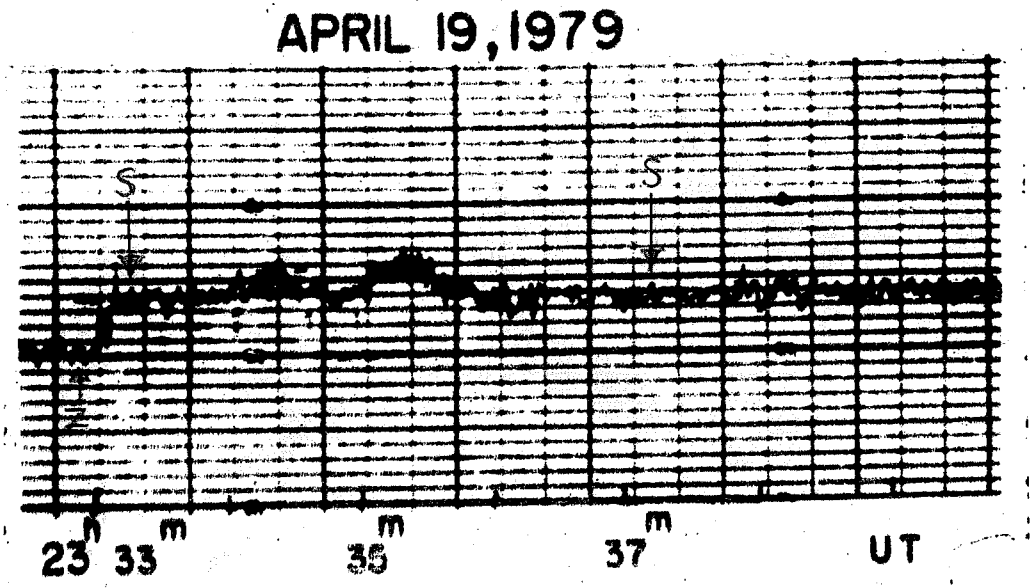

Fig.3.4 : Profile of double enhancement in K band (2.2 μm) from the Rapid Burster (MXB 1730-335). The steady flux level from Liller I is marked as S and from nearby blank sky as Z.

Table 3.4

Characteristics of double enhancement in K band of MXB 1730-335, on 19-20 April 1979.

Event	Time of occurrence of peak (U.T.)	Duration (s)	Peak luminosity in 0.4 μm bandwith erg s^{-1}	Total energy in 0.4 μm band-width erg
A	$23^h34^m20^s$	30 s	1.83 E 37	2.75 E 38
B	$23^h35^m20^s$	46 s	2.14 E 37	4.82 E 38

Note : " E XX $\equiv 10^{XX}$ "

During August/September 1979 most of the time during 12 observational nights cloudy weather prevailed and we could observe the RB for only 2 hours 40 minutes. No increases exceeding the system noise were observed.

3.5 DISCUSSION

The general characteristics of IR bursts observed by us, except for the rate of occurrence, closely resemble those of the X-ray bursts. However, in absence of simultaneous X-ray coverage of RB during our observations, definite association of the IR bursts with X-ray bursts can not be ascertained. For the present discussion we will assume that the observed IR bursts originate from the RB and make an attempt to develop a scenario that explains the observed facts.

As mentioned in Section 3.2 X-ray bursts from the RB are classified into type I and type II depending on their spectral behaviour and also on the recurrence time of bursts.

As the IR photometer used for our observation was a single channel instrument no spectral information on bursts is available. As the occurrence time of type I

bursts is between an hour and a few days, the 6 observed bursts in $2\frac{1}{2}$ hours could not be associated with type I bursts. Thus if the IR bursts have to be related to the RB X-ray burst activity, a possible association can be done with type II X-ray bursts. However, there may not be one to one correspondence between the IR and type II X-ray bursts from the RB. The recurrence time for type II X-ray bursts is few tens of seconds to minutes. Before proceeding further let us see the constraints put by the IR observations for the IR emission region and emission mechanism.

To explain the characteristics of IR burst emission mechanism the brightness temperature has been calculated. At the infrared wavelengths the blackbody spectrum can be represented by Rayleigh - Jeans distribution. Then the surface brightness of the source $I(\lambda)$ which is the flux emitted normal to the surface per unit solid angle, area and time, at a wavelength λ can be written as

$$I(\lambda) = 2\ kc\ T_b(\lambda)\ \lambda^{-4}\ \text{erg}\ s^{-1}\ cm^{-2}\ sr^{-1}\ cm^{-1} \quad \ldots\ldots (3.3)$$

where k is the Boltzman constant,

c is the velocity of light and

$T_b(\lambda)$ is the brightness temperature.

From the observed peak luminosity, L^p, the surface brightness can be calculated knowing the total emitting area. The 2 to 3 seconds rise time of IR bursts suggests that a major portion of the IR burst emission would be originating in a region having linear dimensions less than 3 light seconds. Substituting the average observed value of $L^p = 2 \times 10^{37}$ erg s^{-1} and noting that this is for a bandwidth of 0.3 μm at 1.6 μm one gets

$$I\ (1.6\ \mu m) = 2.09 \times 10^{18}\ erg\ s^{-1}\ cm^{-2}\ sr^{-1}\ cm^{-1}$$

From equation (3.3) the brightness temperature is obtained as

$$T_b\ (1.6\ \mu m) = 1.65 \times 10^{8}\ K$$

Blackbody spectrum with $T \sim 2 \times 10^7$ K fits into the energy distribution of typical type II X-ray burst. The high value of T_b implies that the IR burst radiation is nonthermal in origin. If the IR radiation

were to be thermal in its origin then the X-radiation from blackbody with $T_b = 1.65 \times 10^8$ K will greatly exceed the observed value.

For type II X-ray bursts from the RB, in mode I the burst energy ranges from 5×10^{37} to 5×10^{39} erg while in mode II the average value of burst energy is $\sim 8 \times 10^{38}$ erg. The average IR burst energy is $\sim 2 \times 10^{38}$ erg. It is important to note that this IR burst energy has the contribution from only 0.3 μm wavelength interval at 1.6 μm. This shows that the IR burst energy is more or less comparable to X-ray burst energy and this is quite different from the case of optical bursts from X-ray burst sources. For the 3 burst sources from which simultaneous X-ray and optical bursts have been detected, the ratios of observed optical to X-ray energy fluxes corrected for interstellar extinction for both persistent emission and bursts are listed in Table 3.5.

Table 3.5+

Source	Eopt/Ex Persistent	Eopt/Ex Burst	Reference
MXB 1735-44	4×10^{-4}	6×10^{-5}	Grindlay et al.(1978)
MXB 1837+05	9×10^{-4}	1×10^{-4}	Hackwell et al.(1979)
MXB 1636-53	4.5×10^{-3}	1.2×10^{-3}	Pedersen et al.(1982)

+ Taken from Lewin and Joss (1981)

It is seen from Table 3.5 that optical burst energy is a small fraction of the X-ray burst energy : $\sim 10^{-4}$ for MXB 1735-44 and MXB 1837+05 and $\sim 10^{-3}$ for MXB 1636-53. Grindlay et al. (1978) note that most likely the optical burst emission arises as a result of reprocessing of part of the X-ray burst flux in the surroundings of the X-ray burst source. Hackwell et al. (1979) from their observations of simultaneous optical and X-ray bursts from MXB 1837+05, arrive at a similar conclusion that a region with 1-2 light seconds linear extent situated 1-2 light seconds from the X-ray burst source is responsible for the major part of the observed optical burst emission. They conjecture that this

emitting region could be either an accretion disc or the photosphere of a companion star.. The reprocessing of X-rays in surroundings of the burst source cannot explain the occurrence of IR bursts from the RB since the observed energies of IR bursts are comparable to X-ray burst energies.

The present status of the models of X-ray bursts has been reviewed by Lewin and Joss (1981). All the proposed models consist of a compact object and can be broadly classified into two groups: (i) a system intermittently releasing gravitational energy acquired during the accretion of matter onto a compact object (Baan 1976, 1979; Lamb et al. 1977) and (ii) run-away nuclear fusion of the accreted material on the surface of a neutron star (Woosley and Taam, 1976; Maraschi and Cavaliere, 1977). Till 1978 these two were competing theories. In 1978 when Hoffmann et al. recognised that the X-ray bursts could be classified into 2 types it appeared that both kinds of models could be correct, with one of the two possibly explaining type I bursts and the other type II bursts. Detailed numerical calculations of the nuclear flash model by different groups (Joss 1977, 1978, 1979; Taam 1980; Fujimoto et al. 1981; Wallace& Woosley,1981) have

reproduced a large number of observed features of type I X-ray bursts like, the typical burst rise times, decay time scales, peak luminosities, total emitted energies, spectral properties, recurrence intervals which come out to be a few hours which holds true in most of the cases. However, for only a few systems some difficulties still exist with these models, for e.g. regarding the observations of repeated type I bursts within minutes from MXB 1743-28 (Lewin et al. 1976b) and 4U1608-52 (Murakami et al. 1980).

In the accretion models the inflow of matter needs to be modulated to reproduce the temporal characteristics of X-ray bursts. As pointed out by Lamb et al. (1977) the rise time of the X-ray bursts gives a clue about the location of the region where instability takes place. Rise times of 0.1 to 1 second require that the instability zone lie within a distance of 10^8-10^9 cm from the centre of a compact object. The magnetosphere radius R is given by (Vasyliunas, 1979)

$$\frac{R}{R_x} = 2.9 \times 10^2 \left(\frac{B_x}{10^{12} G} \right)^{4/7} \left(\frac{R_x}{10^6 \text{ cm}} \right)^{3/7} \left(\frac{M_x}{M_\odot} \right)^{1/7} \left(\frac{10^{37} \text{ erg s}^{-1}}{L} \right)^{2/7} \quad \ldots (3.4)$$

where R_x , M_x and B_x are the radius, mass and surface magnetic field of the compact object & L is the luminosity resulting from gravitational accretion of matter.

Hence the magnetosphere presents itself as a potential candidate since its radius not only matches the required positioning of the instability zone but also provides a gating mechanism for the flow of material towards the compact object. As a result various investigators have considered instabilities at the magnetopause of compact objects. Lamb et al. (1977) have considered spherically symmetric flow of matter onto the magnetopause of the compact object. They show that such a situation under certain conditions results in Rayleigh-Taylor instabilities and makes the magnetosphere unstable. This leads to burst-type behaviour. The effect of rotation of the neutron star on the instabilities taking place at magnetopause has been considered by Svestka (1976), Henriksen (1976), Baan (1979) and Joss and Rappaport (1977). For the RB, Baan (1979) has shown that Rayleigh-Taylor instabilities at the magnetopause of an accreting and rotating neutron star result in burst energy histogram that qualitatively matches with the observed one. He also shows that low values of

accretion rate, $\dot{M}$, leads to the bursting behaviour while higher values of $\dot{M}$ result in steady X-ray emission.

Apparao and Chitre (1980) have suggested electron cyclotron maser instability operating at a few tens of neutron star radii above the poles of a magnetised neutron star in a binary system which results in the infrared emission. The electrons acquire the necessary energy from protons. Further they adopt a model in which instability in the accretion flow gives rise to type I X-ray bursts as well as IR burst. Their suggestion is based on the assumption that IR burst radiation is coherent since the brightness temperature inferred is very large ($T_b \sim 10^{16}$ K). However, the large brightness temperature only suggests that the radiation is non-thermal and not necessarily coherent. Also as discussed at the beginning of the present sub-section (3.5) the association of IR bursts with type I X-ray bursts is unlikely because of the discrepancy in recurrence rate.

Presently, nuclear flash model is generally accepted for type I X-ray bursts as it successfully reproduces most of the observed features. Simultaneous observations of X-ray and IR bursts fished out from 1977 data by Lewin et al. (1980) showed that

MXB 1837+05 (Ser X-1) did not produce bright IR bursts simultaneously with the type I X-ray bursts. This goes against Apparao and Chitre's prediction that IR bursts should be in general observable from type I X-ray burst sources.

The occurrence of only 6 IR bursts during two and half hours suggests that the necessary conditions to be fulfilled for IR bursts to occur are very stringent. It appears that whenever the accreting material succeeds in reaching the neutron star surface, on most of the occasions the gravitational potential energy acquired is emitted as an X-ray burst. So all type II X-ray bursts are not accompanied by IR bursts.

Following our April 1979 observations, on 5th September 1979, IR group of Imperial College, London, detected 2 IR bursts from the RB at 2.2 μm during 5^h15^m of observation (Jones et al. 1980). The profiles of these bursts are shown in Fig.3.5 & they are similar to those of ours. An additional feature is the presence of 3 highly narrow spikes superimposed on each of the 2 bursts. Again there was no simultaneous X-ray coverage. However, the occurrence of only 2 bursts during 5^h15^m of observation time once again suggests

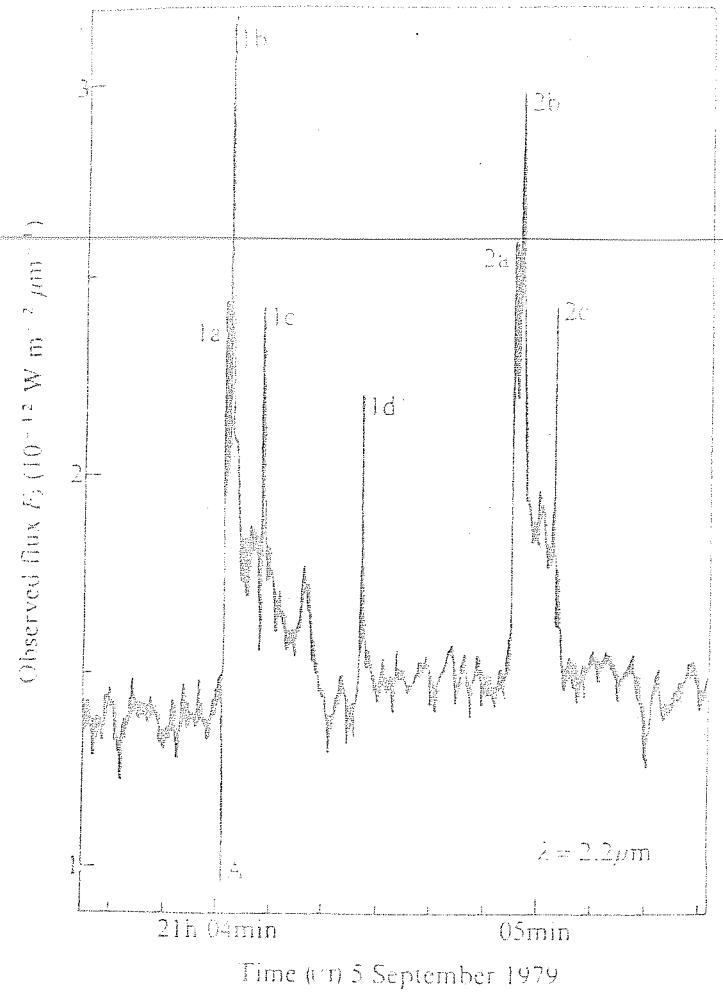

Fig.3.5 : Profiles of two IR (2.2 μm) bursts from the Rapid Burster (MXB 1730-335). Note the presence of 7 brief flashes. The flux scale is not corrected for interstellar absorption. This figure is from Jones et al. (1980).

that IR bursts may not have one to one association with type II X-ray bursts.

During the burst active period of the RB in August 1979 (Inoue et al. 1980), observation times of two groups (Sato et al. 1980; Lawrence, 1982) that have acquired IR data, overlap with the Hakucho X-ray observations. Sato et al. monitored the RB simultaneously in 4 bands viz., I, H, K and L using a multicolour photometer. They have observations lasting 6^h12^m spread over 9, 11 and 12 August 1979. There is one instance of the occurrence of X-ray burst during 6^h12^m of IR observations. However, in none of the 4 IR channels any increase associated with the X-ray burst was seen. The X-ray data is available for the onset and first 126s of the burst duration only, since the X-ray observations were later interrupted. It is worth noting that at the time of this IR observation the RB's X-ray bursting pattern was unusual and very different than the previously observed behaviour. From 8 to 16 August 1979 the RB was emitting trapezoidal X-ray bursts (Inoue et al. 1980).

Glass and Carter (Lawrence et al. 1982) have also obtained IR observations of the RB during its August 1979 active period. They monitored the RB at 2.2 μm on

16 and 21 August (total duration not specified) and did not detect any IR bursts. The upper limit to the IR burst flux is 0.26 Jy. However, on 8 occasions - once on 16 August and 7 times on 21 August 1979 - Hakucho detected type II X-ray bursts from the RB. The 7 bursts on 21 August occur within 1 hr 30 min. The rapid burster after its initial unusual behaviour had started emitting type II X-ray bursts from 16 August.

All IR observations of the RB discussed till now suggest that the necessary conditions for the occurrence of IR bursts are indeed very stringent and only occasionally they are satisfied. The absence of IR bursts accompanying X-ray bursts (Sato et al. 1980; Lawrence et al. 1982) on 9 occasions indicates that all X-ray bursts are not accompanied by IR bursts. On the other hand whether IR bursts from the RB are accompanied by X-ray bursts is not certain because of the non-availability of X-ray data at the time of IR bursts.

We try to explain the mechanism of IR burst emission by adopting a low mass binary system where in the magnetised neutron star is accreting matter lost from the late type companion. No attempt is made to work out the details of instabilities that possibly give rise

to burst type behaviour. Only the possibility of IR emission in the assumed model is suggested.

Cyclotron emission is likely to occur in the surroundings of a highly magnetised neutron star. The largest IR burst energy suggests that emission region is close to the neutron star surface. Assuming dipole field and a value of 10^{12} Gauss for the surface magnetic field of a neutron star, we rule out electron-cyclotron emission mechanism since the corresponding frequency near the surface of the neutron star will then lie in X-ray region.

We propose that proton-cyclotron emission mechanism operating near the neutron star surface is responsible for the IR bursts. For the emission to appear at 1.6 μm the required magnetic field can be calculated as follows:

The cyclotron angular frequency is given by (Tucker, 1975)

$$\omega = \frac{Ze\ B}{mc} \text{ radian } s^{-1} \qquad \ldots\ (3.5)$$

where Ze is the charge of the particle

B is the magnetic field

and m is the mass of the particle.

$\lambda = 1.65\ \mu$m corresponds to $\omega \simeq 1.14 \times 10^{15}$ rad sec^{-1}. Substituting this value of ω , . Ze and m values appropriate for proton, one obtains

$$B \simeq 1.2 \times 10^{11}\ G$$

The neutron star magnetic field is given as

$$B_X(R) = B_X \left(\frac{R_X}{R} \right)^3 \qquad \ldots\ (3.6)$$

where

$B_X(R)$ is the magnetic field at a distance R,

B_X the surface magnetic field, and R_X the radius of neutron star.

Hence if $B_X = 10^{12}$ G, at a distance $R \simeq 2\ R_X$ the magnetic field value is such that the proton cyclotron frequency matches $\lambda = 1.65\ \mu$m.

Now the proton-cyclotron emission will be radiated only if the following conditions are satisfied.

(1) Protons should emit the energy by cyclotron process before transfering their energy to electrons by collisions.

(2) The medium through which the cyclotron radiation has to traverse should be optically thin.

(3) The plasma frequency should be less than the radiation frequency.

On most of the occasions when the accreted material reaches the neutron star surface, the conditions there might be such that all the 3 above mentioned conditions are not simultaneously fulfilled. As a result all type II X-ray bursts need not be accompanied by IR bursts.

To understand the nature of IR bursts an extensive world-wide campaign was carried out in 1980 (Lawrence et al. 1982). X-ray observations from Hakucho were taken from 14 to 21 April 1980 and 14 July to 26 September 1980. During the same period, May to September 1980, IR observations were obtained by different groups. Neither X-ray nor IR bursts were detected. Therefore no conclusion regarding simultaneous occurrence of IR and X-ray bursts could be drawn in this campaign. The RB appears to have decided not to divulge any more clues by not becoming X-ray active in 1981 and 1982 (till June).

More simultaneous IR and X-ray observations of the RB are necessary to understand the nature of IR bursts and their relationship with X-ray bursts.

CHAPTER IV

THE Be STARS

4.1 INTRODUCTION

The discovery of emission line B type stars was an outcome of attempts to systematically classify the stellar spectra. Angelo Secchi in 1866 noticed that Hα was in emission in the spectra of γ Cas. The first systematic observational studies of emission line stars was undertaken by R.H.Curtiss in 1911. P.W.Merrill, D.B.McLaughlin, O.Struve and others continued this program and their work resulted in the first catalogue (Merrill and Burwell,1933) of emission line stars.

The spectra of Be stars consist of continuous energy distribution alongwith the usual absorption lines of hydrogen, helium and other atoms as in normal B type stars. In addition, bright emission lines of hydrogen are superposed on the first few members of the Balmer series. The emission disappears in the higher members of Balmer series, usually at H8 to H15, and the remaining Balmer lines are in absorption as in the normal B type stars. The Balmer absorption lines in B as well as Be stars disappear beyond H16 to H20. The absorption lines broaden due to Stark effect. They start overlapping and

result in a continuum beyond a certain member of Balmer series. The absorption lines of Be and normal B type stars, however, differ in one respect. The absorption lines are broader and shallower in Be stars than in normal B type stars. There is an interesting relationship associated with the broadening of absorption lines in Be stars. In 1931, Struve first pointed out that the widths of the absorption lines are proportional to the widths of emission lines. In some Be stars the lines of FeII, Ti II and Si II show up in emission (Jascheck et al. 1980).

Some Be stars show shell lines in addition to the hydrogen emission lines of Balmer series. The shell lines manifest themselves as sharp and deep absorption cores. The shell absorption cores are superposed on the emission lines in the case of hydrogen and on normal stellar absorption lines for ionised metals like FeII, Cr II, etc. It has been recognised now, that the orientation of the rotational axis of the star with respect to the observer decides whether the stellar spectrum will contain shell lines or not. Only when the rotational axis is either normal or very close to normal to the observer, the shell lines will be present in the observed spectrum.

4.2 CHARACTERISTICS OF Be STARS

In literature various investigators have used the word 'Be star' meaning some what different things. To avoid ambiguity we adopt the following definitions of Be and B type shell stars as recommended at I.A.U. Symposium No.98 (1981) at Munich, Germany (Jaschek et al. 1981).

Be Star

"A non-supergiant B type star whose spectrum has or had at some time, one or more hydrogen lines in emission" and

B-type shell star:

"A Be star whose spectrum is characterised by the simultaneous presence of (a) broad absorption lines and (b) sharp absorption lines which arise from ground states or metastable levels".

Since their discovery in 1866, Be stars have attracted the attention of many observational astronomers and a lot of data has been collected. Some of the salient features of Be stars in optical region are summarised below.

4.2:1 Spectral type and luminosity class:

The frequency distribution of Be stars by spectral type shows two maxima, one around B2 (Mendoza 1958) and the other at B8 (Jascheck et al. 1980). The minimum is around B5. On the other hand the frequency of normal B type stars increases monotonically towards later spectral type.

By definition, the Be stars are confined to the luminosity classes III to V.

The early photometric studies of Be stars by Mendoza (1958) suggested that, on an average they have $M_V = -3.^m6$ and are thus about 1 magnitude above the zero age main sequence in the H-R diagram. However, the recent studies (Abt and Levato, 1977) indicate that some Be stars can also occupy the region of zero age main sequence.

4.2:2 Rotation and Polarisation:

As recognised by Struve in 1931 Be stars, as a class, are rapid rotators; while the average rotational velocity of Be stars is $\sim$ 200 km s^{-1} (Allen, 1976), the maximum rotational velocity observed for Be stars

is as high as $\sim$ 420 km s^{-1} (Slettebak, 1976). The frequency distribution of rotational velocities ($v \sin i$) of Be stars shows a maximum at about 300 km s^{-1} (Slettebak, 1979). With the availability of good quality spectroscopic data and improved stellar atmosphere models, the initial picture of a Be star rotating at critical velocity is slightly modified. According to the present picture Be stars are most likely rotating close to but not at break-up velocities.

Of the observed $\sim$ 70 Be stars about 50% show intrinsic polarisation, the average value being $\sim$ 0.9% (McLean and Brown, 1978; Poeckert et al. 1979). The peculiar characteristics of the wide and intermediate band polarimetry in the visual region of the spectra are (Coyne and Kruszewski, 1969; Serkowski, 1970) (i) a more rapid decrease in the polarisation towards the UV region of the spectrum compared to the interstellar polarisation curve and (ii) a minimum polarisation just to the blue side of the Paschen limit. An interesting recent development has been the detection of changes in the polarisation across the emission lines (Clarke and McLean, 1974; Poeckert, 1975). As compared to the nearby continuum the polarisation in the wings of emission

lines is less and at the line center the polarisation increases in comparison to polarisation of the wings but is still less than nearby continuum polarisation (McLean et al. 1979).

4.2:3 Variability:

The Be stars have shown spectroscopic, photometric and polarimetric variations ranging over wide time scales. So it is convenient to classify these variations into two main groups as (a) long term and (b) short term and rapid.

(a) Long term - time scale of years:

Quite understandably all the initial investigations of Be stars were spectroscopic in nature and these studies showed that the emission lines exhibit impressive variability. McLaughlin, based on a systematic variability study of Be stars found out the following details (Hack and Struve, 1970). The emission line strengths change drastically; this is known as E/C variation where E refers to the emission lines and C to the nearby continuum. Certain Be stars develop strong emission components over different intervals of time and also at

times no trace of emission is present and what was once a prominent Be star looks like an ordinary B type star. As noted earlier (4.1) in many cases the emission line is split into two components. The ratio of intensity of the "violet" to the "red" component changes and this is called V/R variation. Normally V/R variation consists of a change in relative intensities of individual components, with the total emission line intensity remaining more or less the same. Usually either V/R or R/V ratio does not exceed 3. Yet another manifestation of spectroscopic variability of Be stars is the occasional appearance and disappearance of "shell" absorption lines. It should be noted that these three kinds of spectroscopic variations are not mutually exclusive.

Similarly considering the photometric observations of Be stars in UBV bands spread over 16 years, Feinstein and Marraco (1980) have found out that about 70% of them vary in V and (U-B) and 50% in (B-V). Also most of these variations are of long term character and often more during the shell activity. The maximum amplitude of variation in V is $\sim 0^{m}.15$.

Though there are limited repeated polarimetric observations of Be stars available, the existing data

demonstrate the presence of changes in polarisation with time scales of some hundreds of days (Coyne, 1976). Since the existing observations are non-uniformly scattered in time it is not possible to make periodicity studies. On an average the change in amplitude of polarisation (Δp) is $\sim$ 40% of the mean value of polarisation. However, in the case of Z CMa and p Car the amplitudes of the changes in polarisation are larger than mean polarisation itself (Serkowski, 1970). In the case of o And polarisation and spectroscopic changes appear to be correlated (Poeckert et al. 1979).

(b) Short term and Rapid variability:

The spectra of Be stars also change on a time scale of months and days (Slettebak and Reynolds, 1978). The changes may occur either in Hα equivalent width or line profile. Going further down the time scale, the evidence for changes is some what conflicting. Many irregular night to night or even hourly changes have been reported for various Be stars (Doazan, 1976; Bahng, 1976), but are not extensively discussed and interpreted. Simultaneous measurements with independent telescopes and recording systems are necessary to confirm the existence of rapid variations.

Extended photometric data also show evidence of short time scale - months and days - variability.

The percentage polarisation of the Be stars also changes over an interval of few tens of minutes to days. A change of $\Delta p = 0.3$, within 24 hours has been measured for ζ Tau by Poeckert (1975). Clarke and McLean (1976) have reported for ζ Tau a change of $\Delta p \sim 0.2$ over an interval of 40 minutes in the continuum at $\sim$ 4837 Å.

4.3 REVIEW OF PREVIOUS IR OBSERVATIONS

Johnson (1967) first pointed out the fact that the IR emission from Be stars exhibits excesses and attributed the (K-L) excesses observed for these stars to IR emission from the circumstellar shells. Woolf et al. (1970) extended the observations to 11.5 μm and noted that for the excess IR radiation, in most cases, the thermal free-free radiation fits the data quite well. Allen (1973) from his observations of a large sample of Be stars showed that the IR excess is a general feature of these stars. However, because of limited spectral coverage Allen's data could not distinguish between thermal re-radiation from the circumstellar dust and free-free emission originating in ionized circumstellar shell..

From their observations covering a spectral range from 2.3 μm to 19.5 μm Gehrz et al. (1974) found out that Be stars have a smooth energy distribution devoid of emission features at 10 & 20 μm. The presence of these features (10 & 20 μm) is taken as a strong evidence of the circumstellar dust shells (Woolf and Ney, 1969; Becklin and Westphal, 1966; Low and Krishnaswamy, 1970). So Gehrz et al. ruled out circumstellar dust emission in Be stars and concluded that free-free emission from a hot circumstellar plasma shell is the most likely source of the excess IR radiation of Be stars.

Next advancement that helped in deciding the emission mechanism responsible for the observed IR excess in Be stars was done by Scargle et al. (1978) who obtained spectrophotometric observations of γ Cas. The observations were done with Kuiper Airborne Observatory and spectral scanning was accomplished by a continuously variable filter having 1% resolution and operating in the region 1.2 to 4.1 μm. The availability of large number of data points, compared to broad band photometry, allowed a detailed spectral fitting to be done. Scargle et al. concluded that in the case of γ Cas the IR excess is almost entirely due to the free-free plus

bound-free emission from a shell of gas at $T_s \sim 18,000$ K and with optical depth $\tau \sim 0.5$ at 1 μm.

As described in 4.2.2 the radiation from Be stars is polarised. The theoretical models attribute this polarisation to the existence of an asymmetric envelope around a Be star. The electron scattering in the envelope that is mainly confined to the equatorial region polarises the radiation of the central star. However, electron scattering being independent of wavelength cannot explain the observed wavelength dependance of polarisation mentioned earlier (4.2.2). This wavelength dependance of polarisation is attributed to the absorption by hydrogen plasma in the circumstellar envelope (Coyne, 1976). The fractional contribution from shell increases at infrared wavelengths and as a result the polarisation curve should show a dip beyond 1 μm. This suggestion was confirmed by the IR polarimetric observations of ζ Tauri by Capps et al. (1973). Later polarimetric observations in the infrared (Coyne and McLean, 1975 and Jones, 1979) have confirmed the general validity of the hypothesis that polarisation in Be stars is due to electron scattering of stellar radiation.

4.4 OBSERVATIONAL PROGRAM AND RESULTS

Selection of Program Stars: The programme stars were selected on the basis of their visual magnitude being smaller than 7.0 and their accessibility during the observing periods. The smallest intrinsic $(V-K)_i$ colour amongst the main sequence B subspectral type stars is -0.93 for B0 V (Johnson, 1966). Then for $m_V = 7$, assuming that no IR excess is present, $m_K \sim 8$ and this can be detected with reasonable accuracy (signal to noise ratio S/N $\sim$ 4 for integration time $\sim$ 1s on 1 m telescope with the InSb photometer described in Chapter II). The selected objects consisted of Be stars having no IR data and also having previous IR data in the published literature. 55 Be stars were observed in this program. For 20 of them previous data is not available. The subspectral classes B0 to B8 have been covered by this group of program stars.

Near infrared photometry in the standard J H K L bands was done with a conventional liquid nitrogen cooled InSb photometer described in Chapter II. In most of the cases for calibration the standard stars were selected from the list of Johnson et al. (1966) and further it was seen that during observation, as far as possible,

Table 4.1A

Infrared Magnitudes of program Be stars

Stars for which previous IR observations are not available

S. No.	Star Identification HD No.	HR No.	Sp.Type	V	Date+	J	H	K	L	Reference* Optical
1.	18552	894	B8 Vn	6.10	Oct.80	6.25	6.21	6.28	-	7
2.	23016	1126	B8 Vn	5.56	Oct.80-Feb.81	5.76	5.75	5.91	-	6
3.	29866	1500	B7 IV	6.08	Oct.80	5.96	5.87	5.88	-	7
4.	43285	2231	B5 Vn	6.07	Oct.80	6.42	6.46	6.45	-	7
5.	45995	2370	B2 V	6.14	Jan.81	5.99	5.95	5.63	-	7
6.	54309	2690	B1 V	5.75	Jan.81	5.65	5.63	5.58	-	6
7.	164284	6712	B2 Vn	4.64	Apr 80 / Mar 81	4.43	4.32	4.00	3.6	7
8.	164447	6720	B8 Vn	6.38	Apr 80	6.64	6.78	6.63	-	7
9.	168717	6873	B3 Vn	6.13	"	6.30	6.49	6.28	6.0	7
10.	183362	7403	B2 Vn	6.34	"	6.42	6.44	6.15	6.1	7
11.	187811	7565	B2 V	4.95	"	5.22	5.28	5.19	4.9	7
12.	189687	7647	B3 IV	5.19	"	5.46	5.54	5.40	5.4	7
13.	191610	7708	B2 Vn	4.93	"	5.10	5.08	4.92	4.5	7
14.	192044	7719	B8 Vn	5.92	"	6.06	6.17	6.04	-	7
15.	193911	7789	B8 III	5.43	"	5.69	5.77	5.74	-	7
16.	194335	7807	B2 Vn	5.90	"	6.27	6.32	6.35	-	7
17.	200120	8047	B1.5 V	4.74	Apr.Oct80	5.18	5.17	5.00	-	7
18.	203467	8171	B3 III	5.18	Apr 80	5.15	5.12	4.91	4.5	7
19.	208682	8375	B3 V	5.86	"	5.98	6.05	5.72	5.0	7
20.	214167	8603	B1 V	5.73	Oct 80	6.47	6.39	6.72	-	7

*(Reference optical : MK spectral type and V)

+ Nainital : April/October 80 and March 81; Kavalur: Jan./Feb.1981

Table 4.1B

Stars for which previous IR observations are available

S. No.	Star Identification HD No.	HR No.	Sp.Type	V	Date+	J	H	K	L	Reference* Opt/	IR
1.	5394	264	B0.5 IV	2.47	Oct.80	2.30	2.24	2.08	-	7	1,5,8,9
2.	10516	496	B1 V	4.07	"	3.94	3.82	3.54	-	7	1,5,8,9
3.	20336	985	B3 Vn	4.84	"	5.03	5.07	5.00	-	7	1
4.	22192	1087	B4 V	4.23	Oct.80/J.81	4.30	4.24	4.04	-	7	1,5,11,15
5.	23302	1142	B6 III	3.70	Jan.Feb 81	3.90	3.88	3.95	-	7	5,8
6.	23480	1156	B7 III	4.18	"	4.25	4.22	4.28	--	7	5,8
7.	23630	1165	B7 III	2.87	"	2.95	2.99	2.94	-	7	5,8
8.	23850	1178	B8 III	3.62	"	3.74	3.75	3.77	-	8	
9.	23862	1180	B8 V	5.09	"	5.22	5.31	5.13	-	7	8
10.	32343	1622	B3 V	5.08	Oct.80	5.20	5.13	5.00	-	7	1,11
11.	32990	1659	B2 Vp	5.41	Feb 81	5.53	5.47	5.51	-	2,6	13
12.	35439	1789	B1 V	4.95	Oc.80/JF81	4.98	4.90	4.76	-	7	1,4
13.	37202	1910	B2 III	3.00	Feb 81	3.25	3.13	3.00	-	7	5,8,11
14.	37490	1934	B3 III	4.57	Oc.80/J.81	4.78	4.79	4.76	-	7	4,5,8
15.	37795	1956	B8 V	2.64	Feb.81	2.77	2.79	2.87	-	8	4,5,8
16.	45542	2343	B6 III	4.15	Oc.80/J.81	4.47	4.43	4.47	-	7	5,13
17.	50013	2538	B2 V	3.95	Feb.81	3.78	3.64	3.61	-	8	4,5
18.	56014	2745	B3 IIIp	4.65	J.Feb 81	4.88	4.82	4.82	-	8	8
19.	56139	2749	B3 V	3.82	"	4.39	4.42	4.48	-	8	1,4,8,16
20.	58343	2825	B3 IV	5.33	Feb.81	5.00	4.89	5.04	-	7	4,11,13
21.	58715	2845	B8 Vn	2.90	Jan.81	3.00	3.10	2.99	-	7	5,8
22.	63462	3034	B0 Vp	4.52	J.F.M.81	4.34	4.25	4.08	3.6	8	1,4,5
23.	68980	3237	B1.5 III	4.82	Feb.81	4.89	4.72	4.59	-	12	8
24.	83953	3858	B6 V	4.77	Oc.80J.81	4.90	4.90	4.72	4.4	3,8	1,4,5
25.	109387	4787	B5 IV	3.87	Apr 80/M.81	3.94	3.95	3.84	3.6	7	1,5,8,15

Table 4.1B contd.

26. 138749	5778	B6 Vn	4.14	Apr.80/J.F.81	4.44	4.49	4.48	4.5	7	1,5,11
27. 142983	5941	B 4 III	4.88	" F.M.81	4.90	4.84	4.71	4.3	7	1,4,5,9,10
28. 148184	6118	B1 V	4.42	" "	3.40	3.18	2.88	2.5	7	1,4,5,9,11,14
29. 174638	7106	B p	3.42	April 80	3.37	3.29	3.15	2.9	8	5,8 15
30. 202904	8146	B2 V	4.43	Apr.Oct.80	4.40	4.39	4.16	-	7	11
31. 209409	8402	B6 V	4.69	Oct.80	4.82	4.84	4.85	-	7	5,8
32. 212076	8520	B2 V	5.01	"	5.29	5.38	5.42	-	7	5
33. 212571	8539	B1 V	4.66	"	4.46	4.07	3.82	-	7	1,5,9
34. 217050	8731	B3 III	5.43	"	5.34	5.30	5.16	-	7	1,9
35. 217891	8773	B6 III	4.53	"	4.67	4.81	4.84	-	7	1,5,11

* Reference: Optical - MK spectral type and V; Infrared - previous measurement.

+ Nainital: April/October 80 and Marh 81; Kavalur: Jan.Feb.1981.

References:

1. Allen (1973)
2. Boulan et al. (1975)
3. Dachs et al. (1981)
4. Dachs & Wamsteker (1981)
5. Gehrz et al. (1974)
6. Hoffleit (1964)
7. Jascheck et al. (1980)
8. Johnson et al.(1966)
9. Jones (1979)
10. Neto & Pacheco (1982)
11. Schild (1973)
12. Slettebak (1975)
13. Smyth & Nandy (1978)
14. Whittet & van Breda (1980)
15. Woolf et al. (1970)
16. Glass (1974).

the calibration star was within few degrees of the program star and had nearly same spectral type. The results of Be stars observed in the present investigation are listed in Table 4.1. As noted earlier, the program stars have been categorised into two groups. Table 4.1A covers the Be stars for which observations presented in this thesis are new and Table 4.1B includes Be stars having previous IR observations. The HD and HR numbers, MK spectral type and V magnitude of the star are listed in columns 2 to 5. Observation month and year is given in column 6. J H K L photometry in the form of magnitudes appears in columns 7 to 10. MK spectral types and V magnitudes have been taken from the reference listed under the heading optical in column 11. In Table 4.1B reference to earlier IR work is also included.

4.5 DATA REDUCTION AND ANALYSIS

In this sub-section we shall describe the data reduction procedures and their analyses. Implication of these results will be examined in the Discussion, Section 4.9.

The main objective of the study is to understand the nature of envelopes of the Be stars by estimating

the infrared flux emitted by them. The photometrically observed flux contains (a) the contribution from the central star's photosphere and (b) from its circumstellar envelope. It is then necessary to subtract the contribution due to the underlying stellar photosphere from the observed flux to get the contribution from the envelope alone. After this it becomes possible to calculate different envelope properties and compare them with theoretical model calculations. The photospheric contribution can be estimated from model atmosphere calculations, if spectral type of the star is known. This calculation will give absolute fluxes. To calculate the expected apparent flux the distance to the object should be known. One way to get the apparent flux distribution is to normalise the model atmosphere flux distribution at a desired wavelength. In our calculations the normalisation has been done at V (0.55 μm) with the assumption that the circumstellar envelope contribution is negligible in the V band pass. The interstellar reddening modifies the intrinsic flux distribution of the source. Hence the first step in data reduction is to account for the interstellar reddening.

4.5:1 Interstellar Reddening Corrections:

To remove the interstellar reddening effects the visual data of the program stars has been utilised. The spectral type, V magnitude and (B-V) colours of the program stars are taken mainly from Jaschek et al. (1981) and Johnson et al. (1966). The intrinsic colours $(B-V)_i$, $(V-J)_i$ and $(V-K)_i$ are taken from Johnson (1966). The (B-V) colour excess E_{B-V} is then given by the following relation.

$$E_{B-V} = (B-V) - (B-V)_i \qquad \ldots\ldots \quad (4.1)$$

Assuming that only interstellar reddening contributes to E_{B-V}, the total extinction at V, A_V, is calculated using the standard relation:

$$A_V = R\, E_{B-V} \qquad \ldots\ldots \quad (4.2)$$

where R = 3.1 (Barlow and Cohen, 1977).

As pointed out by Jones (1979) this method of accounting for interstellar reddening results in unreddened magnitude values which are good only to $\pm$ $0^m.15$, since the effects of rapid rotation and envelope emission

of Be stars in the intrinsic colour $(B-V)_i$ have been ignored. A_K, theextinction at K (2.2 μm), is then calculated from Van de Hulst's theoretical curve No.15 for interstellar extinction (Johnson, 1968) which gives

$$A_K = 0.089\ A_V \qquad \ldots\ldots \qquad (4.3)$$

The unreddened magnitudes V_u and K_u of a program star are then given by the following equations.

$$V_u = V - A_V \qquad \ldots\ldots \qquad (4.4a)$$

$$K_u = K - A_K \qquad \ldots \qquad (4.4b)$$

where V and K are observed reddened magnitudes.

4.5:2 Calculation of the continuum envelope flux:

For a given program star we now have the unreddened visual magnitude V_u given by (4.4a). The intrinsic colour $(V-K)_i$ for different subspectral types are available (Johnson, 1966). So the expected stellar magnitude K_* for the K band is given by

$$K_* = V_u - (V-K)_i \qquad \ldots\ldots \qquad (4.5)$$

In most of the cases K_u is the smaller than K_* indicating the presence of envelope contribution at K (2.2 μm) which can also be looked upon as the "IR excess". Let us denote the magnitude and flux values of the central star, envelope and both combined as given below.

Quantity	Object		
	Star	Envelope	Combined
K magnitude	K_*	K_s	K_u
Flux at K	K_K^*	F_K^s	F_K^u

It should be noted that

$$F_K^u = F_K^* + F_K^s$$

$$K_* - K_u = 2.5 \log \left[(F_K^* + F_K^s) / F_K^* \right]$$

Let $$\frac{K_* - K_u}{2.5} = \triangle K$$

$$\therefore \quad F_K^S = F_K^* \left(10^{\Delta K} - 1\right)$$

$$= \frac{3.9 \times 10^{-7}}{(2.5119)^{K_*}} \left(10^{\Delta K} - 1\right) \qquad \ldots (4.6)$$

$$\text{erg s}^{-1}\ \text{cm}^{-2}\ \mu\text{m}^{-1}$$

In the above expression zero magnitude flux value for K band from Johnson (1966) given in Chapter II has been substituted. Similarly, the shell flux at other IR bands J, H and L is computed.

4.5:3 Calculation of the continuum envelope luminosity at specified wavelengths:

To calculate the envelope luminosity at different IR wavelengths one needs to know the distance D to the source. As stated in the beginning the distance D to the source is calculated by normalising the model photospheric flux at V (0.55 μ m) assuming the envelope contribution at V to be negligible.

The observed V flux is

$$F_v = \frac{F(V=0)}{(2.5119)^{Vu}} = \frac{3.92 \times 10^{-5}}{(2.5119)^{Vu}} \text{ erg s}^{-1}\ \text{cm}^{-2}\ \mu\text{m}^{-1} \qquad \ldots (4.7)$$

Taking blackbody distribution for photospheric emission, the expected flux at V is

$$\frac{4\pi R_*^2}{4\pi D^2} \quad \mathcal{F} \quad (T_*) \qquad \ldots\ldots \quad (4.8)$$

where $\mathcal{F}$ (T_*) is the blackbody emittance per unit wavelength, and R_* and T_* are the stellar radius and temperature respectively.

$$\mathcal{F} \quad (T_*) = \frac{c_1}{\lambda_v^5} \cdot \frac{1}{e^{c_2/\lambda_v T_*} - 1}$$

Substituting numerical values one gets

$$\mathcal{F} \quad (T_*) \quad = \frac{7.435 \times 10^2}{e^{2.6161/T4_*} - 1} \quad \text{erg s}^{-1} \text{ cm}^{-2} \mu \text{m}^{-1}$$

where $T4_*$ is stellar temperature in units of 10^4 K.

Substituting the observed and expected fluxes in equations 4.7 and 4.8, one obtains the value for distance D as

$$D^2 = \frac{1.897 \times 10^{39} (R11_*)^2 (2.5119)^{V_u}}{e^{2.6161/T4_*} - 1} \text{ cm}^2 \quad \ldots (4.9)$$

where $R11_*$ is the stellar radius in units of 10^{11} cm.

Then the envelope luminosity L_λ at any given wavelength λ, is given by

$$L_\lambda = 4\pi D^2 F_\lambda \text{ erg s}^{-1} \mu \text{ m}^{-1} \quad \ldots . (4.10)$$

Combining Equations 4.6, 4.9, and 4.10 one obtains

$$L_{2.2} = 9.3 \times 10^{33} (R11_*)^2 (2.5119)^{(V-K)_i} \times \frac{(10^{\Delta K} - 1)}{e^{2.6161/T4_*} - 1} \text{ erg s}^{-1} \mu \text{ m}^{-1} \quad \ldots . (4.11)$$

4.5:4 Calculation of total continuum emission of circumstellar envelope:

Having obtained the envelope flux at different IR wavelengths next quantity to be found out is the total continuum emission of circumstellar envelopes of Be stars. Since our observations for most of the program stars do not extend beyond 2.2 μm, a procedure is found out to estimate the total continuum flux of the envelope from the available J H K observations. As mentioned in Sec.4.3 Gehrz et al. (1974) with the help of extensive wavelength coverage from visible to about 20 μm showed that the observed continuum energy distributions of the envelopes fit reasonably well with free-free emission spectrum (4.3). In the following calculations free-free emission mechanism for the continuum radiation from the envelope is considered. Also the envelope is taken to be optically thin in the near IR region.

The free-free emission at a given wavelength per unit solid angle, volume, time and wavelength range is given by (Allen, 1976)

$$j = 1.633 \times 10^{-24} \lambda^{-2} Z^2 g T^{-\frac{1}{2}} N_e N_i \exp(-c_2/\lambda T)$$

$$\text{erg cm}^{-3} \text{ s}^{-1} \text{ sr}^{-1} \mu\text{m}^{-1} \qquad \ldots (4.12)$$

(λ in μm)

where Z is the ion charge

g is the Gaunt factor

N_e, N_i are electron and ion number densities in cm^{-3}.

Integrating Equation 4.12 over the whole wavelength range one obtains

$$j_{tot} = 1.142 \times 10^{-28} Z^2 g. T^{\frac{1}{2}} N_e N_i$$

$$\text{erg cm}^{-3} \text{ s}^{-1} \text{ sr}^{-1} \qquad \ldots\ (4.13)$$

Now it becomes possible to estimate the total free-free continuum flux of the circumstellar envelope (equation 4.13) from the flux at one given wavelength (equation 4.12) which has been obtained observationally. The fractional contribution from the circumstellar envelope increases as one goes to longer wavelengths in the J H K L region. So to minimise the effect of observational errors in the computation of total continuum flux of the envelope it is advisable to use the longest available wavelength observations. Since we do not have L measurements for all the program stars we have taken K band observations to calculate the total continuum flux of the envelope. Also it is seen from equations (4.12) and (4.13) that the free-free emission spectrum has a

weak temperature dependance and consequently assuming it to be uniform throughout the envelope will not introduce uncertainties in the calculations of more than a factor of 2. Substituting $\lambda = 2.2\ \mu m$, $T = 1.4 \times 10^4$ K (Gehrz et al. 1974), $Z = 1$ (most of the material is hydrogen) and $g = 1$ in equations (4.12) and (4.13) and taking their ratio we obtain

$$j_{tot} = 7.56\ (j_{2.2}\ \mu m^{-1}) \qquad \ldots\ (4.14)$$

The luminosity is obtained by integrating the emission throughout the volume i.e.

$$L = \int 4\pi\, j\ dV \qquad \ldots\ (4.15)$$

Since the continuum flux from the circumstellar envelope is predominantly emitted in the infrared spectral region, henceforth the continuum luminosity is denoted by L_{IR}. From 4.14 we get

$$L_{IR} = 7.57\ (L_{2.2}\ \mu m^{-1}) \qquad \ldots\ (4.16)$$

Table 4.2 lists the properties of main sequence normal B type stars, necessary to calculate the total

continuum envelope luminosity. The MK spectral type, radius, temperature, intrinsic colors $(B-V)_i$ and $(V-K)_i$, and bolometric luminosity are given in coloumns 1 to 6 respectively. These values have been taken from Collins (1974) and Johnson (1966). Also given in Table 4.2 are I°_{L} the stellar flux shortward of Lyman limit, $I_{H\alpha}$ and $I_{H\beta}$ the luminosities of the $H\alpha$ and $H\beta$ lines in units of erg s^{-1} $\AA^{-1}$. These three parameters are referred to in the following sections 4.6, 4.7 and 4.9.

The calculated values of total continuum luminosity of the circumstellar envelopes are given in Table 4.3 alongwith the ratios L_{IR}/L°_{L} and L_{IR}/L_{*}. The calculations are done only for the program stars of luminosity class IV and V. The program stars have been grouped according to their MK spectral types. The observed (B-V) colors taken from published literature to estimate the interstellar reddening correction are also listed in Table 4.3. 14 out of 40 stars listed in Table 4.3 do not exhibit IR excess. The implications of this fact will be considered in the Section 4.9.

Table 4.2

Properties of the Main sequence normal B-type stars[a]

Sp. Type	Radius ($R/R_\odot$)	Temperature K	$(B-V)_i$	$(V-K)_i$	L_* erg s^{-1}	L_L° erg s^{-1}	$L_{H\alpha}$ erg s^{-1}	$L_{H\beta}$ erg s^{-1}
B0	5.7	30 000	-0.30	-0.93	1.48 E 38	1.94 E 37	5.66 E 32	1.62 E 33
B1	6.3	24 000	-0.26	-0.81	3.59 E 37	4.49 E 36	4.96 E 32	1.37 E 33
B2	4.8	21 000	-0.24	-0.74	1.48 E 37	8.39 E 35	2.34 E 32	6.25 E 32
B3	4.4	18.000	-0.20	-0.61	6.24 E 36	1.64 E 35	1.52 E 32	3.88 E 32
B4	4.2[b]	16 500[b]	-0.18[b]	-0.54[b]	4.50 E 36[c]	5.93 E 34	1.28 E 32	2.95 E 32
B5	4.0	15 000	-0.16	-0.47	2.77 E 36	1.86 E 34	9.01 E 31	2.16 E 32
B6	3.8[b]	14 300[b]	-0.14	-0.41	2.08 E 36[c]	9.28 E 33	7.41 E 31	1.74 E 32
B7	3.6	13 600	-0.12	-0.35	1.37 E 36	4.62 E 33	6.06 E 31	1.40 E 32
B8	3.2	12 200	-0.09	-0.24	7.80 E 35	8.40 E 32	3.82 E 31	8.35 E 31
B9	2.8	11 000	-0.06	-0.14	4.29 E 35	1.35 E 32	2.32 E 31	4.79 E 31

$R_\odot$ = 6.96 E 10 cm

a From Collins (1974) and Johnson (1966)

b Interpolated values

c L_* calculated using the relation $L_* = 4\pi R_*^2 \sigma T_*^4$ erg s^{-1}

Table 4.3

Total continuum luminosity of the circumstellar envelope for the program Be stars.

S. No.	Star	Sp.Type	(B-V)	L_{IR} erg s^{-1}	L_{IR}/L_L°	L_{IR}/L_*
1	264	B0.5 IV	-0.15	4.32 E 35	0.02	0.29 E -2
2	3034	B0 Vp	-0.05	2.82 E 35	0.02	0.19 E -2
3	496	B1 V	-0.04	3.02 E 35	0.07	0.84 E -2
4	1789	B1 V	-0.20	3.72 E 35	0.08	1.04 E -2
5	2690	B1 V	-0.18	3.24 E 35	0.07	0.90 E -2
6	6118	B1 V	+0.28[a]	8.04 E 35	0.18	2.24 E -2
7	8047	B1 V	-0.05	No Excess	-	-
8	8539	B1 V	-0.03	4.87 E 35	0.11	1.36 E -2
9	8603	B1 V	-0.15	No Excess	-	-
10	1659	B2 Vp	+0.06	"	-	-
11	2370	B2 V	-0.08	1.73 E 35	0.21	1.17 E -2
12	2538	B2 V	-0.23	2.62 E 35	0.31	1.77 E -2
13	6712	B2 Vn	-0.03	1.69 E 35	0.20	1.14 E -2
14	7403	B2 Vn	-0.14	1.30 E 35	0.15	0.88 E -2
15	7565	B2 V	-0.14	3.52 E 34	0.04	0.24 E -2
16	7708	B2 Vn	-0.13	7.95 E 34	0.09	0.54 E -2
17	7807	B2 Vn	-0.20	2.83 E 34	0.03	0.19 E -2
18	8146	B2 V	-0.11	1.29 E 35	0.15	0.87 E -2
19	8520	B2 V	-0.13	No Excess	-	-
20	985	B3 Vn	-0.15	3.76 E 34	0.23	0.60 E -2
21	1622	B3 V	-0.08	4.34 E 34	0.26	0.70 E -2
22	2749	B3 V	-0.18	No Excess	-	-
23	2825	B3 IV	-0.05	6.26 E 34	0.38	1.00 E -2
24	6873	B3 Vn	-0.04	No Excess	-	-
25	7647	B3 IV	-0.17	3.85 E 34	0.23	0.62 E -2
26	8375	B3 Vn	-0.06	4.36 E 34	0.27	0.70 E -2
27	1087	B4 V	-0.06	4.05 E 34	0.68	0.90 E -2
28	2231	B5 Vn	-0.13	No Excess	-	-
29	4787	B5 IV	-0.13	3.48 E 34	1.87	1.26 E -2
30	3858	B6 V	-0.12	2.89 E 34	3.11	1.39 E -2
31	5778	B6 Vn	-0.13	No Excess	-	-
32	8402	B6 V	-0.06	"	-	-
33	1500	B7 IV	+0.06	"	-	-
34	894	B8 Vn	-0.06	"	-	-
35	1126	B8 V	-0.01	"	-	-
36	1180	B8 V	-0.08	6.37 E 33	7.58	0.82 E -2
37	1956	B8 V	-0.12	No Excess	-	-
38	2845	B8 Vn	-0.09	5.52 E 33	6.57	0.71 E -2
39	6720	B8 Vn	-0.06	No Excess	-	-
40	7719	B8 Vn	-0.11	4.35 E 33	5.18	0.56 E -2

a $E(B-V) = +0.35$ adopted from Snow (1975).

4.6 CORRELATION STUDIES OF IR EXCESS WITH STELLAR PARAMETERS

4.6:1 Continuum flux shortward of the Lyman limit:

The physical conditions in the shell around the central B star are determined by the heating and cooling processes operating in the envelope. As pointed out in 4.3 the most widely accepted explanation attributes the excess IR radiation from Be stars to electron-proton scattering in the circumstellar material which is ionised by the Lyman continuum radiation from the central star. Gehrz et al. (1974) have noted that the infrared excess in Be stars increases as spectral type becomes earlier and ascribe it to the increased stellar flux shortward of the Lyman limit (hereafter denoted by L_L°). They also observe that the total continuum envelope flux, L_{IR}, does not increase in direct proportion with the stellar flux shortward of Lyman limit as one goes to earlier spectral type and interpret this as limited amount of available material in the envelope for ionisation. To study the dependance of L_{IR} on L_L°, these two quantities have been calculated by us for 9 of the 10 stars given in Table 5 of Gehrz et al. (1974). The tenth star ξ Per was not included in the present calculations since its spectral type is O7 ne.

The total shell flux is obtained by the equation (4.13) as

$$L_{IR} = 1.435 \times 10^{-27} \; g \; T_S^{\frac{1}{2}} \; N_e^2 \; V_S \; \text{erg s}^{-1} \qquad \ldots\ldots \quad (4.17)$$

where V_S is the shell volume. The shell volume is calculated by assuming a disc geometry as was done by Gehrz et al. (1974).

$$V_S = \pi \; R_S^2 \; H \qquad \ldots\ldots \quad (4.18a)$$

where R_S is the disc radius and H is the disc thickness. The typical value of H is $R_S/5$ (Gehrz et al. 1974). Hence

$$V_S = \frac{\pi \; R_S^3}{5} \qquad \ldots\ldots \quad (4.18b)$$

The stellar flux shortward of Lyman limit L_L° is calculated by using the relation

$$L_L^\circ = 4\pi \; R_*^2 \int_{\nu_o}^{\infty} \mathcal{F}_\nu(T_*) \; d\nu \qquad \ldots\ldots \quad (4.19)$$

where R_* is the stellar radius, ν_o is the frequency at the Lyman limit (3.29×10^{15} Hz) and $\mathcal{F}_\nu(T_*)$ is the emittance per unit frequency range of a blackbody with temperature T_*, the effective stellar temperature.

Table 4.4 lists the results of the calculations alongwith the ratio (L_{IR}/L_L°) and other relevant parameters. Having done these calculations let us see how the observed values of L_{IR}/L_L° compare with the expected value. The expected value can be estimated from the geometrical considerations as follows.

The fractional solid angle Ω_s subtended by the circumstellar envelope at the central star is

$$\Omega_s = \frac{2\pi R_s H}{4\pi R_s^2} = \frac{1}{2}\frac{H}{R_s} \qquad \ldots\ (4.20a)$$

The shell geometry is assumed to be such that at any given distance d, from the central star the ratio $\frac{H(d)}{R(d)}$ remains the same. The typical value of (H/R_s) is given as 1/5 by Gehrz et al. (1974). Hence

$$\Omega_s \sim 0.1 \qquad \ldots\ (4.20b)$$

This means that only 10 percent of the central star's radiation is intercepted by the envelope. Assuming that all the stellar flux shortward of Lyman limit (L_L°) is absorbed by the envelope and re-radiated as the free-free continuum flux one obtains

Table 4.4

Circumstellar Envelope parameters for the stars from Gehrz et al. (1974)

Star Name	Sp.Type	L_{IR} erg s^{-1}	L_L° erg s^{-1}	L_{IR}/L_L°	L_* erg s^{-1}	L_{IR}/L_*
γ Cas	B0 IVp	2.29 E 35	1.14 E 37	0.02	8.14 E 37	0.28 E -2
π Aqr	B1 V	1.25 E 35	1.80 E 36	0.07	3.46 E 37	0.36 E -2
χ Oph	B2 V	3.75 E 34	2.36 E 35	0.16	1.20 E 37	0.31 E -2
ζ Tau	B2 IV	5.67 E 34	2.36 E 35	0.24	1.20 E 37	0.47 E -2
HD 217050	B2 IV	6.69 E 34	2.36 E 35	0.28	1.20 E 37	0.56 E -2
ω Ori	B3 III	5.73 E 34	9.64 E 34	0.59	7.47 E 36	0.77 E -2
ϕ Per	B3 III-V	5.84 E 34	7.38 E 34	0.79	5.72 E 36	1.02 E -2
48 Lib	B5 p	2.66 E 34	1.06 E 34	2.51	2.46 E 36	1.08 E -2
β Psc	B5 p	7.40 E 33	1.06 E 34	0.70	2.46 E 36	0.30 E -2

(R_*, T_*, R_S, T_S and N_e required for above calculations are taken from Gehrz et al . 1974).

$$\frac{L_{IR}}{L_L^{\circ}} \sim 0.1 \qquad \ldots\ldots \quad (4.21)$$

It should be noted that the value of 0.1 is an upper limit since the shell also looses energy in the form of optical emission lines.

As noted in 4.2.2 Be stars as a class are fast rotators, as indicated by their $\upsilon \sin i$ values, resulting in flattening of polar region, non-uniform surface gravity and temperature distribution. The polar region temperatures would be higher and relatively more continuum radiation shortward of Lyman limit would be emitted from these (polar) regions than the equatorial regions. Since the circumstellar envelopes are flattened and mainly confined to the equatorial region, the polar region ultraviolet flux is not utilised in ionising the envelope material. So the disc type geometry of the circumstellar envelope and the preferential emission of stellar flux shortward of Lyman limit from the polar regions put an upper limit for L_{IR}/L_L°. From Table 4.4 it is seen that for 7 out of 9 stars L_{IR}/L_L° values are appreciably greater than 10 percent which is expected upper limit. Hence it appears that though the ionization

in the shell is due to the stellar flux shortward of Lyman limit the energetics of IR radiation is not governed entirely by the amount of available Lyman continuum flux.

For the Be stars observed in our program, the continuum luminosities of the circumstellar envelopes (L_{IR}) have been calculated by the procedure described in 4.5 and listed in Table 4.3. From Table 4.3 it is seen that the ratio L_{IR}/L_L° in general is appreciably greater than 0.1. This fact points out the inadequecy of Lyman continuum flux in supplying the input energy to the circumstellar envelope. Apart from the energy input by Lyman continuum flux, an additional energy source is necessary to explain the higher values of the ratio L_{IR}/L_L°.

4.6.2 Bolometric Flux:

It was seen in the previous section that it is not possible to account for the observed continuum luminosity of the envelope (L_{IR}) if one considers the energy input to the envelope only by photoionizations. To gain an understanding about other possible energy input mechanisms, the central star's bolometric luminosity, L_*, is compared with L_{IR}. The stellar bolometric luminosity is obtained by using the relation

$$L_* = 4\pi R_*^2 \sigma T_*^4 \text{ erg s}^{-1} \quad \ldots\ldots (4.22)$$

where $\sigma = 5.67 \times 10^{-5}$ erg cm^{-2} deg^{-4} sec^{-1} is the Stefan-Boltzman constant.

The ratios of L_{IR}/L_* are obtained for 9 Be stars listed by Gehrz et al. (1974) and are given in Table 4.4. From this table it is seen that for all the 9 stars the ratio L_{IR}/L_* is constant within a factor of 2 with an average value of $\sim 0.6 \times 10^{-2}$ though both L_{IR} and L_* individually vary by a factor of 30. This hints at the importance of the role played by the stellar bolometric luminosity in determining the energy balance of the circumstellar envelopes of Be stars.

To check the general validity of the close dependance of L_{IR} on L_* rather than L_L°, L_{IR} values for our program stars have been plotted against corresponding L_* in Fig.4.1 and also the ratios (L_{IR}/L_*) for all the program stars are listed in Table 4.3. From Fig.4.1 it is seen that the L_{IR} increases in proportion with L_*. Consequence of this is examined in the subsection "discussion" (4.9.2).

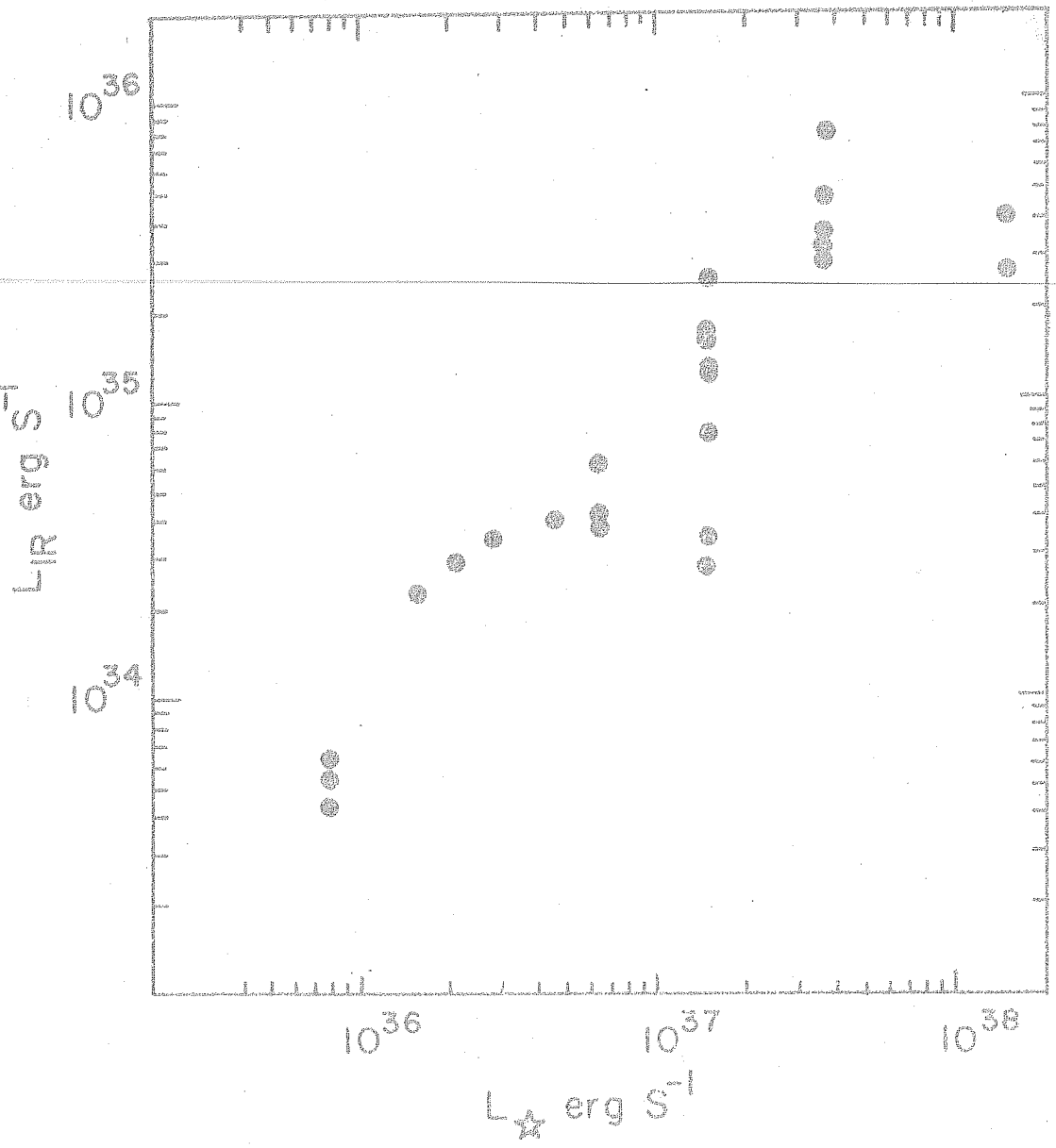

FIG.4·1 THE CONTINUUM INFRARED LUMINOSITY L_{IR} OF CIRCUMSTELLAR ENVELOPES OF PROGRAM Be STARS AS A FUNCTION OF CENTRAL STAR'S BOLOMETRIC LUMINOSITY $L_{\star}$

4.7 CORRELATION STUDIES OF IR EXCESS WITH HYDROGEN EMISSION LINES

In Be stars the hydrogen recombination lines and IR free-free emission originate in the same circumstellar envelope. As a result it is of interest to see whether or not any correlation exists between the infrared continuum radiation from the envelope and properties of the visual spectrum. In particular, is IR excess from Be stars correlated with Balmer emission line strength? In the following paragraphs such comparative study has been made.

As described in 4.2.3 the emission lines of Be stars exhibit variability. So it is desirable to have simultaneous IR photometric and visual spectroscopic data for the purpose of correlation studies. The Hα equivalent widths obtained by Andrillat and Fehrenbach (1982), which are sufficiently close in time, have been taken for the correlation studies. For 18 of our program stars Hα equivalent widths are available.

We have considered only Hα line as it is the most prominent spectral feature that distinguishes a Be star. Hα line strength, i.e. the total energy present in the line, is estimated from the observed

equivalent width. Assuming that the underlying continuum, in terms of which the equivalent widths are measured, arises from a star radiating as a blackbody at temperature T_* and with radius R_* one can write for the line luminosity the following equation

$$L_{H\alpha} = \frac{c_1}{\lambda^5} \frac{10^{-8}}{\exp(c_2/\lambda T_*) - 1} W\, 4\pi R_*^2 \quad .. (4.23)$$

$$\text{erg s}^{-1}$$

where

$c_1 = 3.7419 \times 10^{-5}$ erg cm^2 s^{-1}

$\lambda = 0.6563 \times 10^{-4}$ cm

$c_2 = 1.43883$ cm K

W = observed equivalent width in Å.

Similar equation is given by Burbidge and Burbidge (1953). The $L_{H\alpha}$ values have been calculated for our program stars that have Hα equivalent width data. They are given in Table 4.5. Also listed in Table 4.5 are other pertinent data like date of observation of Hα and its equivalent width. L_{IR} is plotted against $L_{H\alpha}$ in Fig.4.2. It is seen from this figure that significant correlation exists between L_{IR} and $L_{H\alpha}$. The correlation coefficient of

Table 4.5

Continuum lumi-nosity of circumstellar envelopes and Hα emission line luminosity of program Be stars

S. No.	Star HR No.	Sp.Type	IR Data Date	L_{IR} erg s^{-1}	Hα emission line data Date	W Å	$L_{H\alpha}$ erg s^{-1}	$\frac{L_{IR}}{L_{H\alpha}}$
1	264	B0.5 IV	15/16-10-80	4.32 E 35	26-12-80	21.3	1.21 E 34	36
2	496	B1 V	"	3.02 E 35	26-12-80	49.7	2.47 E 34	12
3	1789	B1 V	16-10-80/ 25/26-1-81	3.72 E 35	28-12-80	8.4	4.17 E 33	89
4	6118	B1 V	23/24/26-3-80	8.04 E 35	1-3-80	32.8	1.63 E 34	49
5	8539	B1 V	15-10-80	4.87 E 35	30-12-80	31.9	1.58 E 34	31
6	2370	B2 V	11-01-81	1.73 E 35	26-12-80	30.1	7.04 E 33	25
7	6712	B2 Vn	23/24-03-80	1.69 E 35	4-4-80	44.0	1.03 E 34	16
8	8520	B2 V	15/16-10-80	-	28-12-80	18.3	4.28 E 33	-
9	985	B3 Vn	15-10-80	3.76 E 34	30-12-80	5.5	8.36 E 32	45
10	1622	B3 V	16-10-80	4.34 E 34	26-12-80	24.2	3.68 E 33	12
11	2825	B3 IV	9-2-81	6.24 E 34	30-12-80	8.5	1.29 E 33	48
12	1087	B4 V	16-10-80/ 10-1-81	4.05 E 34	25-12-80	41.0	5.25 E 33	8
13	2231	B5 Vn	16-10-80	-	12-2-81	1.6	1.44 E 32	-
14	4787	B5 IV	16-3-81	3.48 E 34	30-12-80	9.1	8.20 E 32	42
15	5778	B6 Vn	11-1-81	-	30-12-80	-5.6	-	-
16	894	B8 V	15-10-80	-	29-12-80	18.9	7.22 E 32	-
17	1180	B8 V	14-2-81	6.37 E 33	12-2-81	12.0	4.58 E 32	14
18	2845	B8 Vn	25-1-81	5.52 E 33	26-12-80	6.0	2.29 E 32	24

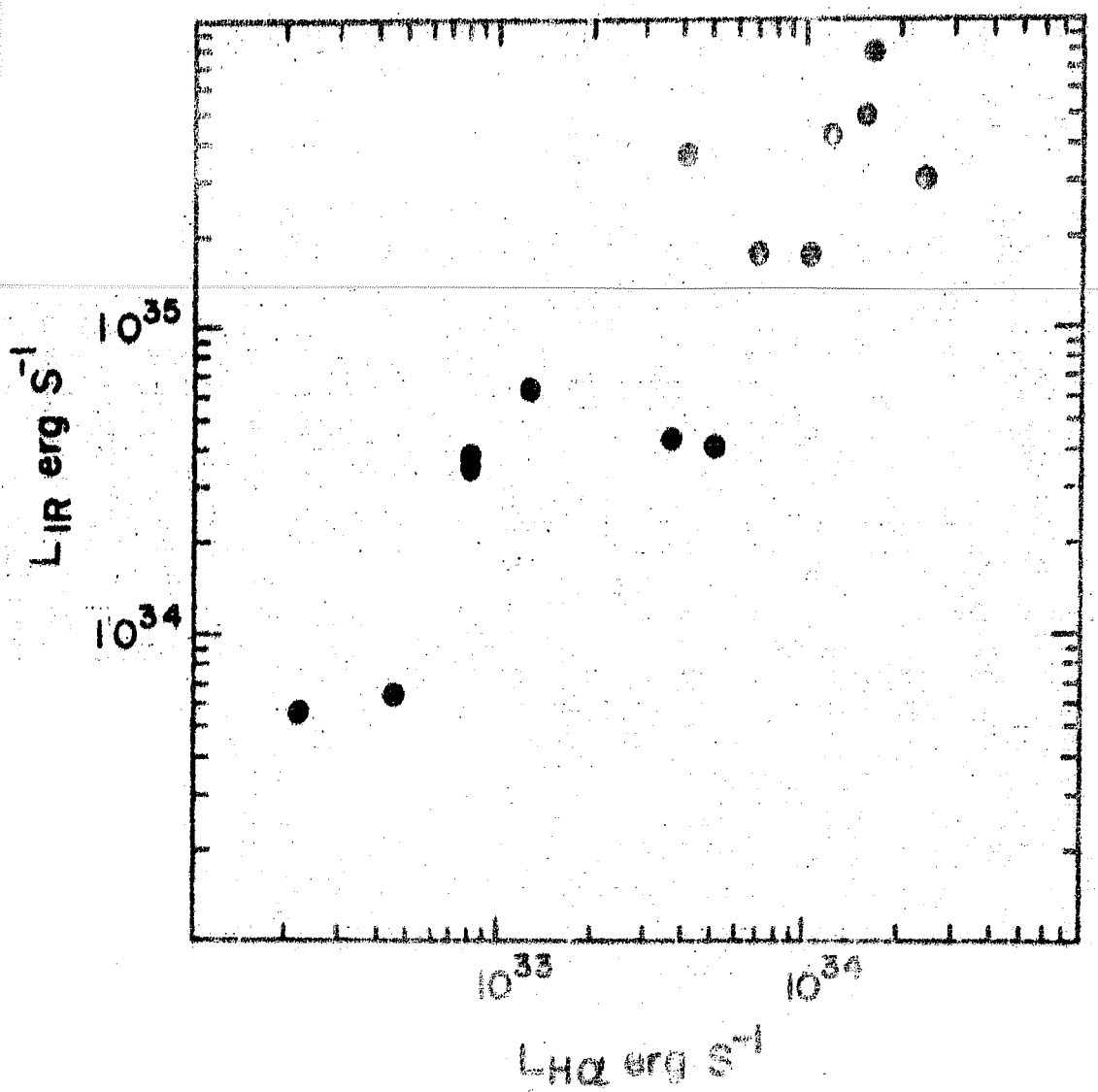

FIG4·2THE CONTINUUM INFRARED LUMINOSITY L_{IR} OF CIRCUMSTELLAR ENVELOPES OF PROGRAM Be STARS AS A FUNCTION OF BALMER H_α LINE LUMINOSITY $L_{H\alpha}$

the linear regression curve of Log L_{IR} and Log $L_{H\alpha}$ is 0.9. Part of the scatter in Fig.4.2 arises because IR and line measurements have not been done simultaneously. In the time interval separating the two observations either IR continuum or line emission could have varied. However, the important thing to notice is the fact that the ratio $L_{IR}/L_{H\alpha}$, for the majority of the stars listed in Table 4.5, is constant with average value 32, within a factor of 2 though both L_{IR} and $L_{H\alpha}$ change by two orders of magnitude.

4.8 INFRARED VARIABILITY

The existence of correlation between Hα line strength and the IR continuum flux from the circumstellar envelope suggests that Be stars should exhibit IR variability since Hα line strength varies as described in 4.2.3. Systematic infrared photometric studies of Be stars to look for IR variability have not been done. The data of Woolf et al. (1970) hinted at IR variability of Be stars. However, Gehrz et al. (1974) reported that during their observational period of one year they did not find any evidence of IR variability in Be stars. Recently Elias et al. (1978) have reported infrared

variability in the Be star o Cas. Since 1964 beginning with Johnson's (1967) observations sporadic infrared observations are available for o Cas. These observations show that o Cas was quiscent between 1964 and 1976 and since 1976 it has shown considerable IR variability. Elias et al. (1978) also have optical spectroscopic data for o Cas which shows that infrared variations are correlated with variations in the Balmer emission lines.

Our set of program stars contains 35 Be stars for which already published IR data exist. For comparison previous J H K L magnitudes for these stars have been taken mainly from the papers of Johnson et al. (1966); Allen (1973) and Gehrz et al. (1974) and these have been pooled together with our data to obtain a data set that spans the time period from 1965 to 1981. This combined data set reveals that in the case of 4 of our program stars the IR magnitudes have significantly varied. The maximum change $\triangle m_K$ in K magnitude lies in the range 0.5 to 0.8, while typical uncertainities in our measurements are $\pm$ $0^m.07$. For these 4 stars all the available J H K L magnitudes alongwith our observations are listed in Table 4.6.

Table 4.6

List of Be stars showing IR variability ($\Delta m_K \gtrsim 0.5$)

S. No.	HR No.	Observer	Date	IR magnitudes J	H	K	L	Equivalent width data Date	W Å
1.	1789	Allen	1971-72	-	5.44	5.47	-	Dec.75	3.78
	B1 V	Dachs	Feb.79	5.15	5.16	5.16	4.97	Nov.76	-2.87
	25 Ori	Present work	Oct.80/J.F 81	4.98	4.90	4.76	-	Jan.77	0
2.	1934	Johnson	1965	4.75	-	4.82	4.81	Oct.74	12.5
	B3 III	Gehrz	1972-73	-	-	4.32	4.01	Dec.75	13.1
	ω Ori	Dachs	Feb.79	4.53	4.51	4.51	-	Nov.76	10.5
		Present work	Oct.80/J.F.81	4.78	4.79	4.76	-	Jan.77	7.8
								Jan.78	4.8
								Oct.Nov.78	7.6
								Feb.Mar 79	7.0
3.	2749	Johnson	1965	4.32	-	4.28	-	Jan.Feb.78	14.2
	B3 V	Allen	1971-72	-	4.06	3.89	3.48	Oct.Nov.78	12.9
	ω CMa	Glass	1972-73	4.17	4.12	3.99	-		
		Dachs	Feb.79	4.21	4.26	4.30	4.20		
		Present work	Jan.Feb.81	4.39	4.42	4.48	-		
4.	6118	Woolf		-	-	-	3.56	May 72	66.7
	B1 V	Schild	1970	-	3.43	3.15	2.92	May 76	45.4
	χ Oph	Allen	1971-72	-	3.68	3.42	2.79	June 77	42.8
		Gehrz	1972-73	-	-	3.60	3.14	July 77	44.0
		Jones	1976	3.42	-	3.03	-	Feb.78	41.3
		Whittet	1976-77	3.50	3.29	3.04	2.71	Oct.78	39.4
		Dachs	Feb.1979	3.33	3.20	2.97	2.56	Mar.79	36.9
		Neto	May 80	3.46	-	2.89	2.28	May 80	33.7
		Present work	Apr 80/F.M.81	3.40	3.18	2.88	2.5		

4.9 DISCUSSION

4.9:1 Models:

The first explanation for the peculiar nature of Be stars was given by Struve (1931). It was observed that all hydrogen (emission) lines in any individual Be star have widths proportional to their wavelengths. This suggests Doppler broadening and it is the main foundation of the rotational model proposed by Struve. Aided by fast rotation the material is able to escape from the star and form a shell mainly confined to the equatorial region. This simple model could explain the available data reasonably well. Even now these concepts suggested by Struve form the basis of some of the well developed models. The present status of models of Be star envelopes is discussed in the review articles by Marlborough (1976) and Poeckert (1981). Following is the brief summary of the Be star models.

Marlborough (1969) developed a model for the Be star envelope by assuming the envelope to be in a steady state and fed by rotational ejection of matter at a constant rate from the equatorial region of the star. The available Hα emission line data was taken to check

the capability of the model. For electron and ion densities in the range 1 x 10^{11} to 5 x 10^{12} cm^{-3} Marlborough's model showed reasonable agreement between theoretical and observed Hα line profiles.

Johnson's (1967) data indicated the existence of nonstellar IR emission in Be stars. These and later IR observations provided new data supporting the presence of circumstellar envelopes in Be stars. The disc like circumstellar envelopes in the Be star models developed by Woolf et al. (1970); Gehrz et al. (1974) and Scargle et al. (1978) give rise to the observed IR excess.

Further evidence for the disc like geometry for Be star envelopes came from polarisation measurements. The scattering in the asymmetrically shaped envelope surrounding the central star gives rise to the observed polarisation. Capps et al. (1973) and Jones (1979) have developed equatorial models capable of producing polarisation as well as its wavelength dependance.

With the availability of diverse observations of Be stars in recent years, Poeckert and Marlborough (1977, 1978a) have made an improvement over the work done by Marlborough (1969) in model building by considering

both the Hα line profile and continuum polarisation. In general, there is good agreement between their model calculations and observations. However, there are some shortcomings like model calculations resulting in larger polarisation than observed though they show correct wavelength dependance. Poeckert and Marlborough (1978b) have investigated the observable effects introduced by different model parameters and have identified some sensitive parameters in certain wavelength ranges. They have finally demonstrated the necessity of simultaneous observations spanning a large wavelength region and involving different techniques to arrive at a model having well defined parameters.

One of the major short-comings of steady stellar wind models for Be stars (Marlborough, 1969) is their inability to explain the observed temporal variations. Limber (1969) has suggested variable mass loss rate as a possible cause for producing temporal variations.

An alternative model for Be star envelope in the form of elliptical ring around the central star, proposed by Struve in 1931, was quantitatively developed by Huang (1972, 1973). In this model apparently periodic V/R variations (Sec. 3.2.3) appear as a natural outcome

of apsidal motion of the ring. However, there are several difficulties with the elliptical model like, its inability to produce deep shell absorption lines (Marlborough, 1976), unlikely synchronised precession of large family of rings to result in apsidal motion etc.

In recent years an interesting alternative scenario to explain the formation of Be stars and their properties is gaining grounds (Plavec, 1976). Plavec discusses the hypothesis that a significant number of Be stars are probably interacting binaries. This formulation admits the existence of several possible models so that objects similar in appearance but different in origin can exist. According to Plavec (1976), the idea of binary model was thought of, not because the Struve's model of fast rotating single star was unsatisfactory but because the models of interacting binaries indicated that one can get something similar to Be star in this situation as well. To start with, a normal B type star is one of the components in the binary system. The companion of this B type star, at a certain stage in its evolution starts loosing mass through Roche lobe overflow (Peters, 1976). The mass loss leads to the formation of a shell around B star and what was once a B star becomes a Be star.

As already noted in Sec. 4.5.4 in the present investigation we adopt the model in which a disc shaped envelope surrounds the central B type star. The radiation shortward of Lyman limit from the central star ionises the material in this envelope. The bright emission lines seen are the hydrogen recombination lines originating in the circumstellar envelope. The thermal bremsstrahlung process operating in the same circumstellar envelope gives rise to the continuum infrared radiation.

4.9:2 The dependance of L_{IR} on stellar parameters:

It was found out in 4.6.1 that the Lyman continuum flux which is capable of photoionising the envelope material and depositing energy, is not able to account for the amount of observed continuum IR radiation from the circumstellar envelope. It was further shown in 4.6.2 L_{IR} is proportional to L_* which suggests that the non-ionising component of the stellar radiation plays an important role deciding the energetics of the circumstellar envelope. As shown in 4.8 the IR flux from circumstellar envelopes of Be stars exhibit appreciable temporal variation. The stellar luminosity is considered to be constant. Only when Be stars exhibit IR excess

the L_{IR} values are proportional to L_{*}. The envelope continuum luminosity of the program stars spans a range of two orders of magnitude from 10^{36} to 10^{38} erg s^{-1} and all through this range the ratio L_{IR}/L_{*} is remarkably constant. The physical implications of correlation between L_{IR} and L_{*} is not clear. However, it is interesting to note that mass loss rates of O and B stars depend on their bolometric magnitudes (Lamers, 1981). Lamers has derived mass loss rates for a large sample of O and B stars. He has determined empirical relation of mass loss rate on basic stellar parameters L, M and R. The derived functional dependance of $\dot{M}$, the mass loss rate on basic stellar parameters is given in Equation (4.24).

$$\dot{M} \propto L^{1.42}\ M^{-0.99}\ R^{0.61} \qquad \ldots\ (4.24)$$

The mass loss rates of OB stars were obtained by Lamers from single observation for each program star. The observed correlation of $\dot{M}$ with L, M and R suggests that these stars are continuously undergoing the mass loss at the derived rates. As noted earlier the IR excess radiation of circumstellar envelopes is variable in time. So the mass loss, which depends upon the rate $\dot{M}$, by stellar wind cannot be directly associated with the material

present in the circumstellar envelope. The Be episode involves occasional ejection of material, most likely from the equatorial region, aided by fast rotation. This process in some way might be dependant upon L_* and as a result the total amount of material is related to L_*. The total amount of material in the circumstellar envelope determines the number densities N_e and N_i which in turn decide L_{IR}.

4.9:3 Correlation of L_{IR} and $L_{H\alpha}$:

To understand the physical processes responsible for the observed correlation of IR excess emission and line emission from Be stars let us see the details of line formation. The characteristic emission lines of Be stars are the result of recombination processes occurring in the circumstellar envelopes. In the recombination process, recaptures occur to excited levels and the excited atoms thus formed then decay to lower levels by radiative de-excitation giving the observed line photons. Balmer series of emission lines results from the de-excitations occurring to the level n=2.

In general the emission at frequency ν due to radiative transition from level n to m is given by

$$j_{nm} = \frac{1}{4\pi} N_n A_{nm} h\nu_{nm} \text{ erg cm}^{-3} \text{ sec}^{-1} \text{ sr}^{-1} \quad .. (4.25)$$

where N_n is the number of atoms in the higher level n

A_{nm} is the transition probability

$h\nu_{nm}$ is the energy of the emitted photon.

The initial energy spectrum of the electrons produced in the photoionisation process depends on the spectral distribution of central star's Lyman continuum photons. However the predominance of elastic scattering results in Maxwell-Boltzmann energy distribution. So in general the population N_n can be written as (Lang, 1974)

$$N_n = b_n N_e N_i \frac{h^3}{(2\pi m kT)^{3/2}} \frac{g_n}{2} \exp(I_n/kT) \quad \ldots (4.26)$$

where $I_n = h\nu_o - \chi_n = (h\nu_o/n^2)$ is the ionisation potential of the level n

$h\nu_o$ is the ionisation potential of atom in the ground level

χ_n is the excitation potential of the level n

$g_n = 2n^2$ is the statistical weight of the level n

N_e, N_i are the electron and positive ion number densities and

b_n is the deviation from thermodynamic equilibrium at local T, N_e and N_i.

The details of optical recombination lines are available for two situations (Osterbrock, 1974). The first one known as case A considers optically thin condition i.e. all the line photons emitted in the recombination process escape. In case B all ground state recombinations are effectively cancelled out by immediate photo-ionisation. Case B is the appropriate one for Be star envelopes. Tucker (1975) has given an analytic expression for the emissivity of a Balmer Hn line as a function of temperature

$$j_{n2} = \frac{1}{4\pi} \times 10^{-23} N_e N_i a_{n2} T^{-\frac{1}{2}} \ln (h\nu_0/kT)$$

$$\text{erg cm}^{-3} \text{ s}^{-1} \text{ sr}^{-1} \qquad \ldots (4.27)$$

$$a_{32} (H\alpha) = 1.29$$

$$a_{42} (H\beta) = 0.449$$

To check the validity of Equation (4.27) in the case of Be star envelopes, $j(H\alpha)/j(H\beta)$ ratios have been

calculated and listed in Table 4.7 for a sample of 17 stars for which Dachs et al. (1981) have given Hα and Hβ equivalent widths. The expected ratio using Equation (4.27) is

$$\frac{j\,(H\alpha)}{j\,(H\beta)} = 2.87$$

The general agreement of the observed $j\,(H\alpha)/\,j\,(H\beta)$ ratios with the expected ones shows that case B conditions hold good for Be star envelopes.

The H_α luminosity of the circumstellar envelope of a Be star assuming the shell to be optically thin can then be written as

$$L_{H\alpha} = \int 4\pi\, j_{H\alpha}\, dV$$

$$= \int 10^{-23}\, N_e\, N_i\, a_{n2}\, T^{-\frac{1}{2}}\, \ln\,(h\nu_o/kT)\,dV \quad ..(4.28)$$

Comparisom of the Equation (4.28) with Equations (4.12), (4.15) and (4.16) shows that both L_{IR} and $L_{H\alpha}$ have the same functional dependance on the product $N_e\ N_i$ apart from the weak dependance of temperature. Hence the existemce of correlation between L_{IR} and $L_{H\alpha}$ is understandable.

Table 4.7

Luminosity ratios of Hydrogen Balmer lines Hα and Hβ of Be stars observed by Dachs et al. (1981)

S. No.	HR No.	Sp.Type	$W_{H\alpha}$ Å	$L_{H\alpha}$ erg s^{-1}	$W_{H\beta}$ Å	$L_{H\beta}$ erg s^{-1}	$\frac{L_{H\alpha}}{L_{H\beta}}$
1	3034	B1 IV	14.8	7.32 E 33	1.85	2.53 E 33	2.89
2	8539	B1 IV	37.0	1.83 E 34	3.3	4.51 E 33	4.06
3	2538	B1.5 IVn	17.8	8.83 E 33	1.7	2.32 E 33	3.79
4	2749	B2 IV	14.2	3.32 E 33	1.55	9.69 E 32	3.42
5	4009	B2 IVpn	38.5	9.01 E 33	4.6	2.87 E 33	3.14
6	4621	B2 IVn	42.3	9.93 E 33	3.8	2.37 E 33	4.18
7	6118	B2 V	66.7	1.56 E 34	8.3	5.19 E 33	3.01
8	6304	B2 IVn	29.6	6.93 E 33	3.7	2.31 E 33	3.00
9	6510	B2 Vn	39.1	9.15 E 33	2.9	1.81 E 33	5.06
10	6929	B2 IVp	29.7	6.95 E 33	4.1	2.56 E 33	2.71
11	8520	B2 IV-V	21.5	5.03 E 33	2.59	1.62 E 33	3.10
12	2825	B2.5IV	11.3	2.65 E 33	1.6	1.00 E 33	2.65
13	2785	B3 V	44.7	6.79 E 33	3.8	1.47 E 33	4.62
14	2911	B3 V	45.0	6.84 E 33	3.7	1.44 E 33	4.75
15	3964	B4 V	33.3	4.26 E 33	3.2	9.44 E 32	4.51
16	4140	B4 Vn	35.6	4.56 E 33	2.9	8.56 E 32	5.33
17	5316	B4 Vn	41.7	5.34 E 33	2.7	7.97 E 32	6.70

It may be noted from Table 4.5 that out of 18 stars listed, 4 do not have measurable IR excess. This could be explained as follows:

(a) As described in 4.8 the Be stars show IR variability. For a given Be star the IR excess will be present only when there is sufficient amount of material in the circumstellar envelope. So the depletion of material in the envelope results in the absence of IR excess. From the previous discussion it is also implied that the absence of IR excess should result in smaller equivalent width of H emission line or even absence of Hα line in emission. This is corroborated by 2 of the stars listed in Table 4.5 that do not have IR excess. 1.6 Å Hα equivalent width of HR 2231 is the lowest of all the 18 stars and in the case of HR 5778 Hα is in absorption.

(b) The other 2 stars - HR 8520 and HR 894 - that do not have IR excess, however, have appreciable equivalent widths. This apprent contradiction may be due to the changes in physical

conditions of the circumstellar envelope in two months separating IR and the Hα observations.

The examination of Table 4.3 shows that in addition to the 4 stars discussed earlier, the following 10 stars viz., HR 8047, HR 8603, HR 1659, HR 2749, HR 6873, HR 8402, HR 1500, HR 1126, HR 1956 and HR 6720, do not exhibit IR excess during our observations. The reason for the absence of IR excess appears to be the same as before - absence of Be episode at the time of IR observations. It will be interesting and valuable to confirm this inference drawn from IR observations.

To make quantitative comparison between the observations and the theoretical estimates let us calculate the ratio of L_{IR} to $L_{H\alpha}$. From equations (4.13), (4.15) and (4.28) we obtain

$$\frac{L_{IR}}{L_{H\alpha}} = \frac{\int 1.435 \times 10^{-27} T^{\frac{1}{2}} N_e N_i \, dV_{IR}}{\int 1.29 \times 10^{-23} T^{-\frac{1}{2}} \ln (h\nu_o/kT) N_e N_i \, dV_{H\alpha}}$$

It should be noted that the circumstellar envelope has been considered to be optically thin to both continuum and line radiation to obtain the above expression.

Assuming that the temperature is uniform throughout the envelope the above expression reduces to

$$\frac{L_{IR}}{L_{H\alpha}} \simeq 0.4 \left(\frac{T}{10^4}\right) \frac{\int N_e \; N_i \; dV_{IR}}{\int N_e \; N_i \; dV_{H\alpha}}$$

From Table 4.5 it is seen that the average value of observed ratio L_{IR}/L_H is $\sim$ 32 significantly different from the theoretical estimate of 0.4 if the emission measures for continuum and line radiation were same. The large value of $L_{IR}/L_{H\alpha}$, 35, shows that the effective emitting volumes of continuum and line radiation are not identical. Most likely line radiation does not escape freely all through the envelope.

During the final part of the present work we noticed that Neto and Pacheco (1982) and Dachs and Wamsteker (1982) have independently arrived at similar conclusions regarding the IR excess and line emission from Be stars.

The foregoing discussion has shown that IR excess is a good indicator of envelope activity of Be stars. As a result Be stars can be more profitably monitored in IR. IR photometric observations are less time

consuming compared to spectroscopic method and also for a given telescope IR observations extend to fainter magnitudes covering larger samples.

4.9:4 Temporal variations:

To get an insight into the IR variability of Be stars, let us first consider the explanations given for Hα variations since both of them are related. It should be noted that here we are concerned mainly with long time scale variations, say few years. As noted by Poeckert and Marlborough (1978) the changes occurring in mass loss rate, expansion velocity and scale height of circumstellar disc are the parameters controlling temporalvariations of Be stars. The emission line data of Be stars obtained by Dachs et al. (1981) show evidence for variations in the size of circumstellar envelopes. They find inverse correlation between the equivalent width (W) and half-intensity width (H). The increased equivalent width suggests extra input of material to the circumstellar envelope. Other parameters such as T, N_e, N_i remaining constant the increase in equivalent width, W, implies an increase in R_s resulting in the increased emission measure.

The material in the envelope is in Keplerian orbit around the central star and rotation velocity decreases with increasing orbital radius. With decrease in velocity the rotational broadening decreases resulting in smaller half-intensity width (H). The same processes which are responsible for changes in line strength can also account for IR variability.

In the following paragraphs a comparative study of all the available optical spectroscopic and IR photometric data for the 4 Be stars that have shown considerable IR variability ($\triangle m_K \gtrsim 0.5$) is done to look for their correlated behaviour.

25 Ori(HR 1789):

According to our IR observations of Jan-Feb.1981, 25 Ori was at K = $4^m.76$. The earliest available observation is that of Allen (1973) for the epoch 1971-72 and the reported value is K = $5^m.47$. Dachs et al. (1982) obtained K = $5^m.16$ in Feb. 1979. These observations show that between 1971-72 and 1981, 25 Ori has brightened by $0^m.7$ at 2.2 μm. The optical spectroscopic data since its discovery has shown that 25 Ori exhibits alternating periods of emission and pure photospheric absorption. The optical spectroscopic data of

Slettebak and Reynolds shows that in Dec.1975 25 Ori was exhibiting considerably low Be activity with Hα equivalent width W = 3.78 Å which is small for B1 spectral type star. Further by November 1976, 25 Ori had entered quiscent phase with Hα in absorption. The observed equivalent width of 8.4 Å in Dec.1980 (Andrillat and Fehrenbach, 1982) indicates that Be activity in 25 Ori has reappeared. Our IR observations show that in Jan-Feb. 1981 25 Ori has appropriate IR excess expected of a B1 V type star. This suggests correlated optical and IR variability similar to that of o Cas (Elias et al. (1978).

ω Ori (HR 1934):

Our observations show that IR excess radiation for ω Ori has decreased from 1972-73 (Allen, 1973) to 1980-81. Our observations of 1980-81 are compatible with 1965 observations of Johnson et al. (1966). K magnitude value of ω Ori in Feb.1979 (Dachs et al. 1982) is in between those of 1972-73 and 1980-81. The optical spectroscopic data shows that Hα equivalent width has decreased from 1974 to 1978. Baliunnas et al. (1975) and Cester et al. (1977) using Hα filter photometry have shown that ω Ori varies on time scale of years.

ω CMa(HR 2749):

Out of the available K magnitudes, ω CMa has the faintest value in1981 and shows no IR excess. In 1971-72 it was brighter by $0^m.6$ at 2.2 μm compared to 1981. 1978 Hα equivalent width data reveals that ω CMa was in a normal emission phase with $W_{H\alpha}$ = 14 Å. As per our IR observations between November 1978 and January 1981 the emission lines should have disappeared.

χ Oph (HR 6118):

χ Oph is one of the well studied Be stars. Along with ϕ Per it has the distinction of having the largest recorded Hα equivalent width of 67 Å (Dachs et al. 1981). The IR coverage for χ Oph is reasonably good - from 1970, K magnitudes are available at more or less regular interval of 1-2 years. At IR wavelengths χ Oph decreased in brightness from 1970 to 1973 and since 1973 its brightness has increased. Hα equivalent width has monotonically decreased from 66.7 Å in 1972 to 33.7 Å in 1980. However, V magnitude brightened by $0^m.5$ between 1972 and 1978, resulting in constant Hα line intensity.

4.10 SUMMARY

Infrared photometric studies of Be stars have been done. J H K magnitudes of 55 Be stars are presented. For 20 of the Be stars the photometric observations reported in this thesis are new. The new results that have emerged from the present investigations are listed below.

1. The observed IR continuum luminosity L_{IR} of the circumstellar envelope of the Be stars exceeds the energy input by the Lyman continnum luminosity L_L^o of the central star. This points to the necessity of an additional energy source to maintain the thermal balance of circumstellar envelopes.

2. The existence of a correlation between the continuum luminosity L_{IR} of the circumstellar envelope and bolometric luminosity L_* of the central star is demonstrated. This correlation suggests that the bolometric luminosity L_* plays an important role in deciding the energetics of the circumstellar envelope. Over two orders of magnitude L_{IR} varies in proportion to L_*.

3. The IR continuum luminosity L_{IR} of the circumstellar envelope is correlated to the Balmer Hα luminosity $L_{H\alpha}$. This provides an additional evidence for the free-free process as the dominant emission mechanism which gives rise to the IR excess from Be stars.

4. The effective volumes which emit Hα line and IR continuum emission are different.

5. The comparison of present observations with the previous available data shows that 4 Be stars - 25 Ori, ω Ori, ω CMa and χ Oph - have varied at K (2.2 μm). The amplitude of this variation lies between $0^m.5$ and $0^m.8$ and the time scale is a few years. The IR variations have also been correlated to the optical variations.

CHAPTER V

RCB STARS

5.1 INTRODUCTION

The variable stars have played a very important role in the development of astrophysical ideas. The study of variable stars has provided new knowledge of the structure and evolution of stars which could not be obtained from the investigations of stars which are steady. RCB stars form a very peculiar group of variable stars. The sudden decreases in intensity by factors as large as $\sim 10^4$ experienced by RCB stars identified them as a separate class of variable stars. Except for the occasional dramatic fadings, the RCB stars are relatively quiscent rest of the time. The spectral studies of RCB stars showed that they are overabundant in carbon and deficient in hydrogen. This spectroscopic property was subsequently added as an additional characteristic property of the RCB group of variable stars. It is pertinent to note here that there are also hydrogen deficient carbon rich stars which do not undergo large decreases in their intensity. These stars are usually referred to as HdC stars.

Obscuration of the star by intervening material in its surroundings is responsible for the visual fading

of RCB stars in the hypothesis of Loreta-O'Keefe (O'Keefe, 1939). Observational evidence for the presence of particulate matter was provided by the discovery of IR excess from the two prominent members of the class viz., R CrB and RY Sgr (Stein et al. 1969 and Lee & Feast, 1969). The IR excess from these stars was attributed to the blackbody radiation from circumstellar dust. Later IR observations (Feast and Glass, 1973; Glass, 1978; Gaustad, 1972; Rao, 1980 a) have shown that the IR excess is a general property of RCB stars. Alongwith the RCB stars Feast and Glass (1973) also observed HdC stars. An interesting outcome of their observations was the absence of IR excess in HdC stars. This showed that the IR excess is not a general property of HdC stars. The occurrence of IR excess is connected to the visual fadings experienced by the RCB stars.

An alternative hypothesis for the IR excess in the case of R CrB was put forward by Humphreys and Ney (1974). In the scenario suggested by them R CrB is a binary system. The companion star has a very low surface temperature and predominantly emits in the IR. The observational result that prompted Humphreys and

Ney to propose the binary model was the 3.5 μm light curve of R CrB which showed a period of $\sim$ 3.5 years. However, later observations by Feast et al. (1977) have shown that all RCB stars are not binaries. In particular the IR excess from RY Sgr at 3.5 μm follows the visual 38.6 days period which is intrinsic to the optical star. Hence it is difficult to associate the observed 3.5 μm excess with the companion star.

5.2 IR EXCESS AND RCB PHENOMENON

The occurrence of IR excess is possibly connected with the visual fadings - RCB phenomenon - of the star. The excess IR radiation fits into the model of thermal re-radiation by the circumstellar material. If this material is replenished by the occasional ejection of matter by the star then the IR excess should be related to the recurrence rate of the visual fadings and also the amount by which the star's intensity decreases in each fading. This inference has been put to an observational test in the case of XX Cam.

5.2:1 XX Cam:

The spectral characteristics (Bidelman, 1948) and the occurrence of a visual minimum during 1939-40

(Yuin, 1948) suggested that XX Cam is a member of the RCB group of variable stars. Yuin made a search for light variability for the years 1898 to 1948. Since 1948 no visual fadings have been reported. It appears that in the last ~ 85 years XX Cam has undergone only one light minimum. It is also interesting to note that the depth of this minimum is small viz., $1^{m}.7$ at V. These facts suggest that XX Cam should have either very little or no IR excess. We have obtained IR observations of XX Cam to see whether it has any IR excess.

IR Observations:

J, H and K band observations of XX Cam were obtained using 1 m telescope at Kavalur. InSb photometer described in Chapter II was used to obtain these observations.

To obtain a reasonably complete energy distribution, the average UBV magnitudes reported by Fernie et al. (1972) and IR observations available with Kameshwara Rao (Rao et al. 1980b) have been utilised. Using a value of E (B-V) = 0.30 (Rao et al. 1980b) the interstellar reddening corrections were done as described in Sec.4.5:1.

All the magnitude and flux values are listed in Table 5.1. The observed energy distribution is plotted in Fig.5.1. The energy distribution of a blackbody at temperature T = 7000 K fits the observational curve reasonably well and shows that no IR excess is present in the wavelength region 1 to 10 μm. The absence of IR excess corroborates the optical data of only instance of light minimum and suggests that XX Cam has probably become stable against RCB phenomenon.

Table 5.1

Energy distribution of XX Cam

Filter	λ (μm)	mag	F (watts/cm^2 μm)	Date
U	0.36	8.48	1.76×10^{-15}	Oct.1966-Feb.1967
B	0.44	8.20	3.78×10^{-15}	
V	0.55	7.35	4.50×10^{-15}	
J	1.25	5.63	1.90×10^{-15}	Dec.1973
K	2.2	5.36	2.80×10^{-16}	
	2.2	5.5	2.47×10^{-16}	Feb.1974
	3.6	5.38	4.16×10^{-17}	
	10	4.5*	2.06×10^{-18}*	
J	1.26	5.80	1.627×10^{-15}	Feb.1980
H	1.65	5.70	5.972×10^{-16}	
K	2.23	5.55	2.350×10^{-16}	

* 10 micron measurement is an upper limit to the flux.

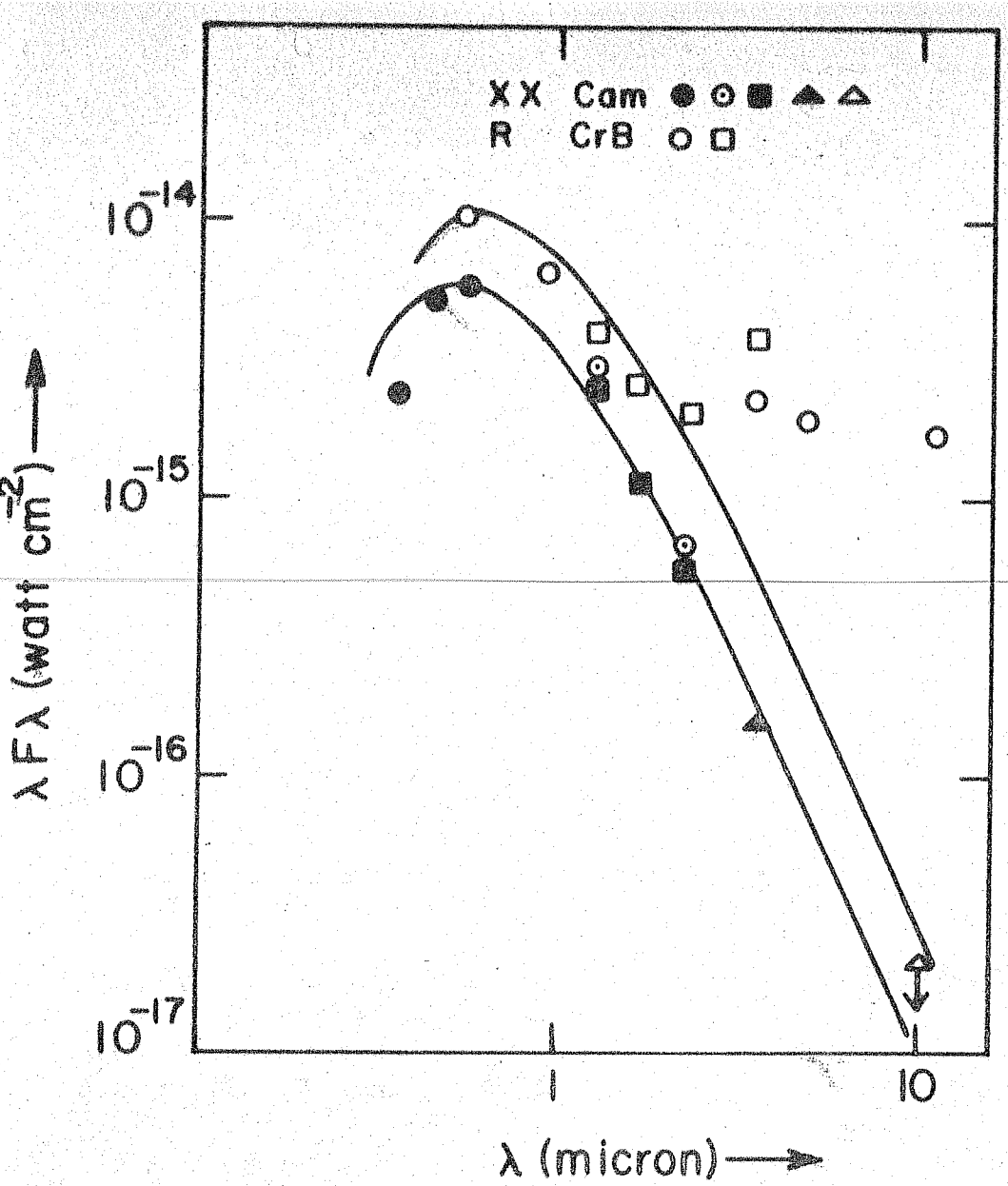

Fig.5.1 : Energy distribution of XX Cam corrected for E (B-V) = 0.30. The observations fit into blackbody energy distribution for T = 7000 K. The energy distribution of R CrB which has large infrared excess is also shown.

BB : Blackbody energy distribution
XX Cam observations :

- ● Fernie et al. (1972), ◎ Dec. 1973
- ▲ Feb 1974, open triangle denotes upper limit
- ● Present observations, Feb.1980. R CrB Obs:
- ○ Humphreys and Ney (1974)
- □ Present observations Feb. 1980.

REFERENCES

Abt, H.A. and Levato, H.	1977	PASP 89, 797.
Allen, D.A.	1973	MNRAS, 161, 145.
Allen, C.W.	1976	Astrophysical Quantities.
Alvarez, J.A., Furniss, I., Jennings, R.E., King K.J. and Moorwood, A.F.M.	1974	H II regions and the Galactic Center. Proc. 8th ESLAB Symp. ed. AFM Moorwood, ESRO SP-105, p.69.
Allen, D.A. and Barton, J.R.	1981	PASP 93, 381.
Andrillat, Y. and Fehrenbach, Ch.	1982	Astron. Astrophys. Supp. Ser. 48, 93.
Apparao, M.V.K. and Chitre, S.M.	1979	Private communication.
Apparao, M.V.K. and Chitre, S.M.	1980	Astrophys. Sp.Sc. 72, 127.
Baan, W.A.	1977	Ap J. 214, 245.
Baan, W.A.	1979	Ap.J. 227, 987.
Bahng, J.D.R.	1976	Rapid variations of Hα in Be stars, in Slettebak A (ed) 'Be and shell stars' IAU Symp. No. 70, 41.
Baliunas, S.L., Ciccone, M.A. and Guinan, E.F.	1975	PASP 87, 969.
Barlow, M.J. and Cohen, M.	1977	Ap. J. 213, 737.
Becklin, E.E. and Westphal, J.A.	1965	Ap. J. 145, 445.

Beckman, J.E. and Moorwood, A.F.M.	1979	Rep Prog. Phys. 42, 87.
Bidelman, W.P.	1948	Ap. J. 107, 413.
Blanco, A., Bussoletti, E., Melchiorri, B., Melchiorri, F. and Natale, V.	1976	Infr. Phys. 16, 569.
Blumenthal, G.R. and Tucker, W.H.	1974	Ann. Rev. Astron. Astrophys. 12, 23.
Boulon, J., Doazan, V. and Letourneur, N.	1975	Astron. Astrophy. 40, 203.
Bradt, H,, Doxsey, R.E. and Jernigan, J.G.	1979	Advances in Space Exploration (eds) W.A.Baily and L.E.Peterson Vol.3, p.3.
Burbidge, G.R. and Burbidge, E.M.	1953	Ap. J.117, 407.
Canizares, C.R., McClintock, J.E. and Grindlay, J.E.	1979	Ap. J. 234, 556.
Capps, R.W., Coyne, G.V. and Dyck, H.M.	1973	Ap. J. 184, 173.
Cester, B., Giuricin, G., Mardirossian F., Pucillo, M., Castelli, F. and Flora, U.	1977	Astron. Astrophys. Suppl. Ser. 30, 1.
Clarke, D. and McLean, I.S.	1974	MNRAS 167, 27p.

Clarke, D. and McLean, I.S.	1976	MNRAS 174, 335.
Collins,	1974	Ap. J. 191, 157.
Cooke, B.A., Ricketts, M.J., Maccacaro, T., Pye, J.P., Elvis, M., Watson, M.G., Griffiths, R.E., Pounds, K.A., McHardy, I., Maccagni, D., Seward, F.D., Page, C.G. and Turner, M.J.L.	1978	MNRAS 182, 489
Coyne, G.V. and Kruszewski, A.	1969	A. J. 74, 528.
Coyne, G.V. and McLean, I.S.	1975	A.J. 80, 702.
Coyne, G.V.	1976	Be and Shell stars, (ed) A.Slettebak, IAU Symp. No.70, p.233.
Dachs, J. et al.	1981	Astron. & Astrophy. Suppl. Ser. 43, 427.
Dachs J. and Wamsteker, W.	1982	Astron. Astrophys. 107, 240.
Doazan, V.	1976	Be and Shell Stars, (ed) A.Slettebak, IAU Symp. 70, 37.
Elias, J., Lanning, H. and Neugebauer, G.	1978	PASP 90, 697.

Ennis, D., Becklin, E.E., Beckwith, S., Elias, J., Gatley, I., Matthews, K., Neugebauer, G. and Willner, S.P. 1977 Ap. J. 214, 478.

Fazio, G.G. 1976 Frontiers of Astrophysics, ed. Avrett E.H. (Harvard University Press), p.203.

Feast, M.W. and Glass, I.S. 1973 MNRAS 161, 293.

Feast, M.W., Catchpole, R.M., Lloyd Evans, T., Robertson, B.S.C., Dean, J.F. and Bywater, R.A. 1977 MNRAS 178, 415.

Feinstein, A. and Marraco, 1979 A. J. 84, 1713.

Fernie, J.D., Sherwood, V. and Dupuy, D.L. 1972 Ap. J. 172, 383.

Fujimoto, M., Hanawa, T. and Miyaji, S. 1981 Ap. J. 247, 267.

Forman, W., Jones, C., Cominsky, L., Julien, P., Murrays, S., Peters, G., Tananbaum H. and Giacconi, R. 1978 Ap. J. Suppl. 38, 357.

Frank, J., King, A.R., Sherrington, M.R., Giles, A.B. and Jameson, R.F. 1981 MNRAS 196, 921.

Gatley, I. and Becklin, E.E. 1981 Infrared Astronomy (eds.) CG Wynn Williams and DP Cruikshank, IAU Symp. No.96, p.281.

Gaustad, J.	1972	Mem.Soc.R. Sci. de Liege 6^{e} serie, Tome III, 87.
Geballe, T.R., Wollman, F.R., Lacy, J.H. and Rank, D.M.	1977	PASP 89, 840.
Gehrz, R.D., Hackwell, J.A. and Jones, T.W.	1974	Ap. J. 191, 675.
Gehrz, R.D., Grasdalen, G.L., Hackwell J.A. and Ney, E.P.	1980	Ap. J. 237, 855.
Glass, I.S.	1974	Monthly Notes Astron. Soc. South Afr. 33, 53.
Glass, I.S.	1978	MNRAS 185, 23.
Grindlay, J. and Heise, J.	1976	IAU Cir No.2879.
Grindlay, J., Gursky, H., Schnopper, H., Parsignault, D.R., Heise, J., Brilnkman,A.C. and Schrijver, J.	1976	Ap. J. Lett. 205, L127.
Grindlay, J.E., McClintock, J.E., Canizares, C.R., Van Paradijs, J., Li, F.K. and Lewin,W.H.G.	1978	Nature 274, 567.
Hack, M. and Struve, O.	1970	Stellar spectroscopy - peculiar stars, Observatorio Astronomico di Trieste, p 20.

Hackwell, J.A., Grasdalen, G.L., Gehrz, R.D., Van Paradijs, J., Cominsky, L. and Lewin, W.H.G.	1979	Ap. J. Lett. 233, L115.
Hardie, R.H.	1962	Astronomical Techniques (ed) WA Hilther, The University of Chicago Press, p.178.
Harvey, P.M., Campbell, M.F. and Hoffmann, W.F.	1976	Ap. J. 205, L69.
Hayakawa, S., Ito, K., Matumoto, T. Ono, T. and Uyama, K.	1976	Nature, 261, 29.
Henriksen, R.N.	1976	Ap. J. 210, L19.
Hoffleit, D.	1964	Catalogue of Bright Stars, Yale University Observatory.
Hoffmann, W.F., Frederick, C.L. and Emery, R.J.	1971	Ap. J. 164, L23.
Hoffman J.A., Marshall, H.L. and Lewin, W.H.G.	1978	Nature 271, 630.
Hudson, R.D.	1969	Infrared System Engineering John Wiley and Sons Inc.
Huang, S.S.	1972	Ap. J. 171, 549.
Huang, S.S.	1973	Ap. J. 183, 541.
Humphreys, R.H. and Ney, E.P.	1974	Ap. J. 190, 339.

Inoue, H., Koyama,K., Makishina K., Matsuoka, M., Murakami, T., Oda, M., Ogawara, Y., Ohashi, T., Shibazaki, N., Tanaka, Y., Tawara, Y., Kondo, I., Hayakawa, S., Kunieda H., Makino, F., Masaai, K., Nagase, F., Miyamoto, S., Tsunemi, H. and Yamashita, K.	1980	Nature 283, 358.
Jascheck, M., Hubert-Delplace, A.M., Hubert, H. and Jaschek, C.	1980	Astron. Astrophys. Suppl. Ser. 42, 103.
Jaschek, M., Slettebak, A. and Jaschek, C.	1981	'Be Star Newsletter', p.9.
Johnson, H.L.	1966	Ann.Rev.Astron.Astrophy. 4, 193.
Johnson, H.L., Mitchell, R.I., Iriarte, B. and Wisniewski, W.Z.	1966	Comm. Lunar Planet. Lab. No.63, p.99.
Johnson, H.L.	1967	Ap. J. Lett. 150, L39.
Johnson, H.L.	1968	Nebulae and Interstellar matter, (eds) BM Middlehurst and LH Aller, University of Chicago Press, p.193.
Jones, A.W., Selby, M.J., Mountain, C.M., Wade, R., Magro, C.S. and Munoz, M.P.	1980	Nature 283, 550.
Jones, T.J.	1979	Ap. J. 228, 787.

Joss, P.C.	1977	Nature 270, 310.
Joss, P.C.	1978	Ap. J. 225, L123.
Joss, P.C.	1979	Comm. Astrophys. 8, 109.
Joss, P.C. and Rapport, S.	1977	Nature 265, 222.
Kleinmann, D.E., Kleinmann, S.G. and Wright, E.L.	1976	Ap. J. Lett. 210, L83.
Kulkarni, P.V., Ananth, A.G., Sinvhal, S.D. and Joshi, S.C.	1977	Bull. Astron.Soc. of India, 5, 52.
Lamb, F.K., Fabian, A.G., Pringle, J.E. and Lamb D.Q.	1977	Ap. J. 217, 197.
Lamers, H.J.G.L.M.	1981	Ap. J. 245, 593.
Lang, K.R.	1974	Astrophysical Formulae, p.244. Springer-Verlag, Berlin.
Lawrence, A. et al.	1982	Preprint, X-ray, Radio and Infrared observations of the RB (MXB 1730-335) during 1979 and 1980.
Lee, T.A. and Feast, M.W.	1969	Ap. J. 157, L173.
Lena, P.	1978	Infrared Astronomy, ed. G.Setti and GG Fazio, (Dordrecht-Reidel).

Lewin, W.H.G., Doly, J., Clark, G.W., Rapport, S.A., Bradt, H.V.D., Doxsey, R., Hearn, D.R., Hoffmann, J.A., Jernigan, J.G., Li, F.K., Mayer, W., McClintock, J., Primini, F. and Richardson, J.	1976a	Ap. J. Lett. 207, L95.
Lewin, W.H.G. et al.	1976b	MNRAS 177, 83p.
Lewin, W.H.G.	1977	MNRAS, 179, 43.
Lewin, W.H.G.	1980	Globular Clusters, eds. D Hanes and B.Madore, (Cambridge University Press).
Lewin, W.H.G., Cominsky, L.R., Walker, A.R. and Robertson, S.C.	1980	Nature 287, 27.
Lewin, W.H.G. and Joss, P.C.	1981	Sp. Sc. Rev. 28, 3
Liller, W.	1976	IAU Cir. No.2929.
Liller, W.	1977	Ap. J. Lett. 213, L21.
Limber, D.N. and Marlborough, J.M.	1968	Ap. J. 152, 181.
Low, F.J. and Smith, B.J.	1966	Nature 212, 675.
Low, F.J. and Aumann, H.H.	1970	Ap. J. 162, L79.
Low, F.J. and Krishnaswamy, K.S.	1970	Nature 227, 1333

Low, F.J. and Rieke, G.H.	1974	Methods of Experimental Physics ed. N Carleton, 12, 415 (New York - Academic).
Maillard, J.P.	1974	Highlights of Astronomy, ed. G.Contopoulos, Dordrecht-Reidel, 3, 269.
Manduca, A. and Bell, R.A.	1979	PASP 91, 848.
Maraschi, L. and Cavaliere, A.	1977	Highlights in Astronomy, 4, Part I, p.127.
Marlborough, J.M.	1969	Ap. J. 156, 135.
Marlborough, J.M.	1976	Be and Shell Stars, (ed) A. Slettebak, IAU Symp. No.70, p.335.
Marshall, H.L., Ulmer, M.P., Hoffmann, J.A., Doty, J. and Lewin W.H.G.	1979	Ap. J. 227, 555.
McClintock, J.E., Canizares, C. and Backman, D.E.	1978	Ap. J. Lett. 223, L75.
McLean, I.S. and Brown, J.C.	1978	Astron. Astrophys. 69, 291.
McLean, L.S., Coyne, G.V., Frecker, J.E. and Serkowski, K.	1979	Ap. J. 228, 802.
Mendoza, E.E.	1958	Ap. J. 128, 207.
Mendoza, E.E.	1966	Ap. J. 143, 1010.
Merril, P.W. and Burwell, C.G.	1933	Ap. J. 78, 87.

Moorwood, A.F.M.	1978	Infrared Astronomy, ed. G.Setti and GG Fazio (Dordrecht-Reidel), p.291.
Murakami, et. al.	1980	Ap. J. Lett. 240, L143.
Neto, A.D. and Pacheco, J.A.F.	1982	MNRAS 198, 659.
Neugebauer, G. and Leighton, R.B.	1969	NASA SP-3047.
Neugebauer, G., Becklin, E. and Hyland, A.R.	1971	Ann. Rev. Astron. Astrophys. 9, 67.
Ney, E.P.	1976	The Study of Comets, (eds) B.Donn, M.Mumma, W.Jackson, M.A'Hearn and R.Harrington, p.334.
O'Keefe, J.A.	1939	Ap. J. 90, 294.
Okuda, H., Maihara, T., Oda, N. and Sugiyama, T.	1977	Nature 265, 515.
Okuda, H.	1981	Infrared Astronomy: IAU No.96, The large scale IR emission in the galactic plane - Observations (eds) CG Wynn-Williams and DP Cruikshank, p.247.
Osterbrock, D.E.	1974	Astrophysics of Gaseous Nebulae Nebulae, W.H.Freeman and Co. San-Francisco.
Pedersen, H. et al.	1979 1982	IAU Cir. No.3399. Pre-print.
Peters, G.R.	1976	Be and Shell Stars, (eds) A.Slettebak, IAU Symp. 70, 417.

Phillips, J.P., Selby, M.J., Wade, R. and Magro, C.S.	1980	MNRAS 190, 337.
Plavec, M.	1976	Be and Shell Stars - (ed) A.Slettebak, IAU Symp. No.70, p.439.
Poeckert, R.	1975	Ap. J. 196, 777.
Poeckert, R. and Marlborough, J.M.	1977	Ap. J. 218, 220.
Poeckert, R. and Marlborough, J.M.	1978a	Ap. J. 220, 940.
Poeckert, R. and Marlborough, J.M.	1978b	Ap. J. Suppl. 38, 229.
Poeckert, R., Bastien, P. and Landstreet, J.P.	1979	Astron. J. 84, 812.
Poeckert, R.	1981	IAU Symp. No.98 -Be and Shell stars.
Price, S.D. and Walker, R.G.	1976	AFGL-TR-76-0208.
Price, S.D., Murdock, T.L. and Shivanandan, K.	1981	SPIE Vol.280, 33.
Rao, N.K.	1980a	Observatory 100, 164.
Rao, N.K., Ashok N.M. and Kulkarni, P.V.	1980b	J. Astr. Astrop. 1, 71.
Rieke, G.H., Telesco, C.M. and Harper, D.A.	1978	Ap. J. 220, 556-567.

Rieke, G.	1978	Infrared Astronomy (ed) by G Setti and GG Fazio (Dordrecht-Reidel), p.159.
Rieke, G.H. and Lebofsky, N.J.	1979	Ann. Rev. Astron. Astrophys., 17, 477.
Robson, E.I., Vickers, D.G., Huizinga, J.S., Beckman, J.E. and Clegg, P.E.	1974	Nature 251, 591.
Sato,S., Kawara, K., Kobayashi, Y., Maihara, T., Okuda, H. and Jugaku J.	1980	Nature 286, 688.
Scargle,J.D., Erickson, E.F., Wittenborn, F.C. and Strecker, D.W.	1978	Ap. J. 224, 527.
Schild, R.E.	1973	Ap. J. 179, 221.
Serkowski, K.	1970	Ap. J. 160, 1083.
Sherrington, M.R., Lawson, P.A., King, A.R. and Jameson, R.F.	1980	MNRAS 191, 185.
Slettebak, A.	1975	Ap. J. 197, 137.
Slettebak, A.	1976	Be and Shell Stars (ed) by A Slettebak IAU Symp. 70, 123.
Slettebak, A. and Reynolds, R.C.	1978	Ap. J. S. 38, 205.
Slettebak, A.	1979	Sp. Sc. Rev. 23, 541.

Smyth, M.J. and Nandy, K.	1978	MNRAS 183, 215.
Snow, T.P.	1975	Ap. J. 198, 361.
Soifer, B.T. and Pipher, J.L.	1978	Ann. Rev. Astron. Astrophys., 16, 335.
Stein, W.A., Gaustad, J.E., Gillett, F.C. and Knacke, R.F.	1969	Ap. J. 155, L3.
Strom, S.E., Strom, K.M. and Grasdalen, G.L.	1975	Ann. Rev. Astron. Astrophys., 13, 187.
Struve, O.	1931	Astrophys. J. 73, 94.
Spinard, H. and Wing, R.F.	1969	Ann. Rev. Astron. Astrophys., 7, 249.
Svestka, J.	1976	Astrophys. Sp. Sc. 45, 21.
Swank, J.H., Becker, R.H., Pravdo, S.H. and Serlemitsos, P.J.	1976a	IAU Cir. No.2963.
Swank, J.H., Becker, R.H., Pravdo, S.H., Saba, J.R. and Serlemitsos, P.J.	1976b	IAU Cir. No.3010.
Swank, J.H., Becker, RH Boldt, E.A., Holt, S.S., Pravdo, S.H. and Serlemitsos, P.J.	1977	Ap. J. Lett. 212, L73.
Szkody, P., Dyck, H.M., Capps, R.W., Becklin, E.E. and Cruishank, D.P.	1979	A. J. 84, 1359.

Taam, R.E.	1980	Ap. J. 241, 358.
Thompson, R.I. and Johnson, H.L.	1974	Ap. J. 193, 147.
Tucker, W.H.	1975	Radiation Processes in Astrophysics, MIT Press, p.110.
Vasyliunas, V.M.	1979	Sp. Sc. Rev. 24, 609.
Wallace, R.K. and Woosley, S.E.	1981	Ap. J. 45, 389.
Walter, F.M., White, N.E. and Swank, J.H.	1981	IAU Cir. No.3611.
White, N.E. and Swank, J.H.	1982	Ap. J. L. 253, L61.
Whittet, D.C.B. and Van Breda, I.G.	1980	MNRAS 192, 467.
Woody, D.P., Mather, J.C., Nishioka, N.S. and Richards, P.L.	1975	Phys. Rev. Lett. 34, 1036.
Woolf N.J. and Ney, E.P.	1969	Ap. J. 155, L181
Woolf, N.J., Stein, W.A. and Strittmatter, P.A.	1970	Astr. Astrophys. 9, 252.
Wynn Williams, C.G. and Cruikshank, D.P.	1981	IAU Symp. No.96 (D.Reidel Publ. Co. Dordrecht-Holland).
Woosley, S.E. and Taam, R.E.	1976	Nature 263, 101.
Yuin, E.	1948	Ap. J. 107, 413.